Regulating DNA replication and mutagenesis in *Bacillus subtilis*

Ariana Nakta Samadpour

A dissertation submitted in partial fulfillment

of the requirements for the degree of

Doctor of Philosophy

University of Washington

2018

Reading Committee:

Houra Merrikh, Chair

Nina Salama

Michelle Reniere

Program Authorized to Offer Degree:

Microbiology

Copyright © 2018

Ariana Nakta Samadpour

.

University of Washington

Abstract

Regulating DNA replication and mutagenesis in *Bacillus subtilis*

Ariana Nakta Samadpour

Chair of the Supervisory Committee:

Assistant Professor Houra Merrikh

Department of Microbiology

All organisms must control the timing of DNA replication to maintain their genomic stability. In bacteria, this is achieved through tightly controlling the frequency of replication initiation. Though it is well established that DNA topology is important for replication initiation, it was unclear whether the enzymes that modulate supercoiling are important for regulating this process. The work presented in this dissertation identifies a novel role for the essential topoisomerase, DNA gyrase, as a negative regulator of the replication initiator, DnaA. We find that gyrase activity is required for proper binding of DnaA to *oriC* and controls replication initiation frequency in the model Gram-positive bacterium, *Bacillus subtilis*. Based on the conservation of both gyrase and DnaA across all bacteria, and the importance of DNA topology for all stages of DNA replication, it is unlikely that this regulatory mechanism is unique to *B. subtilis*, and likely reflects a general strategy widely utilized by prokaryotes.

Creating genetic variability within bacterial populations is important for adaptation and survival. Therefore, cells must balance the need for high fidelity DNA replication with the need for genetic variability. They promote fidelity by accurately copying their DNA and repairing damaged DNA. Cells can increase variability by inducing pathways that introduce mutations. In particular, genome architecture and transcription levels together dictate mutation rates as a result of collisions between DNA replication forks and RNA polymerase. In support of previous work, I found that transcription-coupled nucleotide excision repair facilitates the increased mutation rates of highly transcribed genes in *B. subtilis*. Furthermore, I found that this mutagenesis is dependent on the activity of DNA polymerase I and the translesion synthesis polymerases YqjH and YqjW. My work contributes to our understanding of transcription-associated mutagenesis.

TABLE OF CONTENTS

ACKNOWLEDGMENTS

I am grateful to my advisor, Houra Merrikh for giving me the opportunity to join her lab when I was an undergraduate student. Working in her lab allowed me to experience how rewarding it is to be a part of a research team and fueled my interest in pursuing graduate school. I thank her for supporting my scientific training.

Many thanks to my committee members, Nina Salama, Michelle Reniere, Caroline Harwood and Alan Weiner, for their guidance. Especially Nina and Michelle for their help on my reading committee.

I would like to thank Sam Million-Weaver and Chris Merrikh for patiently answering my many questions when I first started in the lab as an undergrad.

I am grateful for the mentorship and support of the outstanding post-docs in our lab. Especially Ankunda Kariisa and Maureen Thomason for their generous support and encouragement during my graduate training. I am also thankful to Kevin Lang for his mentorship during the ups and downs of my research.

I would like to thank everyone in the Merrikh lab and the microbiology department for making my time here enjoyable. Special thanks to the graduate students in our lab – Mark Ragheb, for his friendship and support over the last three years, and Monica Cesinger for bringing her enthusiasm and positivity.

To Hannah Ledvina, Erin Garcia, and Hannah Tabakh – I could not have asked for a better group of classmates to go through graduate school with. I am excited to see what these talented ladies will accomplish.

To Nickolas Good, for his unwavering support, encouragement, and love. I cannot thank him enough for the many weekends he spent in the lab with me and for keeping me positive throughout graduate school. I am so grateful to have him in my life.

And most importantly, I thank my incredible parents, Dalia Alfi and Mansour Samadpour, for their continual love and support. They are an amazing team. Special thanks to my dad for his humor and my mother for her kindness. I am grateful for the example they have set for me through their hard work and generosity, and for their perspective and mentorship.

LIST OF FIGURES AND TABLES

Chapter 1

Chapter 2

CHAPTER 1. Introduction

1.1 Overview of DNA replication in *Bacillus subtilis*

Like most bacteria, *Bacillus subtilis* has a single, circular chromosome. DNA replication initiates from the origin of replication, *oriC*. The two replisomes assemble at *oriC*, each replicating one arm of the chromosome, until reaching the terminus, as illustrated in **Fig. 1.1**. Recent work from our lab supports a factory model of bi-directional DNA replication, in which the two replisomes stay intact upon assembling at the origin, with the chromosomal DNA pulled through each replisome (1). The *B. subtilis* chromosome is 4.2 mega base-pairs in length, and *in vivo* work indicates that chromosome duplication can be completed in 40 minutes (2). Based on this, it has been estimated that the replication machinery copies DNA at a rate of 1,000 base-pairs per second (2).

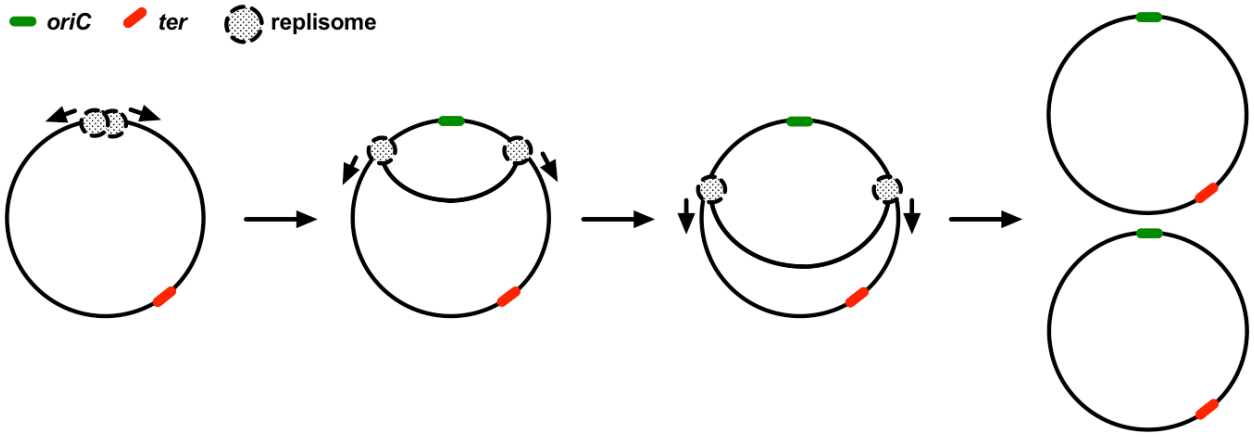

Figure 1.1 Schematic of bi-directional DNA replication from a single, circular chromosome. The two replisomes (patterned circles) assemble at the origin, *oriC* (green). Arrows indicate bi-directional replisome movement along the two arms of the chromosome. Replication ends at the terminus sequence, *ter* (red).

DNA polymerases synthesize DNA in the 5' to 3' direction. Due to the opposing polarity of the two template strands, the two newly synthesized DNA strands are replicated differently. DNA synthesis of the leading strand is continuous, whereas on the lagging strand, DNA is copied in 1-2 kilobase-pair fragments, called Okazaki fragments (3, 4). There are a set of proteins that are required for replicating both daughter strands, as well as several additional proteins that are needed for lagging strand DNA synthesis. The details of this will be further explained below. Upon unwinding of the template DNA, and progression of leading and lagging strand synthesis, two Y-shaped replication fork structures form. A simple depiction of this is shown in **Figure 1.2 A**.

DNA replication is carried out by a set of proteins that operate together to form the replisome. The architecture of the *B. subtilis* replisome is illustrated in **Figure 1.2 B**, with the individual replisome components described in **Table 1.1**. The replication machinery includes the homohexameric helicase, DnaC, which translocates along the lagging strand, unwinding the double helix template ahead of the replication fork (5, 6). Following helicase activity, single-stranded DNA binding proteins (Ssb) coat the DNA, preventing re-formation of the DNA helix and protecting against nucleolytic attacks of exposed single-stranded DNA (7).

Leading strand DNA synthesis is performed by the main replicative polymerase, PolC. Discontinuous DNA synthesis on the lagging strand is completed in 1-2 kilo base-pair fragments, called Okazaki fragments. Each Okazaki fragment is started with the action of primase, which synthesizes an RNA primer that the replicative DNA polymerase DnaE can initiate from to copy the template DNA. Following dissociation of DnaE from the template DNA, the other replicative polymerase, PolC is required to complete Okazaki fragment synthesis, and the resulting gaps from the Okazaki fragments are sealed by ligase. DNA polymerases require association with the β-clamp to be processive. The clamp loader forms a complex with these proteins and the replicative helicase, facilitating the coupling of template unwinding and DNA synthesis. In addition, the type II topoisomerases, gyrase and topoisomerase IV, are required to relieve positive supercoiling generated in front of replication forks, and to decatenate sister chromosomes.

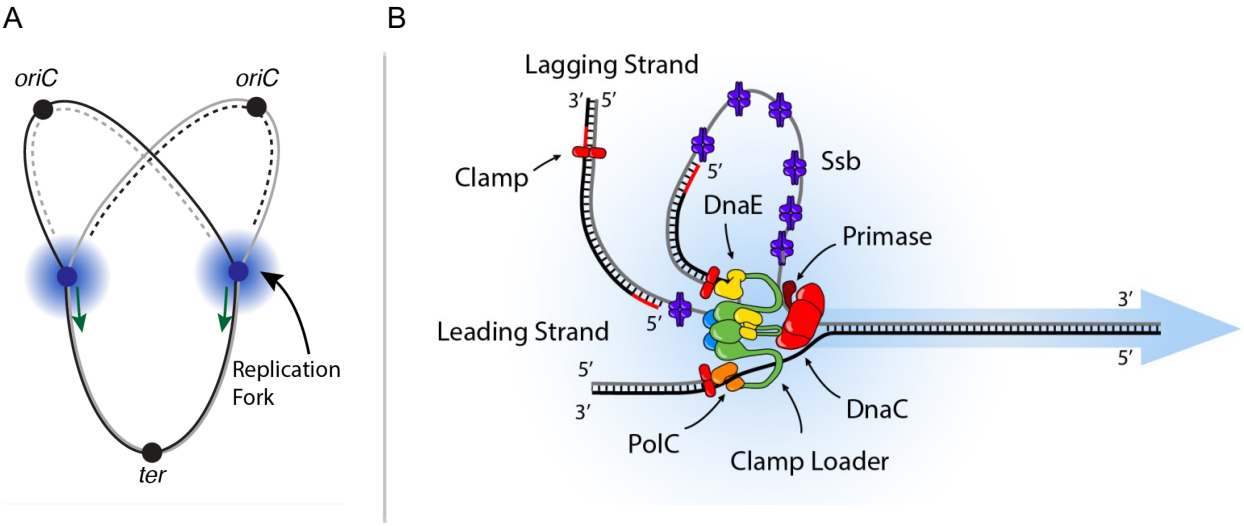

Figure 1.2 A) Diagram of a partially replicated chromosome. Blue shading represents the replication forks, blue dots represent the replisomes. Newly synthesized DNA is depicted by the dotted lines, and the green arrows indicate the direction of replication fork movement. **B)** Architecture of the *Bacillus subtilis* replisome. The clamp loader (green) and clamp (red) interact with the replicative DNA polymerases DnaE (yellow) and PolC (orange). The DnaC helicase hexamer unwinds DNA ahead of the replisome. Lagging strand DNA synthesis requires additionally proteins, including Primase (dark red), and single-stranded DNA binding proteins (Ssb, in purple).

Replisome Component	Protein Composition	Function
Initiator Protein	DnaA (1)	Initiate Replication
DNA Polymerase III	PolC (1)	Leading-strand DNA synthesis Lagging-strand DNA synthesis Proofreading Exonuclease
	DnaE (1)	Lagging-strand DNA synthesis
β-Clamp	DnaN (2)	Processivity Clamp
Clamp Loader	DnaX (3)	Close β-Clamp
	HolA (1)	Open β-Clamp
	HolB (1)	Structural Element
Helicase	DnaC (6)	Unwinds Duplex DNA
Primase	DnaG (1)	RNA Primer Synthesis at Okazaki Fragments
Single-Strand Binding Protein	SSB (4)	Protects ssDNA
Helicase Loader	DnaB (4)	Helicase loading at *oriC* and at stalled replication forks during replication restart
	DnaD (4)	
	DnaI (1)	
Ligase	LigA (1)	Seals Okazaki Fragments
Gyrase	GyrA (2), GyrB (2)	Relaxes positive supercoils Introduces negative supercoils
Topoisomerase IV	ParC (2), ParE (2)	Relaxes positive supercoils Separates linked sister chromosomes

Table 1.1 Components of the replication machinery in *Bacillus subtilis*.

1.2 Initiation of DNA Replication in *Bacillus subtilis*

For cells to begin a new round of replication, the initiator protein, DnaA must first bind to specific 9-mer consensus sequences at the origin of replication, *oriC* (8–10). Upon cooperative binding to these sites, DnaA oligomerization results in bending of the origin sequence, which catalyzes unwinding of an AT-rich region, called the DNA unwinding element (DUE) (11). Following this step, the helicase loaders, DnaB, DnaD and DnaI are recruited to the DUE to facilitate loading of the helicase protein, DnaC (12). Subsequently, replisome proteins are assembled, and replication proceeds bi-directionally.

Origin of Replication

Replication initiates from a specific DNA sequence, called the origin of replication (*oriC*). The length, sequence and structure of *oriC* vary among bacterial species, however they share several key features, which include: DnaA binding sites and an AT-rich region required for melting of the DNA (13, 14). An illustration of the *B. subtilis oriC* structure is shown in **Figure 1.3**.

In *B. subtilis*, *oriC* is bipartite – with two regions containing DnaA binding sites that are separated by the *dnaA* gene (15). This bipartite structure is essential for replication initiation in *B. subtilis* and is thought to facilitate looping of this region during initiation (11). Including the *dnaA* gene, *oriC* is roughly 2.2 kilobase pairs long and contains specific sequences that DnaA binds to called DnaA boxes. The 9 base-pair consensus sequence of these DnaA boxes is: 5'-TTATNCACA-3' (16). There are low and high affinity DnaA boxes. This is particularly important for the regulation of initiation in *E. coli*, where DnaA-ATP can bind to both types of boxes, whereas DnaA-ADP can only bind to the high affinity DnaA boxes (17). However, in *B. subtilis*, DnaA-ATP and DnaA-ADP display minimal differences in their binding efficiencies to these regions (with DnaA-ATP having a higher binding efficiency) (18). Nevertheless, the differences in these

sequences can be important for the ordered assembly of DnaA oligomers (10, 19, 20). Upon DnaA oligomerization, there is opening of the unstable AT-rich DnaA unwinding element (11, 13).

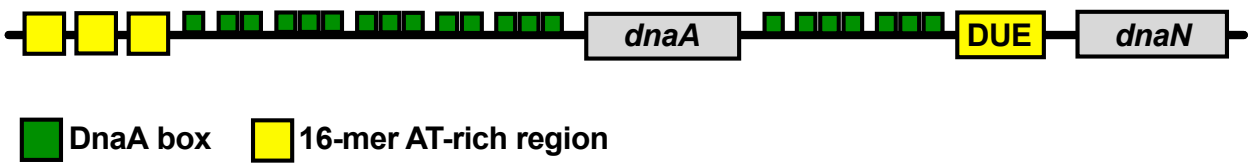

Figure 1.3 Structure of *oriC* in *Bacillus subtilis* (21). The DnaA boxes are depicted by the green boxes, and the 16-mer AT-rich regions are depicted by the yellow boxes. The *dnaA* gene divides *oriC* into two regions.

Structure and Function of DnaA

The replication initiator protein, DnaA, is required for initiation of DNA replication in bacteria and is highly conserved in both Gram-positive and Gram-negative bacteria. Seminal work isolating and characterizing conditional lethal mutations for essential cellular functions in *Escherichia coli* led to the discovery of *dnaA* temperature sensitive (*Ts*) mutants (22). The name of this gene, *dnaA*, originated from their finding that *dnaA Ts* mutants were the first mutants shown to be deficient in DNA replication (22, 23). DnaA is a 50 kilodalton AAA^+ (ATPase associated with diverse cellular activities) type protein that has four domains (24, 25).

The N-terminal DnaA Domain I is critical for interactions with DnaA regulators across bacterial species and allows for helicase loading (21). In *B. subtilis* this region facilitates interactions with SirA (26, 27). DnaA Domain II is poorly conserved across bacteria (28). It acts as a flexible linker between domains I and III, and may be important for the efficiency of replication initiation (29). Domain III contains Walker A and B motifs which allow for ATP binding and hydrolysis. This region is essential for DnaA-DnaA interactions that allow for DnaA oligomerization, as well as for binding to single-stranded DNA (21). In *B. subtilis*, Domain III is also important for

DnaA-YabA and DnaA-DnaD interactions that ensure proper timing of replication initiation during vegetative growth (30–32), and for interactions with Soj and SirA that ensure *oriC* segregation during sporulation (33). The C-terminal Domain IV of DnaA contains a double-stranded DNA binding domain that allows for recognition and binding to DnaA-boxes (34, 35). DnaA is able to bind to DNA through the helix-turn-helix motif of Domain IV that interacts with the major groove of double-stranded DNA (35).

DnaA has a high affinity for ATP (K_d = 30 nM) and ADP (K_d = 100 nM) (36). In cells, it is predicted that newly synthesized DnaA is more often ATP-bound based on the relative concentrations of ATP and ADP. DnaA must be in its ATP-bound form to be "active" – to initiate replication initiation (36). When the DnaA-ATP pool is sufficient, DnaA association at both low and high affinity DnaA binding sites leads to DnaA oligomerization (20). This leads to melting of the DNA unwinding element (DUE) and bending of the origin region (13, 14). ATP hydrolysis thereby inactivates DnaA and prevents premature initiation events. Using its carboxy-terminal double-stranded DNA binding domain, ADP-bound DnaA can bind to high-affinity DnaA boxes. The multi-protein DnaA structures formed with ADP-DnaA are different than the ATP-DnaA oligomers and are unable to catalyze opening of the DUE. Furthermore, in *E. coli*, ADP-DnaA cannot bind to low-affinity DnaA boxes, as is needed for DnaA oligomerization at *oriC* (19).

In addition to its role in replication initiation, DnaA is also a transcription factor (37). This has been demonstrated in *B. subtilis*, *E. coli*, and *Caulobacter crescentus*. Importantly, DnaA represses *dnaA* expression (38–41). DnaA expression levels are autoregulated by DnaA binding to specific DnaA-boxes near the *dnaA* promoter (42). This can have consequences for regulating DnaA levels and DnaA activity as an initiator protein. As a transcription factor, DnaA also controls the transcription of many other genes – and can act as both an activator and a repressor (39, 40, 43). In *B. subtilis*, DnaA alters gene expression in response to replication stress – specifically following inhibition of replication initiation and replication elongation (37, 39). In addition, DnaA

indirectly controls the expression of hundreds of genes through controlling the expression of other transcriptional factors (37).

Regulation of Replication Initiation

Replication initiation is tightly regulated to ensure production of viable progeny. Many of the seminal studies on replication initiation and the mechanisms by which cells regulate this process were done in *E. coli*. Through this work, we have learned a great deal about the structure and function of DnaA, the features of *oriC*, and how cells regulate replication initiation (44). Much of what has been found in *E. coli* is similar in other bacteria. One common mechanism for regulation of replication initiation in *E. coli* and *B. subtilis*, for example, is through DnaA boxes outside of the origin of replication. Sequestration of DnaA at binding sites outside of *oriC* reduces the pool of available DnaA in cells, thus preventing pre-mature initiation events (45, 46). Additionally, autoregulation of *dnaA* is common in both organisms (41, 42, 47). DnaA binds to specific DnaA-boxes near the *dnaA* promoter (42), repressing *dnaA* expression (38–41). This is ultimately important for reducing DnaA pools in cells and controlling replication initiation frequency.

Despite sharing many features, there are significant differences in the control of replication initiation between the Gram-negative bacterium, *E. coli*, and the Gram-positive bacterium, *B. subtilis* (48). One of these fundamental differences is found in the organization of DnaA boxes at the origin of replication. The *oriC* structure is bipartite in *B. subtilis*, with two DnaA box clusters flanking the *dnaA* gene. This is in contrast to the continuous *oriC* sequence in *E. coli* (21). While the bipartite structure of the *B. subtilis oriC* sequence is known to be required for proper replication initiation, and leads to looping of this region during initiation (11), it remains unclear why this bipartite structure is important. Similar bipartite structures exists in other organisms, like *Helicobacter pylori* (49, 50).

Interestingly, none of the DnaA regulators identified in *B. subtilis* have known homologues in *E. coli*. Furthermore, there is a fundamental difference in how replication is controlled among these two organisms that stems from the difference in nucleotide hydrolysis rates for DnaA-ATP, the active form of the initiator protein (48). The DnaA-ATP/ADP half-life is 10-fold higher in *E. coli* as compared to *B. subtilis* (36, 51). Therefore, in *E. coli*, regulation of replication initiation is largely through limiting DnaA-ATP levels in the cell. A primary mechanism for this (which has not been observed in *B. subtilis*) is through stimulating nucleotide hydrolysis of DnaA using a process called regulatory inactivation of DnaA (RIDA) that is dependent on interactions between the DnaA regulator Hda and DnaA (52). Additionally, this can be achieved through DnaA-ATP hydrolysis at the DnaA binding locus, *datA* (53). Furthermore, the stimulated rate of nucleotide exchange in *E. coli* (54) is roughly equivalent to the basal rate of DnaA-ATP hydrolysis in *B. subtilis* (51).

Generally, in *B. subtilis*, DnaA regulation is achieved by controlling DnaA binding and oligomerization at the origin of replication (44, 55, 56). Also, there is an additional layer of regulation that *B. subtilis* uses to facilitate initiation control at the onset of sporulation (26, 57, 58). The specific proteins and their respective regulatory activities are explained further below. Generally, these sporulation-specific DnaA regulators perform the critical function of preventing new rounds of replication prior to sporulation. This regulatory activity ensures that there are only two chromosomes – one which will go to the mother cell, and the other which goes to the spore. *B. subtilis* DnaA regulators that modulate DnaA binding to *oriC* during vegetative growth and prior to sporulation are listed in **Table 1.2** and explained in further detail in subsequent sections.

DnaA Regulator	Type of Regulator	Timing of initiation control
YabA	Negative	Vegetative Growth
DnaD	Negative	Vegetative Growth
SirA	Negative	Onset of Sporulation
Monomeric Soj	Negative	Onset of Sporulation
Dimeric Soj	Positive	Onset of Sporulation

Table 1.2 Summary of *Bacillus subtilis* DnaA regulators.

YabA

YabA is conserved in Gram-positive bacteria with low (G+C) content (59). It was first predicted to act as a regulator of replication initiation through a yeast two-hybrid screen performed in *B. subtilis*, showing that YabA interacts with the replisome proteins DnaA and DnaN (59). Following this screen, further work was performed, characterizing YabA as a negative regulator of replication initiation during vegetative growth. YabA interacts with domain III of DnaA, which is important for DNA binding, ATP hydrolysis and DnaA oligomerization. Through this interaction, YabA prevents cooperative DnaA binding at *oriC*, and controls replication initiation frequency during vegetative growth (31, 60). YabA associates with *oriC* and other DnaA binding regions – and this association is dependent on DnaA (60). An illustration of DnaA control by YabA is depicted in **Figure 1.4**.

Another mechanism by which YabA has been proposed to regulate DnaA activity is through tethering DnaA to the replisome (61). YabA forms a complex with DnaA and the β-clamp protein, DnaN, sequestering DnaA away from the origin (61). DnaA accumulates at the origin of replication when the replisome is assembling or disassembling, and colocalizes with the replisome during the rest of the cell cycle (61). Based on these findings, it was proposed that DnaA sequestration through replisome association may be important for preventing premature replication initiation. However, following this work, the Grossman lab showed that when DnaN is over-expressed (~3.5 fold), DnaA enrichment at *oriC* increases, and YabA enrichment at *oriC* decreases *in vivo* (60). These results indicate that DnaN-YabA interactions inhibit initiation by sequestering YabA (rather than DnaA) from the origin (60).

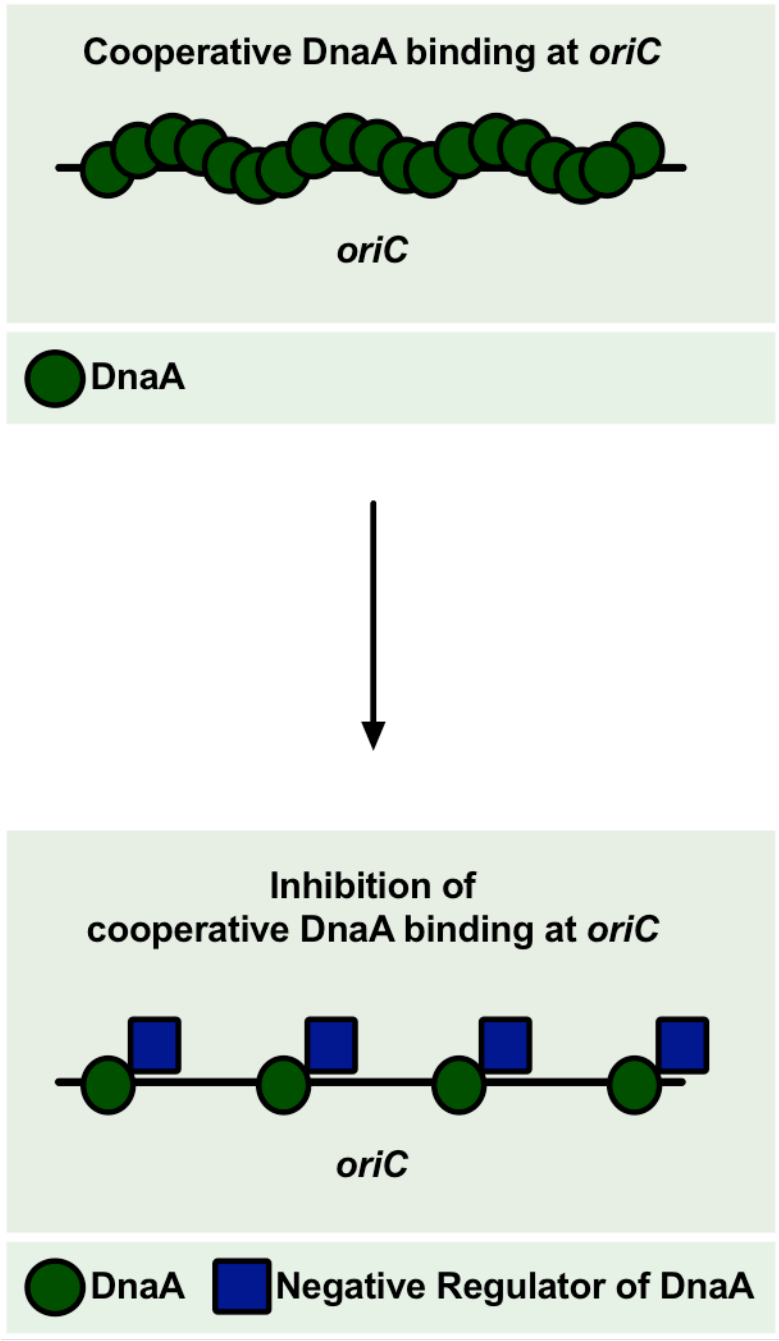

Figure 1.4 Negative regulators of DnaA (YabA, DnaD and SirA) inhibit replication initiation by interacting with DnaA and preventing cooperative DnaA binding at *oriC*.

DnaD

B. subtilis DnaD is required for loading of the replicative helicase, DnaC, at *oriC* during replication initiation, and at stalled replication forks during replication restart. In addition to its function as a helicase loader, DnaD also plays a role in regulation of replication initiation. Specifically, DnaD acts as a negative regulator of DnaA by interacting with domain III of DnaA at *oriC* (62) and at other DnaA binding sites along the chromosome (63). The association of DnaD with these DnaA binding sites is dependent on DnaA (12, 63). Through its recruitment, DnaD inhibits cooperative DnaA binding to these regions (31, 51) and decreases the dissociation constant (K_d) of DnaA to DNA (51). An illustration showing how DnaD inhibits DnaA binding at *oriC* is displayed in **Figure 1.4**.

SirA

SirA is a sporulation-induced protein (57) that inhibits replication initiation (18, 20, 27) and facilitates proper chromosome segregation at the onset of sporulation (33). Under these conditions, SirA negatively regulates DnaA and inhibits replication initiation (18, 20, 27). Specifically, SirA binds to three residues on the surface of domain 1 of DnaA (26), a region required for DnaA dimerization. This interaction prevents cooperative DnaA binding to *oriC* (26). An overview of how SirA inhibits DnaA at the onset of sporulation is illustrated in **Figure 1.4**. In addition to its role in preventing replication initiation during sporulation, SirA works in the same pathway as Soj to facilitate *oriC* segregation at the start of sporulation (33, 58). SirA and Soj both interact with domain III of DnaA for *oriC* capture (33).

Soj

Soj is both an activator and inhibitor of replication initiation. This is dependent on whether it is in its monomeric or dimeric form. As an ATP-bound dimer, Soj binds to DNA and acts as an activator of DnaA (64). Whereas, monomeric Soj is an inhibitor of DnaA (64) – it prevents DnaA oligomerization *in vitro* and *in vivo* (65). In this form, Soj binds to the AAA+ ATPase domain of DnaA and prevents DnaA helix assembly at *oriC* at the onset of sporulation (65). The two mechanisms by which Soj regulates DnaA are illustrated in **Figure 1.5**. Spo0A regulates Soj activity by influencing its conformation. Specifically, Spo0A inhibits Soj dimerization through catalyzing DnaA ATPase activity (64). An additional function of Soj is that it works in the same pathway as SirA to facilitate *oriC* segregation at the start of sporulation (33, 58).

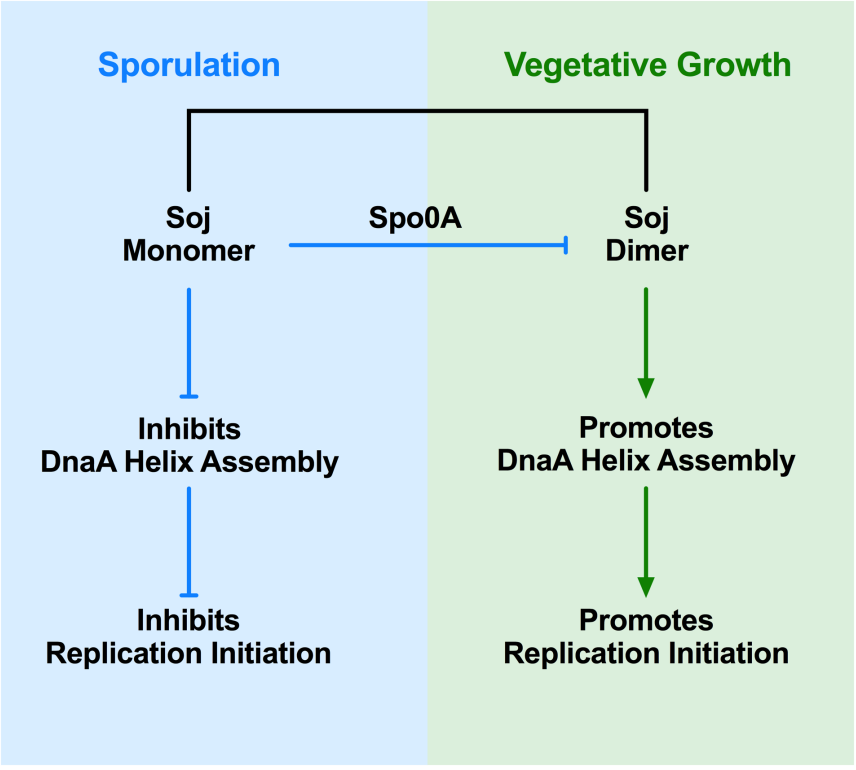

Figure 1.5 Overview of the regulation of replication initiation by monomeric and dimeric Soj in *B. subtilis*.

DnaA-ATP Hydrolysis

The levels of DnaA-ATP and DnaA-ADP are important for regulating replication initiation – as the ATP bound form is required for initiation to occur (36). In *E. coli*, there are various DnaA regulators that promote DnaA-ATP hydrolysis in order to deplete the DnaA-ATP pools and reduce the frequency of replication initiation (53, 66). However, in *B. subtilis*, where nucleotide exchange occurs rapidly without the aid of accessory proteins, analogous regulatory mechanisms have not been described. Furthermore, the basal rate of DnaA nucleotide exchange in *B. subtilis* is essentially the same as the stimulated rate of nucleotide exchange for DnaA in *E. coli* (51, 54).

1.3 Elongation of DNA Replication in *Bacillus subtilis*

Replication fidelity and mutagenesis

Faithful transfer of genetic information to daughter cells is important for bacterial fitness. However, generating genetic diversity is essential for adaptation to new environments and for survival of bacterial species over time. Cells must balance these two contradictory requirements. They are able to achieve this equilibrium through their many redundant mechanisms that work together to reduce replication errors and repair spontaneous chromosomal mutations, and through tightly regulating processes that introduce mutations into the genome.

In order to ensure faithful transfer of genetic information, bacteria use high fidelity DNA polymerases with proofreading functions, and employ back-up mechanisms that fix mistakes made during DNA replication (67). The overall error rate of bacterial DNA replication is very low (67–69). In *E. coli* it is estimated to be as low as 1 mistake per 10^{10} bases inserted (67). The greatest contribution to this low mutation rate is the highly accurate base selection of replicative polymerases, followed by their back-up proofreading functions which immediately correct most mistakes made during replication. In *E. coli*, it is estimated that high-fidelity polymerases make a

single error for every 10^4 – 10^6 bases inserted, and proofreading functions can fix as many as 99.9% of the mistakes made during base selection, further reducing DNA replication error rates 1,000 fold (69). Mismatch repair further reduces the errors made 100-fold, through operating behind the replication forks and fixing most of the mistakes not left unresolved by proofreading (70). Additionally, DNA repair proteins scan the chromosome, working independently of DNA replication to ensure that DNA damage from endogenous and exogenous sources are repaired before they lead to fixed chromosomal mutations that will be passed on to daughter cells. As described above, there are many redundant pathways cells use to ensure the faithful transfer of genetic material to daughter cells. Mutations do get passed on, however, and the genetic variation that results from these mutations is required for the fitness of bacterial populations over time. Furthermore, despite having low base-line rates of mutagenesis, under certain conditions, bacteria increase their mutation rates.

A common way bacteria are able to adapt to stressful environmental conditions is through inducing mutagenic pathways (71–73). These error-prone mechanisms are highly regulated to prevent uncontrolled mutagenesis. Stress-induced mutagenesis is tightly controlled by several master regulators that are often redundant and can be activated during nutrient deprivation and antibiotic treatment, upon heat or cold shock, and when cells must respond to extensive DNA damage (71). Important, widely conserved bacterial stress-response regulators and pathways will be described below.

In *E. coli* and many proteobacteria, the alternative sigma factor RpoS plays a key role in dealing with changes to various environmental conditions (74). RpoS is activated in response to nutrient starvation, growth-rate reduction, and changes in osmotic pressure, pH, and temperature (71). Upon activation, RpoS induces expression of various repair proteins and translesion synthesis (TLS) polymerases (75, 76). In order to survive in the presence of bulky DNA lesions, cells must employ specific TLS polymerases, which are unique in their ability to replicate past

these regions but are also highly mutagenic (76). These TLS polymerases will be re-visited in more detail below, in the section “Translesion Synthesis Polymerases.”

A well-studied mechanism bacteria use to deal with DNA damage is the SOS response (77). Much of what we know about this process comes from more than 50 years of research in the model organism, *E. coli* (78). The SOS response is coordinated by the recombination protein, RecA, which induces expression of genes repressed by the transcriptional regulator, LexA (78). Upon RecA nucleoprotein filamentation, there is self-cleavage of the LexA repressor (79, 80), leading to induction of SOS-regulated genes (81), which are involved in DNA repair (recombination and nucleotide excision repair), as well as TLS polymerases that allow for mutagenic lesion bypass during DNA replication (82). Expression of these genes allows cells to tolerate extensive DNA damage. This response also leads to DNA-damage-induced mutagenesis.

Alarmones are also important for introducing genetic variability under stress-conditions (71). An example of this found in many bacteria, is the second messenger, small nucleotide guanosine tetraphosphate, ppGpp (83, 84). This second messenger is produced under various kinds of nutrient starvation (85) as well as heat shock (86). Upon increased production of ppGpp, there are global changes in gene expression. Depending on the organism, these changes can be a result of its direct interactions with the β’ and ω subunits of RNA polymerase (RNAP), or through changes in guanosine triphosphate concentrations (83). In addition to directly binding and modifying the activity of RNAP, ppGpp can bind to and alter various other proteins, including: cellular GTPases, proteins involved in nucleotide metabolism and lipid metabolism, metabolic proteins, and PLP-dependent basic aliphatic amino acid decarboxylases (87). Based on the range of intracellular ppGpp concentrations under normal growth conditions and upon induction of this signal, and the inhibition constants of ppGpp for these protein targets, it is thought that ppGpp mediated protein inhibition is likely transient and reversible (87).

Another mechanism by which bacteria drive evolution is through genome organization. The majority of genes are encoded on the leading strand in bacteria (88). This orientation bias is

greater for highly transcribed and essential genes, ranging from 75% to 95% across different bacterial species (89–91). And even more striking: 100% of rRNA genes are co-oriented with replication (90, 92–94). Gene orientation has consequences on the severity of collisions between DNA replication and transcription – and this can determine base-line rates of mutagenesis (89). This will be further explained in the next two sections.

Replication-Transcription Conflicts

There are many obstacles to replication fork progression. These include: bulky DNA lesions, DNA-binding proteins, DNA/RNA secondary structures, and transcription machinery. Replication and transcription are happening at the same time, on the same template. This is illustrated in **Figure 1.6**. Without either spatial or temporal separation for these two processes, collisions occur between replication and transcription machineries, which we refer to as "replication-transcription conflicts (95)."

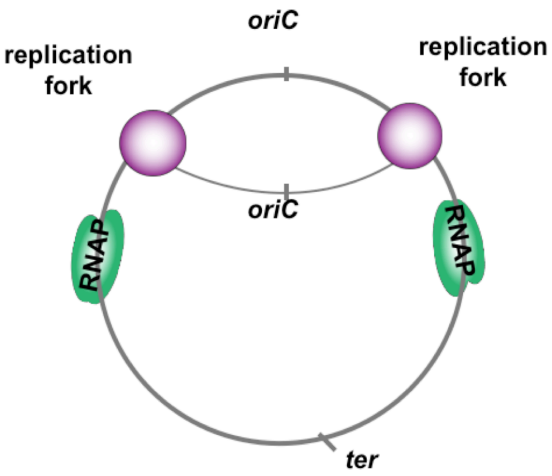

Figure 1.6 DNA replication and transcription occur at the same time, on the same DNA template.

There are two types of replication-transcription conflicts. Co-directional conflicts occur when replication forks collide with transcription of genes encoded on the leading strand, whereas head-on conflicts occur when replication forks collide with transcription of genes encoded on the lagging strand. These two kinds of conflicts are illustrated in **Figure 1.7**. Both types of replication-transcription conflicts result in replisome stalling and genomic instability (95–97). However, the two orientations lead to different consequences for cells. Co-directional conflicts cause replisome

stalling and replication restart (96). Head-on conflicts also lead to these outcomes; however, the consequences of head-on conflicts are much more severe (98), and include: more severe replisome stalling and disassembly (99), single-strand and double-strand DNA breaks (97), insertions and deletions (100), and increased mutagenesis (89, 101, 102).

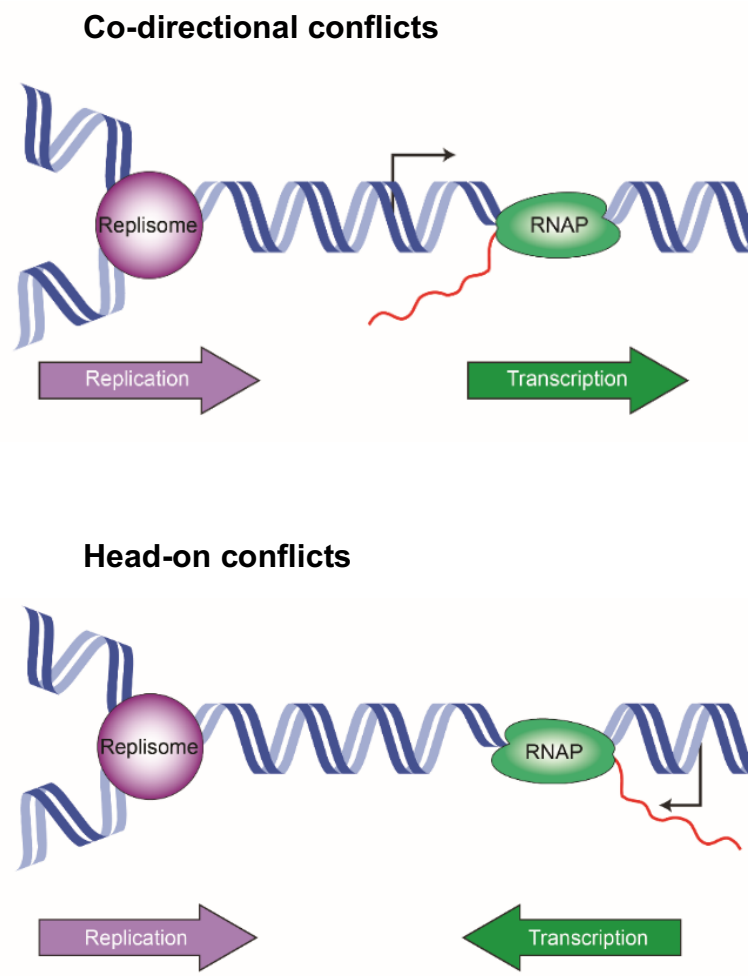

Figure 1.7 Head-on and co-directional replication-transcription conflicts. Head-on conflicts occur when transcription is on the lagging strand. Co-directional conflicts result from transcription on the leading strand.

Bacteria have many different conflict resolution factors, which they rely on to survive these events (103). Conflict resolution factors identified in *E. coli* include the small nucleotide guanosine tetraphosphate ppGpp, which prevents RNAP from blocking replication at DNA lesions (104), transcription factors like the Gre proteins and DksA which remove transcriptional barriers to DNA replication (104, 105), helicase proteins like DinG which can unwind r-loops *in vitro* (106), and the helicase Rho which works together with the Rho cofactors NusA and NusG as transcriptional terminators (107). In *B. subtilis*, known conflict resolution factors include the accessory helicase PcrA (108) and RNAse HIII (101). Additionally, bacterial genomes are organized such that for the majority of genes, transcription and replication are co-oriented, reducing the frequency of more detrimental head-on conflicts (88). This is illustrated in **Figure 1.8**.

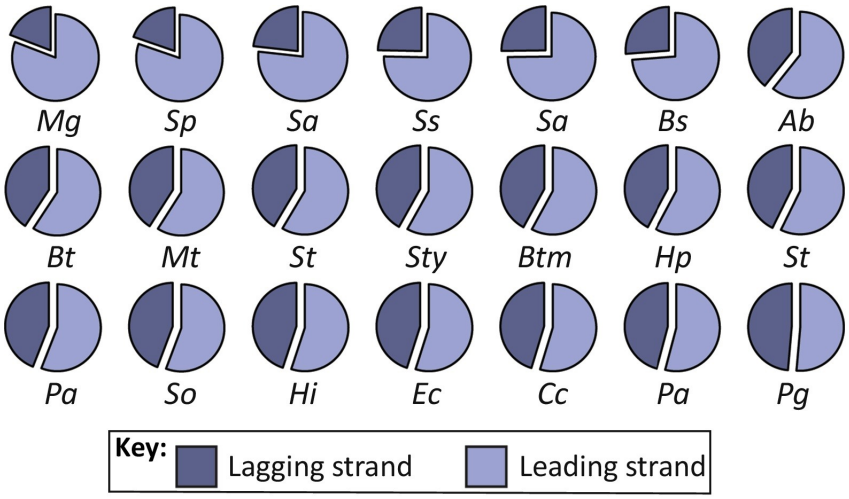

Figure 1.8. Genome orientation bias across different bacterial species. The light purple represents the proportion of genes encoded on the leading strand, that are co-oriented with replication. The dark purple represents the proportion of genes encoded on the lagging strand, that are head-on to replication. While the genome orientation bias varies among the different bacteria presented, in all of these species there are more genes encoded on the leading strand. Top row: *Mg*: *Mycoplasma genitalium* G37 (80.8%); *Sp*: *Streptococcus pneumoniae* TIGR4 (80.3%); *Sa*: *Staphylococcus aureus* NCTC 8325 (76.8%); *Ss*: *Streptococcus sanguinis* SK36 (75.3%); *Sa*: *Staphylococcus aureus* N315 (74.8%); *Bs*: *Bacillus subtilis* 168 (73.8%); *Ab*: *Acinitobacter baylyi* ADP1 (60.7%). Middle row: *Bt*: *Burkholderia thailandensis* E264 (59.3%); *Mt*: *Mycobacterium tuberculosis* H37Rv (59.0%); *St*: *Salmonella enterica serovar* Typhimurium Ty2 (58.6%); *Sty*: *Salmonella enterica* serovar Typhi Ty2 (58.1%); *Btm*: *Bacteroides thetaiotaomicron* VPI-5482 (58.0%); *Hp*: *Helicobacter pylori* 26695 (57.8%); *St*: *Salmonella enterica* serovar Typhimurium 14028S (57.3%). Bottom row: *Pa*: *Pseudomonas aeruginosa* PA01 (55.9%); *So*: *Shewanella oneidensis* MR-1 (55.7%); *Hi*: *Haemophilus influenzae* Rd KW20 (55.0%); *Ec*: *Escherichia coli* K-12 MG1655 (54.9%); *Cc*: *Caulobacter crescentus* NA1000 (54.7%); *Pa*: *Pseudomonas aeruginosa* UCBPP-PA14 (54.1%); *Pg*: *Porphyromonas gingivalis* ATCC 33277 (51.4%). This figure is taken from Merrikh H. *Trends Microbiol* (2017) (88).

Accelerated Evolution of Highly Transcribed Genes

Targeted mutagenesis of highly transcribed genes is an important mechanism by which bacteria selectively drive evolution (88, 89). Our lab has shown that mutation rates increase in a transcription-dependent manner by a factor of 2 to 4 fold (89, 109). There are various factors that contribute to genomic instability at highly transcribed genes. One example of this is the accumulation of RNA-DNA hybrids at these regions. These highly stable structures expose single-stranded DNA that is more prone to DNA damage. Our lab has recently shown that in the absence of factors that remove these hybrids, cells have higher rates of mutagenesis at highly transcribed genes (101). Additionally, recent work by our lab as well as other groups has shown that transcription-coupled nucleotide excision repair (TC-NER) is mutagenic (109–112). The mechanism for this is still largely unknown however and requires further investigation.

Transcription-Coupled Nucleotide Excision Repair

Mfd is a highly conserved bacterial DNA repair protein that promotes mutagenesis through its involvement in transcription-coupled nucleotide excision repair (TC-NER). TC-NER is initiated when RNA polymerase (RNAP) encounters DNA lesions, which inhibit its progression (113–115). To repair these lesions and allow for continued transcription and replication past these sites, RNAP must first be removed. Mfd pushes stalled RNAP off of DNA in an ATP-dependent manner (113), allowing for recruitment of transcription-coupled DNA repair proteins UvrA and UvrB. Upon displacement of RNAP by Mfd, UvrA binds the lesion, UvrB recruits UvrC, and UvrC makes an incision at the lesion site. The helicase protein, UvrD, then removes the excised DNA, and the gap is filled and ligated. Recent work has shown that this DNA repair pathway is mutagenic (110–112). Despite numerous reports that Mfd-mediated repair is mutagenic (110–112), why this repair pathway is error-prone is not well understood. It has been well-established through both *in vitro* and *in vivo* work that Pol I is involved in TC-NER (112, 116, 117). However, how gap filling by a

high-fidelity polymerase, like Pol I, might promote mutagenesis is not clear. We have performed preliminary experiments that indicate Pol I may be introducing mutations during TC-NER through acting in concert with translesion synthesis polymerases.

Translesion Synthesis Polymerases

Bacterial cells are constantly exposed to endogenous and exogenous sources of DNA damage. To counteract this, they have many DNA repair pathways. However, despite having systems in place to fix DNA damage, replication forks can encounter DNA lesions prior to their repair. The main replicative polymerases are unable to replicate past some of these regions. This leads to replisome stalling. In order to replicate past bulky lesions, cells employ the use of translesion synthesis (TLS) polymerases (118, 119). In all domains of life, Y-family polymerases are important for TLS activity (120). TLS polymerases are able to take over and replicate a short patch of DNA, past the lesion, switching places with the main replicative polymerases (121). A schematic showing this process, including: stalled replisomes at a lesion, polymerase switching, and TLS polymerase lesion bypass is shown in **Figure 1.9**.

Translesion synthesis is often error-prone. This is in large part because TLS polymerases lack 3' → 5' exonuclease activity (proofreading functions) (122). They also misincorporate bases at a greater frequency than main replicative polymerases do. On undamaged DNA templates their misincorporation rate is between 10^3 - 10^5, which is roughly 10-fold higher (123). This is because 1) the structure of the little finger domain and active site allows for mismatches to be made (124) and 2) they are often acting on damaged templates and bulky adducts (118). TLS polymerase activity is important for introducing genetic variability within bacterial populations, a process that is essential for maintaining evolutionary fitness (118). However, these polymerases are tightly controlled to prevent excess activity on non-damaged templates where they can also introduce

mutations. As previously described, TLS polymerases are induced under conditions of excess DNA damage and stress, by the SOS-response and the transcription factor RpoS.

Research on TLS polymerase activity in *B. subtilis* by our lab as well as other groups indicate that these polymerases are contributing to transcription-associated mutagenesis (109, 125). Additionally, at least in *B. subtilis*, it appears that the increased mutation rates associated with TLS polymerases is dependent on DNA polymerase I activity (126). This will be further explained in **Chapter 3**.

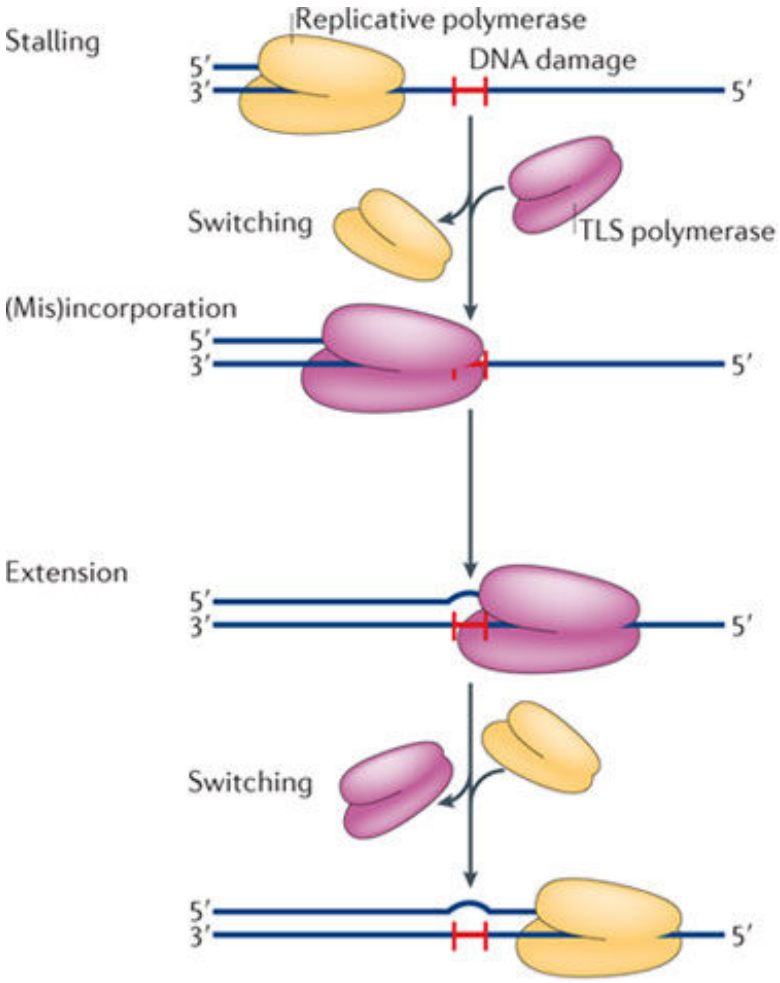

Figure 1.9 Model for polymerase switching and trans-lesion synthesis past bulky lesions. The replicative polymerase (yellow) is unable to replicate past bulky lesions (depicted here by the red "H") – leading to stalling of the replisome. Upon replisome stalling, the TLS polymerase (purple) is recruited to these sites and replaces the replicative polymerase via polymerase switching. TLS polymerases have large active sites that allow them to replicate past these regions and incorporate nucleotides opposite of the lesion. Unlike processive replicative polymerases, TLS polymerases are distributive and dissociate after replicating a short patch of DNA. This allows for a second polymerase switching event, where the replicative polymerase can re-associate with the β-clamp and continue replicating the DNA. This image was taken from Sale JE *et al*, Nature Reviews, 2012 (121).

1.4 Role of DNA topology in DNA replication

DNA topology is critical for all stages of DNA replication – initiation, elongation, and termination. In order for DNA replication to initiate and proceed *in vitro*, the replication machinery requires a negatively supercoiled template (127–131). In addition, DNA replication induces changes in DNA topology both behind and in front of the replication machineries, which introduces impediments to DNA replication progression and termination. Chromosomal DNA becomes over-twisted (positively supercoiled) ahead of the replication forks, causing torsional strain that must be resolved for DNA replication to proceed (132). There is also positive supercoiling generated in the already replicated region which must be resolved to prevent catenation of the chromosomal DNA and to allow for proper segregation of daughter chromosomes upon termination of DNA replication (132). Gyrase activity and transcription also promote under-twisting of DNA (negative supercoiling). Supercoiling generated ahead of and behind of the replisome and RNA polymerase are illustrated in **Figure 1.10**. Many of the topological problems that arise from these processes are resolved by winding solutions (133). This is achieved through the actions of enzymes called topoisomerases (132).

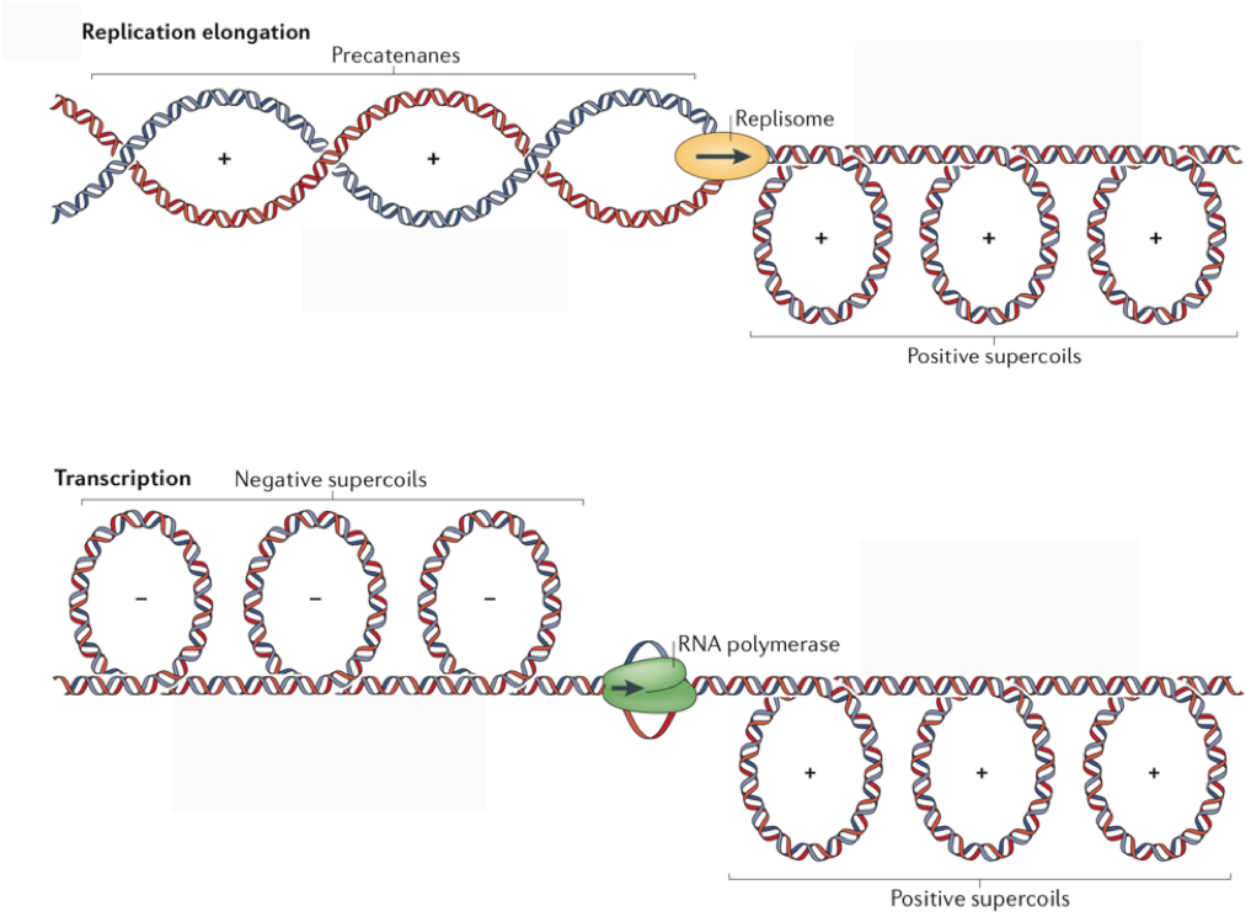

Figure 1.10 Supercoiling generated ahead of and behind of the replisome and RNA polymerase. This image was modified from Vos SM et al, Nature Reviews, 2011 (132). The top panel shows the supercoiling structures that form on either side of the replisome during DNA replication. Positive supercoiling is generated in front of and behind the replication machinery. Positive supercoiling behind the replisome must be resolved to prevent catenated DNA. The bottom panel shows how positive and negative supercoiling form ahead and behind of RNA polymerase during transcription.

1.5 Chromosomal DNA Supercoiling and Topoisomerases

Chromosomal DNA presents many topological challenges to DNA replication. Double-stranded DNA must be melted and separated to create an appropriate template for the replisome to assemble on and copy the DNA. Following this, replicative helicases are needed to unwind the DNA in front of replication forks, and this unwinding activity creates topological changes. The resulting positive supercoils and precatenated DNA structures must be resolved by topoisomerases in order for replication to proceed and for proper chromosome segregation during cell division (134, 135).

Bacteria use various enzymes called topoisomerases to maintain the proper topological status required for DNA replication (136). Topoisomerases alter DNA structures by transiently cleaving the phosphodiester backbone of DNA, passing DNA through the breaks formed, and re-sealing the DNA. All DNA topoisomerases can be divided into one of the following two classes: type I and type II topoisomerases, based on whether they catalyze single-stranded or double-stranded breaks, respectively (132). Topoisomerases each perform different cellular roles and preferentially act on different substrates. The details of how, what, and when topoisomerase I, gyrase, and topoisomerase IV act are described below. This is not a comprehensive review of all topoisomerases, but rather the topoisomerases that have been studied by us and other groups in the context of regulation of replication initiation in *E. coli* and *B. subtilis*.

Topoisomerase I is a conserved type I topoisomerase which relaxes negative supercoiling (137). Topoisomerase I binds to single-stranded DNA near double-stranded DNA. This enzyme directly interacts with RNA polymerase (138) and relieves negative supercoiling generated behind RNA polymerase during transcription (139). This activity is critical for reducing RNA:DNA hybrids at regions of negative supercoiling (140). Topoisomerase I can also alleviate negative supercoiling generated by gyrase (how gyrase introduces negative supercoiling will be discussed

further below) (141). The first major indication that topoisomerase I may be important for reducing supercoiling *in vivo* was that in *E. coli*, *topA* (topoisomerase I) deletion mutants accumulate compensatory mutations in *gyrA* and *gyrB*, the genes that encode for DNA gyrase (142). When these compensatory mutations are introduced into wild-type cells, DNA gyrase activity is attenuated, resulting in the reduction in global supercoiling levels (143).

Bacteria have two essential type II topoisomerases – DNA gyrase and topoisomerase IV (144). These enzymes control DNA topology and are required for all stages of DNA replication (136). The way type II topoisomerases alter DNA topology is by forming double-stranded DNA breaks, passing duplex DNA through these breaks, and then re-sealing the breaks (144). This mechanism of action is illustrated in **Figure 1.11**. Despite their similar amino acid sequences, and seemingly redundant activities – DNA gyrase and topoisomerase IV play distinct roles – each displaying different activities in cells, with different affinities for the various DNA templates found in cells (144–146). Gyrase relaxes positively supercoiled DNA and actively introduces negative supercoils (147). These reactions are required for replication to initiate (127–131, 148) and to resolve excess positive supercoiling generated in front of replication forks during replication elongation (149, 150). Whereas topoisomerase IV can relax positive and negative supercoils (151). Topoisomerase IV has a preference for acting on positively supercoiled (152), and catenated DNA structures (134) – the latter of which is required for unlinking of daughter chromosomes upon termination of DNA replication (153).

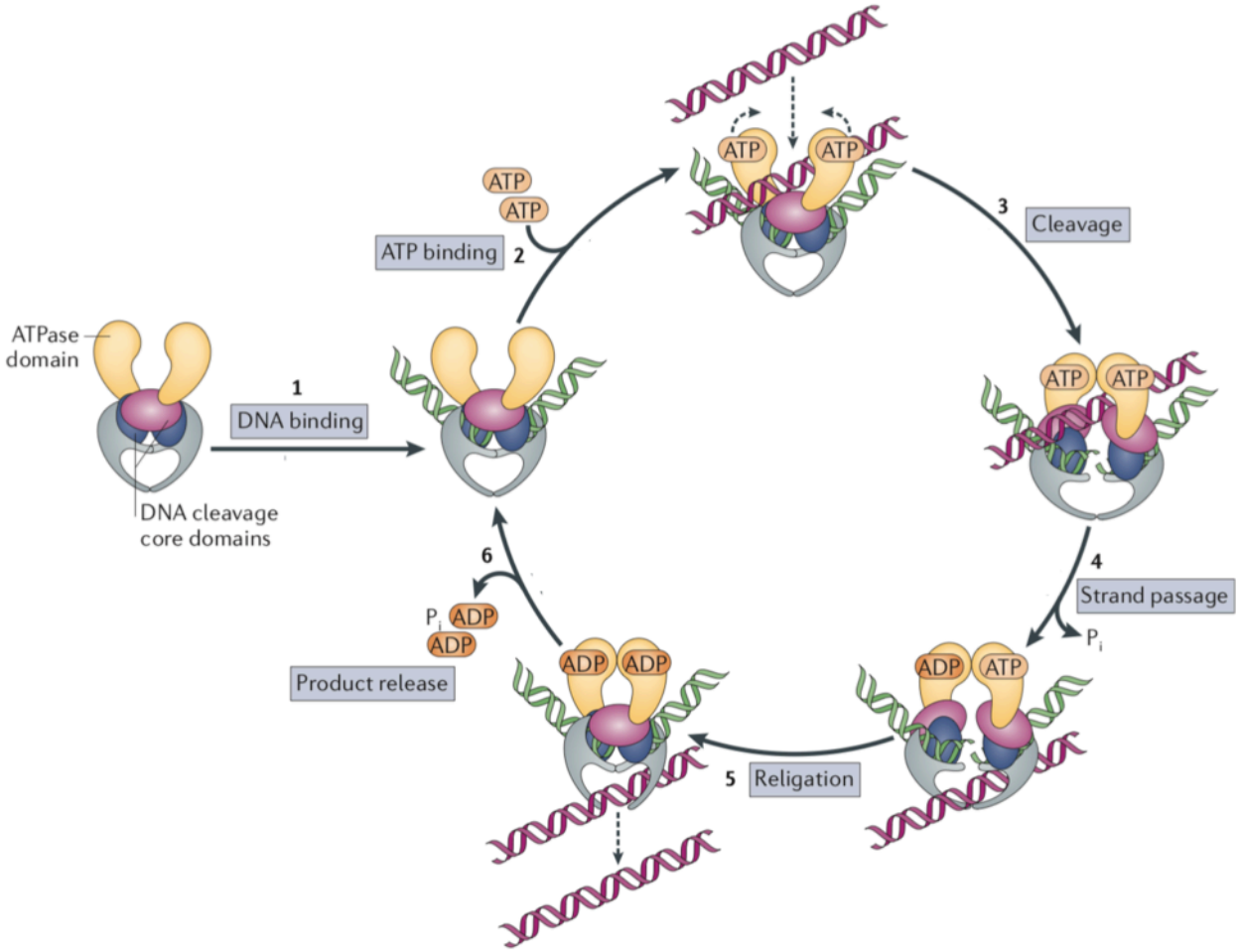

Figure 1.11 Mechanism of action of type II topoisomerases. This image was modified from Vos SM et al, Nature Reviews, 2011 (132). Type II topoisomerases first bind to one duplex DNA segment (shown in green). Following this, they associate with a second duplex DNA segment (shown in purple). ATP-binding stimulates a DNA cleavage reaction, where a double stranded break is made in the bound duplex DNA segment. The second DNA duplex that is associated with the complex can then pass through the opening made in the first DNA duplex. The broken DNA is religated and the DNA products are released from the complex.

CHAPTER 2.

DNA gyrase activity regulates DnaA-dependent replication initiation in *Bacillus subtilis*

Originally published as an article in *Molecular Microbiology*.

Samadpour, A. N. and Merrikh, H. (2018), DNA gyrase activity regulates DnaA-dependent replication initiation in *Bacillus subtilis*. Molecular Microbiology. doi:10.1111/mmi.13920

Summary

In bacteria, initiation of DNA replication requires the DnaA protein. Regulation of DnaA association and activity at the origin of replication, *oriC*, is the predominant mechanism of replication initiation control. One key feature known to be generally important for replication is DNA topology. Although there have been some suggestions that topology may impact replication initiation, whether this mechanism regulates DnaA-mediated replication initiation is unclear. We found that the essential topoisomerase, DNA gyrase, is required for both proper binding of DnaA to *oriC* as well as control of initiation frequency in *Bacillus subtilis*. Furthermore, we found that the regulatory activity of gyrase in initiation is specific to DnaA and *oriC*. Cells initiating replication from a DnaA-independent origin, *oriN*, are largely resistant to gyrase inhibition by novobiocin, even at concentrations that compromise survival by up to four orders of magnitude in *oriC* cells. Furthermore, inhibition of gyrase does not impact initiation frequency in *oriN* cells. Additionally, deletion or overexpression of the DnaA regulator, YabA, significantly modulates sensitivity to gyrase inhibition, but only in *oriC* and not *oriN* cells. We propose that gyrase is a negative regulator of DnaA-dependent replication initiation from *oriC*, and that this regulatory mechanism is required for cell survival.

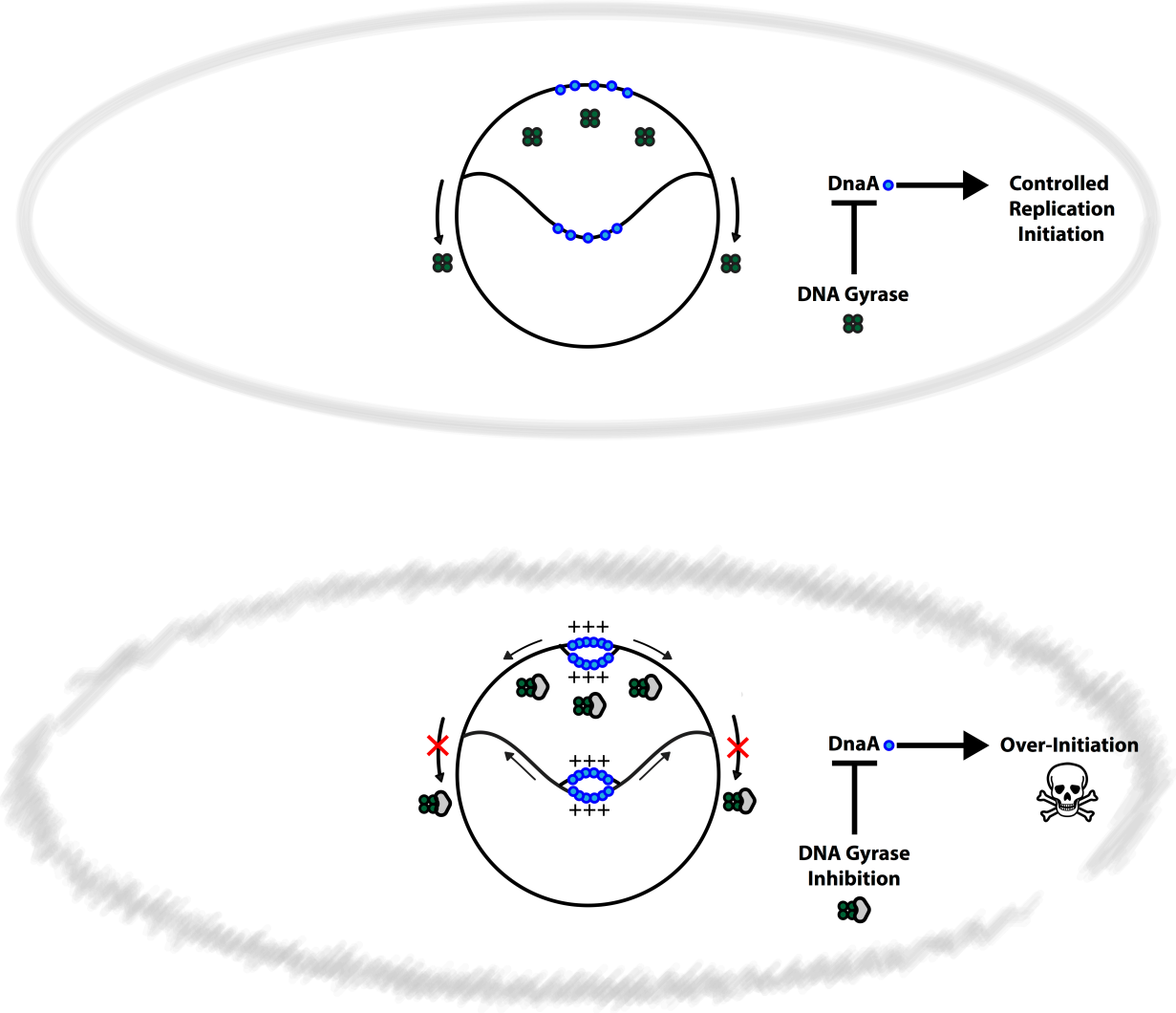

Figure 2.1. Model for control of DnaA-dependent replication initiation by DNA gyrase. DNA gyrase controls replication initiation by inhibiting DnaA binding and activity at the origin of replication, *oriC*. Inhibition of gyrase increases replication initiation frequency and DnaA association with *oriC*, and is harmful to cell survival if replication initiates from *oriC*. We propose a model where modulation of DNA topology by gyrase regulates replication initiation at an early step during orisome assembly.

Introduction

DNA replication is an essential process in all organisms. In bacteria, replication initiates from a single origin of replication, *oriC*, and proceeds bi-directionally until the replication forks reach the terminus, *ter* (154). Replication initiation from *oriC* depends on ordered binding of the replication initiation protein, DnaA, to specific 9-mer consensus sequences (8–10). Oligomerization and cooperative binding of DnaA leads to the melting of the origin at the DNA unwinding element (DUE), and subsequent replisome assembly. Regulation of replication is important for proper cell proliferation and generally occurs at the initiation step through modulation of DnaA binding and activity (44, 55, 56)

The regulatory mechanisms for DnaA association and function with *oriC* in *Bacillus subtilis* and other Gram-positive bacteria are generally different than in Gram-negatives. For example, key regulators of initiation in *B. subtilis* include YabA and SirA, which are not found in *Escherichia coli* (26, 27, 30, 44). Additionally, the mechanism of DnaA regulation is different in *B. subtilis* compared with *E. coli*: YabA disrupts oligomerization and cooperative binding of DnaA to the origin and this type of regulatory mechanism has not been reported for the key *E. coli* initiation regulators such as Hda, SeqA or Dam (44). YabA has also been proposed to sequester DnaA at the replication forks (61).

One critical factor in replication initiation and progression is DNA topology (56, 131, 155). Much of what is known regarding the role of supercoiling in bacterial replication comes from in vitro studies that use plasmid-based systems and proteins purified from *E. coli* (127–131, 148). These studies have established that a negatively supercoiled DNA template is required for replication initiation by DnaA from *oriC* in these reconstituted systems (127–131, 148). Furthermore, *in vitro*, supercoiling can enhance association of *Helicobacter pylori* and *E. coli* DnaA to certain consensus sites at *oriC* (49, 156), and *Aquifex aeolicus* ATP-DnaA oligomerization has been shown to induce positive DNA supercoils (157). In agreement with this,

transcription-induced negative supercoiling near *oriC* activates replication initiation in *E. coli* (158, 159). However, although these studies suggest a role for topology in DnaA association and replisome assembly at the origin for these particular Gram-negative bacteria, whether changes in DNA superhelicity regulate replication timing or frequency *in vivo* or for Gram-positives is unclear.

In vitro, the type II topoisomerase DNA gyrase has been utilized to obtain the necessary supercoiling status for replication reactions to initiate and progress (127–131, 148). Other processes affect DNA topology as well – including DNA replication and transcription (160). Without gyrase, which regulates DNA topology by introducing negative supercoils and relieving excess positive supercoils ahead of replication forks (147, 149), replication cannot proceed (144, 161). Furthermore, *in vitro* studies suggest that negative supercoiling at the origin promotes replication initiation and increases DnaA binding (49, 156), although gyrase is not required for open complex formation or helicase loading (13). If these *in vitro*-based models are correct, then upon gyrase inhibition, the rate of replication initiation as well as DnaA binding to the origin should decrease *in vivo*. These predictions have not been thoroughly tested in living cells. Moreover, the few existing in vivo studies of gyrase contradict the predictions from *in vitro* work. For example, recent work from *E. coli* suggest that gyrase promotes ATP hydrolysis by DnaA, at the DnaA sequestration locus, *datA*, which negatively regulates initiation (53). This is in contrast to *in vitro* work, which suggests that gyrase promotes DnaA-dependent initiation. Therefore, though various studies have suggested that gyrase may influence replication initiation, the mechanism and potential role of gyrase as a regulator of DnaA binding or activity at *oriC in vivo* remain to be determined.

We found that gyrase is an essential, negative regulator of replication initiation *in vivo*, in *B. subtilis*. Our data indicate that gyrase activity decreases DnaA association with *oriC* and inhibits replication initiation. The regulatory function of gyrase is specific to DnaA and *oriC*: replication initiation from an ectopic, DnaA-independent origin, *oriN* is unaffected by gyrase activity.

Furthermore, gyrase inhibition is significantly more detrimental to cell survival when replication initiates from *oriC* compared with *oriN*. Lastly, over-expression of the DnaA negative regulator YabA promotes survival of gyrase inhibition. These results suggest that the essentiality of gyrase stems at least partially from a regulatory activity in *oriC* and DnaA-dependent replication initiation.

Results

Inhibition of type II topoisomerases leads to over-initiation.

To test if and how DNA topology impacts replication initiation *in vivo*, we measured the impact of novobiocin on initiation dynamics. Novobiocin is a useful tool for understanding the importance of DNA topology for essential processes, such as DNA replication and transcription (162–165). Gyrase is the primary target of novobiocin. Novobiocin competitively inhibits ATP binding to the GyrB subunit of DNA gyrase, thus inhibiting its enzymatic activity (165–167). The K(i) (inhibition constant) of novobiocin is over four orders of magnitude less than the K(m) (Michaelis constant) for ATP (165). While novobiocin blocks ATP binding to the GyrB subunit of gyrase, there is no known structural similarity between ATP and GyrB (149).

Following the characterization of novobiocin-mediated gyrase inhibition, topoisomerase IV was identified as a secondary target of novobiocin (151, 168). Gyrase subunits (GyrA and GyrB) share extensive sequence homology with topoisomerase IV subunits (ParC and ParE), respectively. As such, just as novobiocin inhibits GyrB-ATP binding, novobiocin inhibits topoisomerase IV by blocking the ATP binding site of ParE (151). Our understanding of these drug-enzyme interactions are based largely on studies performed in *E. coli*. However, novobiocin

demonstrates a high affinity for *B. subtilis* gyrase as well, suggesting that the preferential effect of novobiocin on *B. subtilis* gyrase is likely similar to that of *E. coli* (169).

To assess the role of DNA topology on replication, we determined the marker frequency pattern along the genome for wild-type cells grown in the presence and absence of novobiocin using whole genome sequencing and quantitative PCR (Fig. 2.2 A and B). Using whole genome marker frequency analyses through next generation sequencing, we found that novobiocin increases DNA copy number near *oriC* two-fold, which gradually decreases to levels exhibited by the untreated control samples (Fig. 2.2 A and B), at around 36° and 340° along the chromosome (Fig. 2.2 A). Consistent with our marker frequency analysis, we also observed this reduction in copy-number at 45 and 315 (indicated as '−45' in the figure) degrees by qPCR (Fig. 2.2 B). These data suggest that changes in DNA topology impact replication initiation *in vivo*.

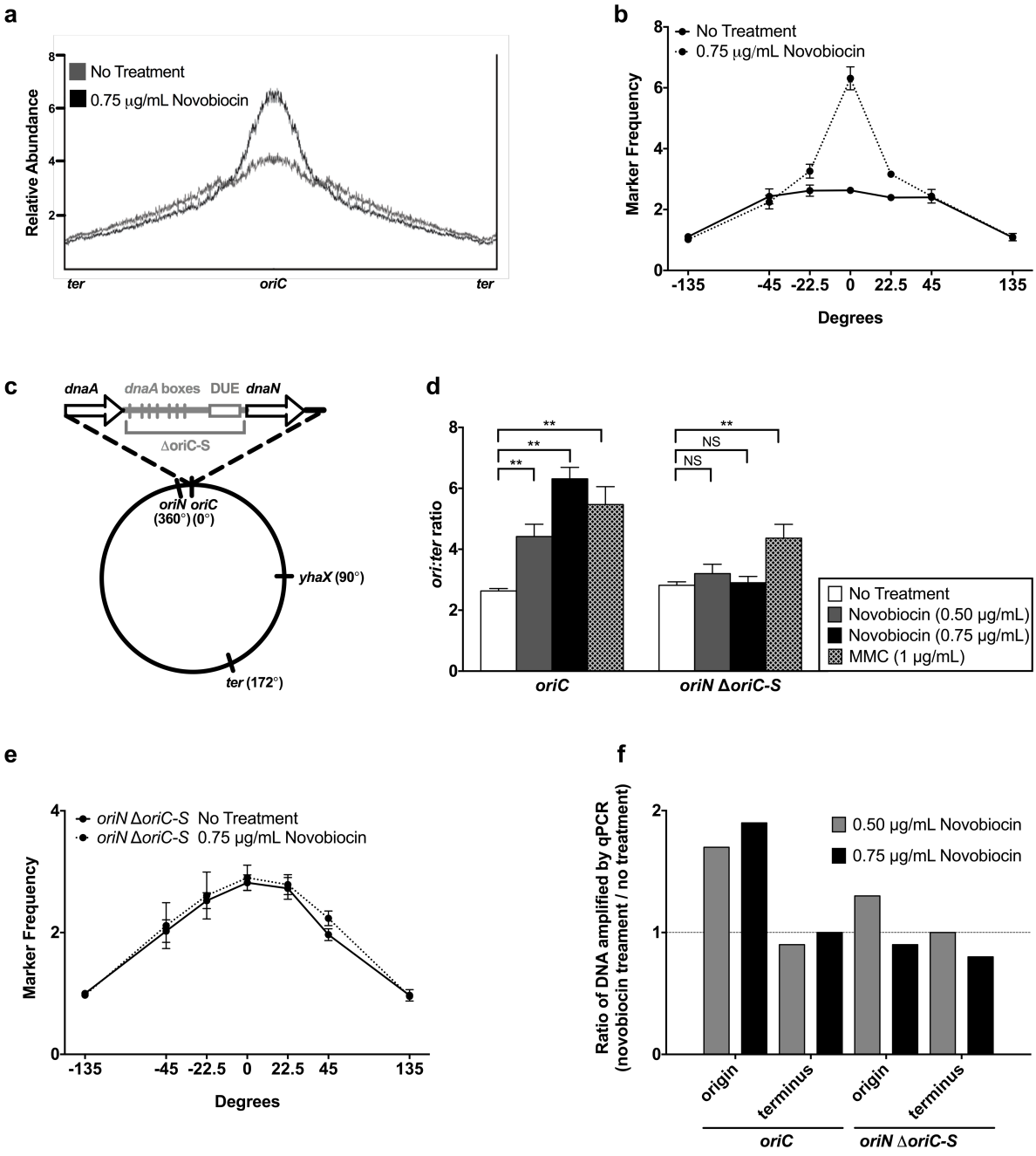

Figure 2.2. Inhibition of type II topoisomerase activity by novobiocin increases *oriC*-dependent replication initiation. A) Marker frequency analysis as measured by deep sequencing for *oriC* cells with no treatment and cells treated with 0.75 μg/mL novobiocin for 40 minutes. The x-axis indicates chromosomal location, and the y-axis represents the abundance of reads relative to the total number of reads in the sequencing library. B) Marker frequency as measured by quantitative

PCR at 0, 45, 135, 225, and 315 degrees along the chromosome for exponential phase *oriC* cultures with no treatment and 0.75 μg/mL novobiocin treatment for 40 minutes. Data shown are averages for at least 9 biological replicates examined on 3 different days. C) *oriN* Δ*oriC-S* mutants initiate replication at *oriN* and have a deletion in the region between *dnaA* and *dnaN*, which includes the DNA unwinding element (DUE) and DnaA binding sites. D) Origin-to-terminus ratios of exponential-phase *oriC* cells increase upon novobiocin and MMC treatment. No effect was observed for *oriN* Δ*oriC-S* cells treated with novobiocin. Origin-to-terminus ratios for *oriN* Δ*oriC-S* cells increase with MMC treatment. Origin-to-terminus ratios of exponential-phase cells grown were grown with no treatment, with 0.50, and 0.75 μg/mL novobiocin, and with 1 μg/mL MMC. Data shown are averages from 6-12 biological replicates. Error bars represent standard error of the mean. Statistical significance was calculated using *t*-test (** $p < 0.01$). E) Marker frequency as measured by quantitative PCR at 0, 45, 135, 225, and 315 degrees along the chromosome for exponential phase *oriN* Δ*oriC-S* cells with no treatment and 0.75 μg/mL novobiocin treatment. Data shown are averages for at least 9 biological replicates. F) For *oriC* cells, but not *oriN* Δ*oriC-S* mutants, treatment with novobiocin increases DNA amplified from the origin, but does not change the amount of DNA amplified from the terminus. Presented here is the ratio of total DNA amplified from the origin and terminus for cultures treated with 0.50 and 0.75 μg/mL novobiocin divided by the amount of DNA amplified from the same regions for cultures without treatment. Absolute levels of DNA used are derived from Cq values from qPCR (raw data). Ratios of DNA amplified for *oriC* cells and *oriN* Δ*oriC-S* mutants are plotted. Data shown are averages from 6-9 biological replicates.

Over-initiation of novobiocin treated cells is specific to *oriC*.

To determine if the impact of novobiocin on replication initiation is specific to cells that undergo DnaA-dependent initiation at *oriC*, we measured the effect of novobiocin on origin-to-terminus ratios for *oriC* cells and *oriN ΔoriC-S* cells that undergo DnaA-independent and

unregulated replication initiation from a heterologous origin, *oriN* (170). *oriN* is the origin of replication used by pLS32, a plasmid present in *Bacillus natto* (a.k.a., hay or grass *Bacillus*) (171, 172). Initiation from *oriN* depends on the initiator protein RepN, which is also expressed in the strains we used in our experiments (Fig. 2.2 C). Both *oriN* and *repN* are integrated at *spoIIIJ* on the chromosome (170). Importantly, the *oriN* strain lacks the DUE region found at *oriC* and thus its replication initiation depends on *oriN* and RepN activity (171, 173) (Fig. 2.2 C).

We measured the ratio of origins to termini upon exposure of cells to increasing concentrations of novobiocin by amplification of *oriC* and *ter* using qPCR. Increased replication initiation generally leads to an increased ratio of origin to terminus DNA. For *oriC* cells, we found that novobiocin treatment increases origin-to-terminus ratios in a dose-dependent manner (Fig. 2.2 D) indicating that cells are over-initiating. In contrast, we did not observe any change in origin-to-terminus ratios in the presence of novobiocin for the *oriN* cells (Fig. 2.2 D). The *oriC* novobiocin phenotype remained the same under slow growth conditions, when cultures were grown in minimal glucose media (Fig. 2.3). Analysis of DNA copy number at several different locations along the genome of the *oriN* cells showed results consistent with this observation: novobiocin did not increase the DNA copy number at any of the loci analyzed around the chromosome (Fig. 2.2 E).

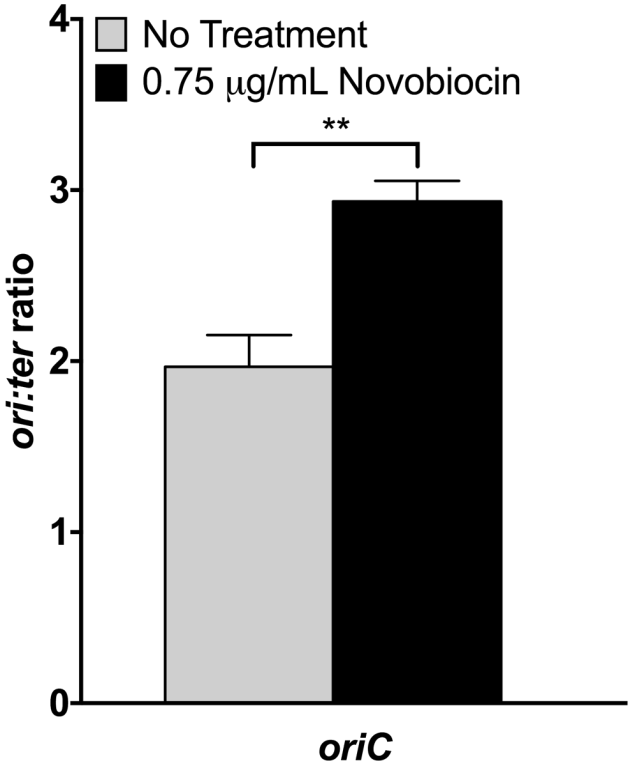

Figure 2.3. Inhibition of gyrase activity increases *oriC*-dependent replication initiation under slow growth conditions. Origin-to-terminus ratios for *oriC* cells grown in minimal glucose media with and without 0.75 μg/mL novobiocin are plotted. Data shown are averages from 3 biological replicates. Error bars represent standard error of the mean. Statistical significance was calculated using *t*-test (**$p<0.01$).

The changes in origin-to-terminus ratios we observed were due to changes in the copy number at *oriC* and not *ter*: (a) the genome-wide marker frequency analysis showed a specific increase in the copy number of origin-proximal DNA (rather than the terminus), and (b) the ratio of total *oriC* DNA, but not *ter* DNA, from the novobiocin treated cells compared with untreated cells was over 1 (Fig. 2.2 F). Furthermore, the increased ratio of origin-proximal DNA was only

detected in *oriC* and not *oriN* cells (Fig. 2.2 F). Together, these results indicate that topoisomerase inhibition by novobiocin impacts replication initiation specifically from *oriC*.

The effect of novobiocin on replication initiation is not due to a general block in replication elongation.

The consensus in the field is that topoisomerase inhibition primarily effects replication elongation. However, the *oriC* specificity of the phenotypes we observed following novobiocin treatment suggests that either gyrase or Topo IV is primarily impacting replication initiation. If inhibition of topoisomerases was primarily affecting replication elongation, then *oriN* cells would also display similar phenotypes to those observed in *oriC* cells given that the elongation complexes (and the chromosome) are the same in both strains. It is formally possible that topoisomerase inhibition does lead to changes in replication elongation and that these changes indirectly modulate initiation from *oriC*. In this scenario, either gyrase or Topo IV would not be primarily acting at the origin, and, other elongation inhibitors would also have an *oriC*-specific effect (there would be over-initiation from *oriC* but not *oriN* upon elongation block through any inhibitor of replication).

To further clarify whether the *oriC*-specific effects of topoisomerase inhibition is due to a replication elongation block, we measured origin-to-terminus ratios for *oriC* and *oriN* cells in the presence and absence of the replication elongation inhibitor, Mitomycin C (MMC) (Fig. 2.2 D). We found that cells treated with MMC over-initiate, but this over-initiation phenotype is not specific to *oriC* (Fig. 2.2 D). In both *oriC* and *oriN* cells, origin-to-terminus ratios increased upon treatment with 1 μg ml^{-1} MMC: a concentration at which replication is inhibited (39). Although this effect was more pronounced for *oriC* cells, the increase in *oriN* cells was statistically significant (P value < 0.01). Together, these results are consistent with our observations that replication

elongation is largely unaltered in *oriN* cells upon topoisomerase inhibition. The results of the *oriN* and MMC experiments together strongly suggest that arrest of replication elongation is unlikely to be responsible for the over-initiation phenotypes we see in *oriC* cells upon inhibition of topoisomerases through novobiocin treatment.

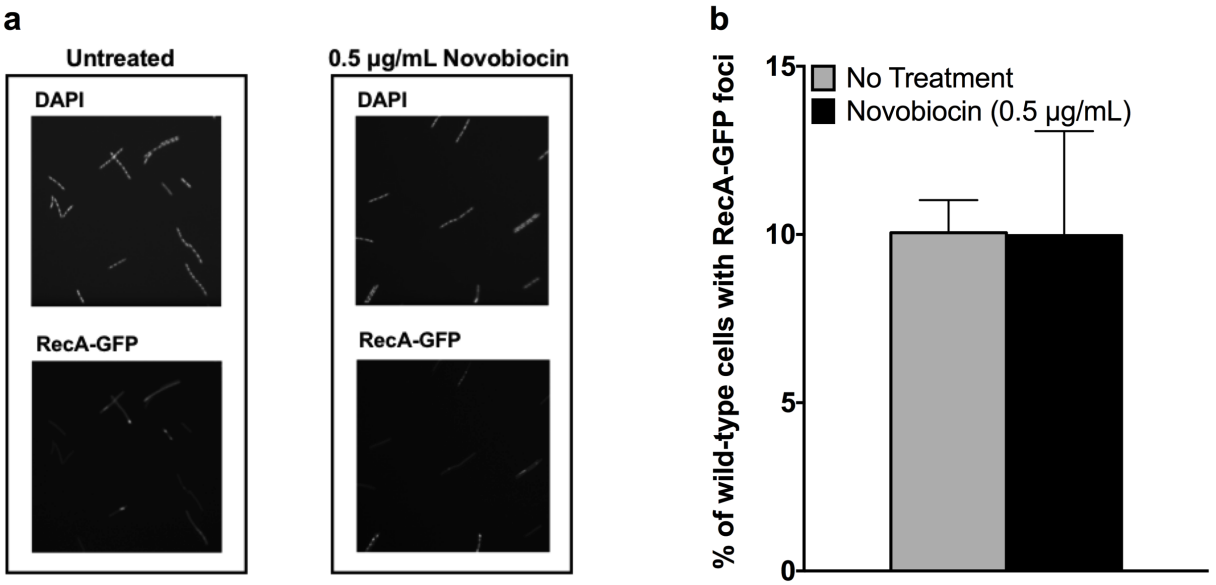

Figure 2.4. Inhibition of gyrase activity does not induce a RecA-dependent DNA damage response. A) Representative DAPI and RecA-GFP microscopy images from *oriC* cells grown with and without novobiocin. B) Quantification of the % of cells with RecA-GFP foci for *oriC* cells grown with and without novobiocin. At least 2,000 cells from 3 biological replicates were counted per condition. Error bars represent standard error of the mean.

Additional experiments were performed to test if novobiocin-induced over-initiation could be leading to replication fork collapse. Microscopy using *oriC*+ *recA-gfp* cells grown in LB and in LB supplemented with novobiocin yielded no obvious cell morphology defects (i.e., filamentous

cells) (Fig. 2.4). The total number of RecA-GFP foci and the total number of cells (DAPI stained nucleoids) were quantified for these two conditions in order to calculate the percentage of cells with RecA foci. We observed no difference in the percentage of cells with RecA-GFP foci, which was roughly 10% under both conditions (Fig. 2.4). Together, these results provide evidence against novobiocin inducing a DNA damage response, which would be expected under conditions of replication fork collisions or collapse.

The over-initiation phenotype of novobiocin treated cells is specifically due to gyrase inhibition.

Novobiocin inhibits both Topo IV and gyrase, therefore it was unclear if the effects we observed were due to the activity of one or the other (or both) enzymes at the origin. To identify which topoisomerase was responsible for the observed effects of novobiocin inhibition, we plated wild-type *B. subtilis* cells on 4 μg ml^{-1} novobiocin, and isolated a novobiocin resistant mutant of gyrase that contained a single mutation in the *gyrB* gene, converting Arginine at the 138 position to Leucine. The R138L mutant carries an amino acid change in the ATP-binding domain of gyrase. This mutation is in the same domain and the amino acid change is analogous to previously identified novobiocin resistant gyrase mutants in other bacteria (168, 174). Mutations that lead to novobiocin resistance can sometimes arise in the *parE* gene, which codes for one of the two subunits of Topo IV (151, 168). We confirmed that there was no mutation in the *parE* gene in the *gyrB* (R138L) mutant by sequencing.

We quantified the survival of wild-type and *gyrB* mutants with increasing concentrations of novobiocin. As expected, the novobiocin resistant mutant can grow on novobiocin, at concentrations which are lethal for wild-type cells. The *gyrB* mutant grew normally on LB supplemented with 0.45, 0.55, 0.65, 0.75 and 0.85 μg ml^{-1} novobiocin, whereas the wild-type strain displayed 1–3-logs (or more) of killing when grown on these concentrations (Fig. 2.5 A).

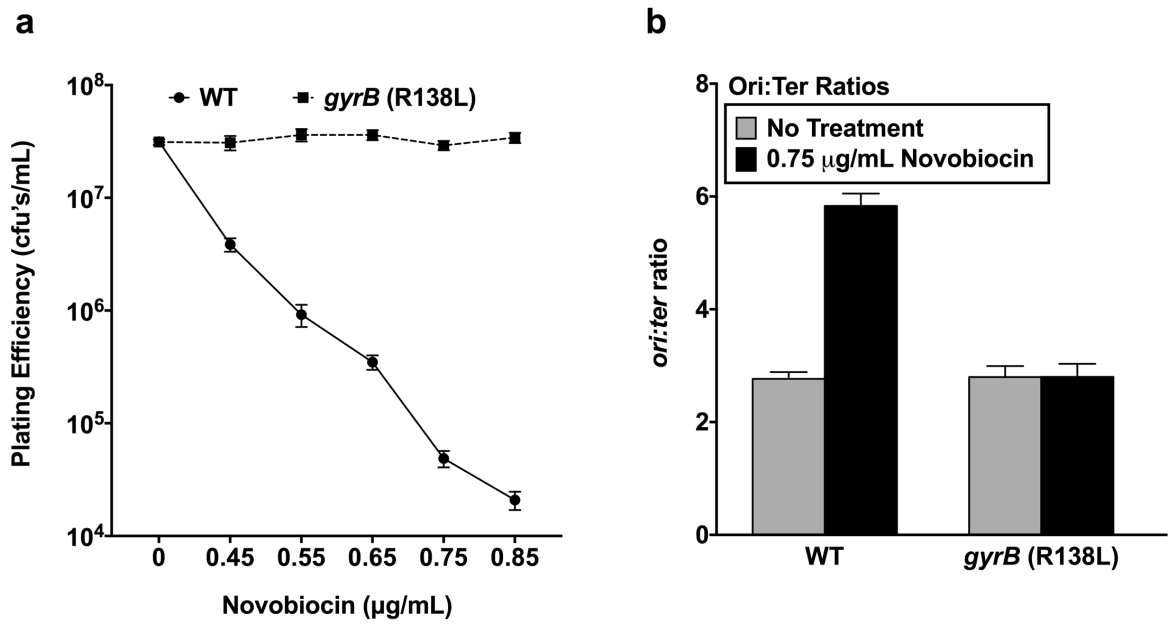

Figure 2.5. The over-initiation phenotype of *oriC*+ cells after topoisomerase inhibition is due to effects on gyrase. A) Plating efficiency of wild-type cells and *gyrB* (R138L) mutants on increasing concentrations of novobiocin. Colony forming units per mL of exponentially growing cultures (OD600 = 0.3) plated on LB or LB supplemented with 0.45, 0.55, 0.65, 0.75, and 0.85 µg/mL novobiocin. Data shown are averages from 12-24 biological replicates. Error bars represent standard error of the mean. B) Origin-to-terminus ratios of exponential-phase wild-type cells increases upon treatment with 0.75 µg/mL novobiocin. No effect was observed for *gyrB* (R138L) mutants. Data shown are averages from 6 biological replicates. Error bars represent standard error of the mean.

We then measured origin-to-terminus ratios for wild-type and *gyrB* mutant cells, in the presence and absence of novobiocin (Fig. 2.5 B). As before, wild-type cells displayed a two-fold increase in origin-to-terminus ratios; however, the gyrase mutant did not show an increase in origin-to-terminus ratios (Fig. 2.5 B). This indicates that the impact of novobiocin on initiation frequency is through inhibition of gyrase, and is unlikely to be related to inhibition of Topo IV.

Gyrase inhibits DnaA association with *oriC*

The effect of gyrase inhibition on replication initiation, but not elongation, led us to investigate its impact on DnaA association at *oriC*. *oriN* cells do not use DnaA to initiate replication, therefore, one explanation for how gyrase might modulate initiation in an *oriC*-specific manner is through modulation of DnaA binding or activity. To test this, we performed Chromatin Immunoprecipitations (ChIPs) of DnaA for *oriC*, *oriN* and *gyrB* (R138L) mutant cells. We measured DnaA association at two different loci within *oriC*: upstream of *dnaA*, (P*dnaA*), and at the DUE using anti-DnaA rabbit polyclonal antiserum. We normalized the signal for the various loci in *oriC* to a previously established control locus (26, 60, 63), *yhaX*, with and without novobiocin treatment (Fig. 2.6).

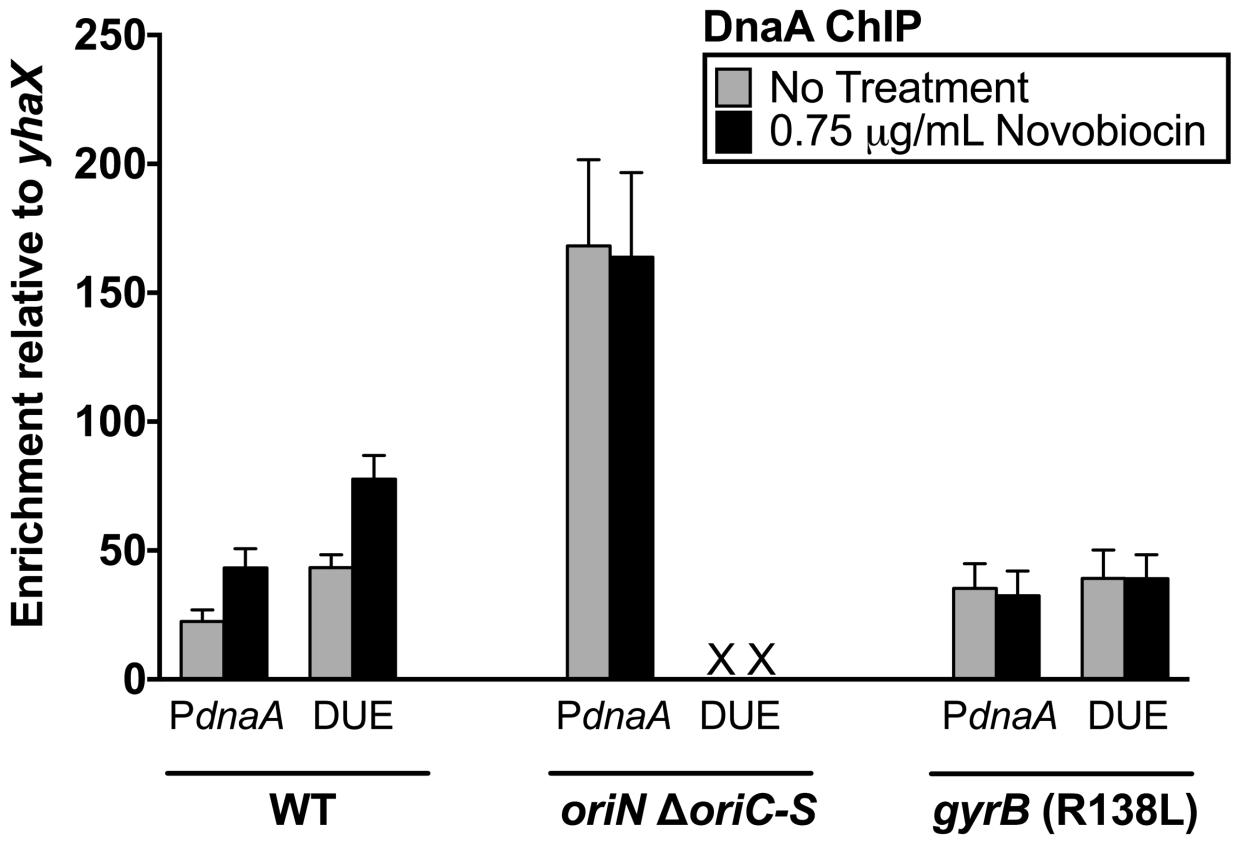

Figure 2.6. Inhibition of gyrase activity increases DnaA association at *oriC*. DnaA enrichment was measured at the DUE and P*dnaA* by ChIP-qPCR (relative to a locus outside of the origin, *yhaX*). DnaA ChIPs were performed from WT, *oriN ΔoriC-S*, and *gyrB* (R138L) cells, grown in the presence or absence of 0.75 μg/mL novobiocin. Data shown are averages from at least 6 biological replicates. Error bars represent standard error of the mean.

In *oriC* cells, DnaA enrichment at P*dnaA* and DUE increased roughly two-fold upon treatment with novobiocin (Fig. 2.6). Interestingly, although the overall levels of DnaA found at *oriC* were higher in the *oriN* strain, novobiocin treatment did not lead to any further increase in DnaA enrichment at P*dnaA* in the *oriN* background (Fig. 2.6). DnaA association with the DUE region could not be measured, as the DUE is deleted in this strain background. DnaA ChIPs were also performed in the novobiocin resistant *gyrB* mutant. Novobiocin treatment did not change DnaA binding patterns at the two loci tested in this strain (Fig. 2.6). These results suggest that gyrase activity modulates DnaA association with *oriC*, which is consistent with the over-initiation phenotypes observed in *oriC* cells.

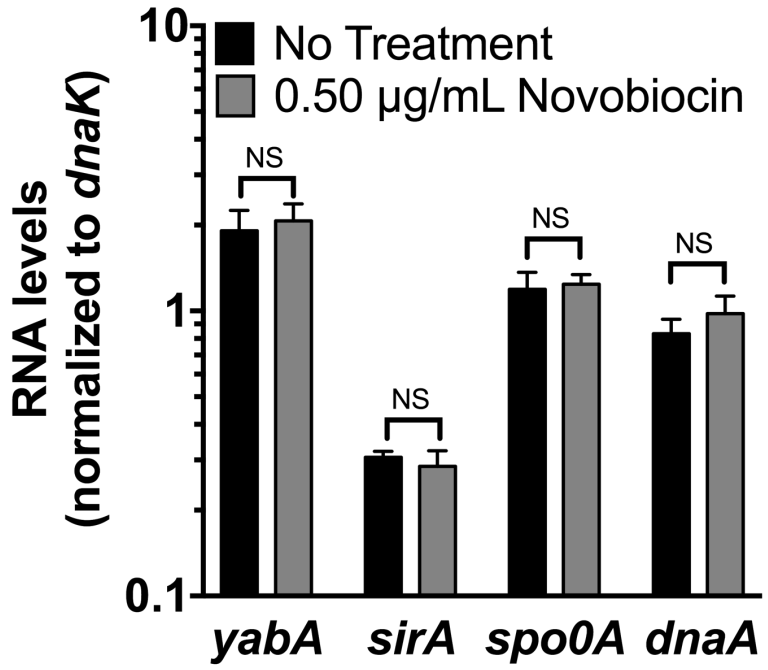

Figure 2.7. Inhibition of gyrase activity does not change expression levels of known DnaA regulators: YabA, SirA, Spo0A or DnaA. RNA levels for *yabA, sirA, spo0A, and dnaA* (normalized to *dnaK*) for *oriC*+ cells. Data shown are averages from 6 biological replicates. Statistical significance was calculated using *t*-test (NS P>0.05).

Given the impact of gyrase inhibition on initiation frequency and DnaA association at *oriC*, we wanted to test if inhibition of gyrase activity indirectly impacted DnaA through its known regulators. For this, we measured expression levels of several known DnaA regulators with and without novobiocin. RNA levels were quantified for *yabA, sirA, spo0A* and *dnaA*, and normalized to *dnaK* for *oriC*+ cells grown in the presence and absence of novobiocin (Fig. 2.7). We did not detect any changes in expression profiles for these DnaA regulators after novobiocin treatment (Fig. 2.7).

Initiation from *oriN* decreases sensitivity to gyrase inhibition.

Genome-wide marker frequency, origin-to-terminus ratios, and DnaA ChIP analyses all showed that gyrase inhibition alters DnaA-dependent initiation from *oriC*, but not RepN-dependent initiation from *oriN*. Given the importance of well-timed replication initiation and gyrase activity for DNA replication, we were curious if *oriC* cells are more susceptible to gyrase inhibition than cells initiating replication from *oriN*. To test this, we measured the survival efficiency of *oriC* and *oriN* cells upon exposure to novobiocin. Interestingly, we found that strains initiating from *oriN* are significantly less sensitive to gyrase inhibition, showing minimal survival defects when plated on concentrations of novobiocin that reduce survival of wild-type cells by up to 3-logs (Fig. 2.8 A). In order to ensure that secondary mutations are not responsible for the increase in novobiocin survival observed among the *oriN* strains, we sequenced the *gyrB* and *parE* genes, where mutations that lead to resistance usually arise in response to novobiocin treatment. No mutations were found in these genes in the *oriN* strains.

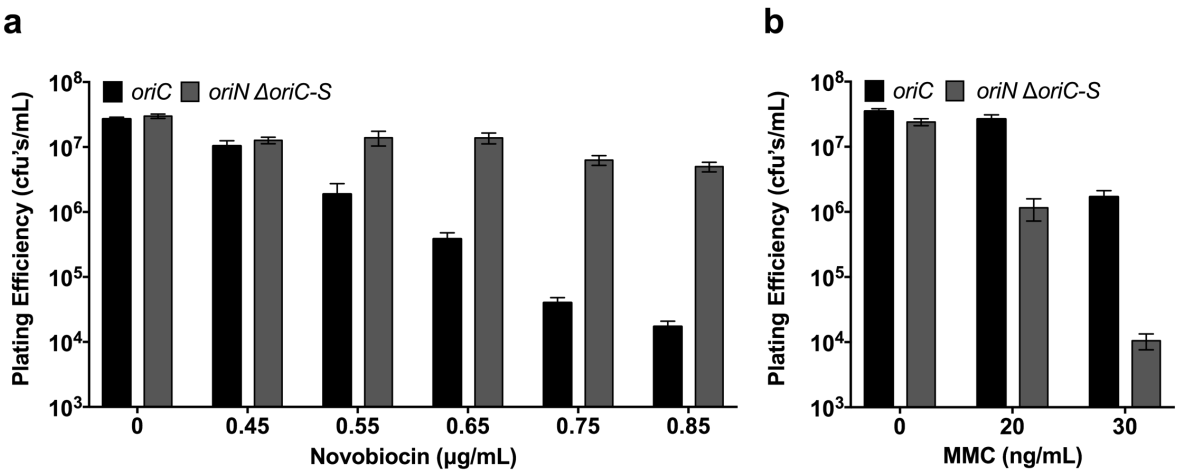

Figure 2.8. The survival defect observed upon topoisomerase inhibition is *oriC*-dependent. Plating efficiencies of *oriC* and *oriN* cells on increasing concentrations of novobiocin and MMC are presented. A) Colony forming units per mL on LB and LB supplemented with 0.45, 0.55, 0.65, 0.75 and 0.85 μg ml^{-1} novobiocin were quantified. Data shown are averages from at least 10 biological replicates. Error bars represent standard error of the mean. B) Colony forming units per mL on LB and LB supplemented with 20 and 30 ng ml^{-1} of mitomycin C (MMC) were quantified. Data shown are averages from four biological replicates. Error bars represent standard error of the mean.

We confirmed that the decrease in colony forming units on LB supplemented with novobiocin is due to cell death, rather than growth inhibition. To do this, wild-type exponential phase cells were plated on novobiocin. After 24–48 hours of incubation at 30°C, colony forming units were quantified and replica plating was performed to transfer cells to LB plates, which were incubated overnight. Colonies did form in the same places as observed on the antibiotic plates, however, there was no increase in colony forming units on LB plates compared with LB supplemented with novobiocin (data not shown).

To determine if the resistance of *oriN* cells to novobiocin is related to replication elongation, we performed plating efficiency experiments on MMC. We found that, as expected, *oriC* cells are

sensitive to MMC treatment (Fig. 2.8 B). Importantly, however, unlike what we observed with novobiocin, *oriN* cells did not show any resistance beyond that of *oriC* cells to MMC. In fact, *oriN* cells were 1–2 logs more sensitive to various concentrations of MMC, as compared with *oriC* cells (Fig. 2.8 B). In the context of our novobiocin experiments, these data again confirm that the *oriC*-specific growth defects observed upon gyrase inhibition are unlikely to be related to a block in replication elongation.

YabA–DnaA interactions at *oriC* can counteract gyrase inhibition.

YabA is a negative regulator of DnaA that lowers rates of replication initiation through disrupting oligomerization and cooperative binding of DnaA to *oriC* (31, 60) and tethering DnaA to the replisome (61). Deletion of *yabA* leads to over-initiation of replication, whereas over-expression of *yabA* inhibits this process (175). If gyrase has an essential role in regulating DnaA-dependent initiation dynamics, then known regulators of DnaA may be important for modulating the impact of gyrase inhibition on replication initiation and survival. To test this model, using *yabA* deletion and over-expression mutants, we investigated the impact of YabA on modulating novobiocin susceptibility. In addition, we wanted to determine whether, specifically, the interaction of YabA with DnaA is important for novobiocin susceptibility. For this, we constructed a strain that harbors a mutant of YabA (*yabA-aim*) containing a previously characterized single point mutation that disrupts interactions between YabA and DnaA (*yabA*-N85D) (176). The mutant allele of *yabA* was placed under an IPTG-inducible promoter, in a *yabA* deletion background. Both *yabA-aim* expression and *yabA* over-expression were confirmed by measuring RNA levels (Fig. 2.9 A).

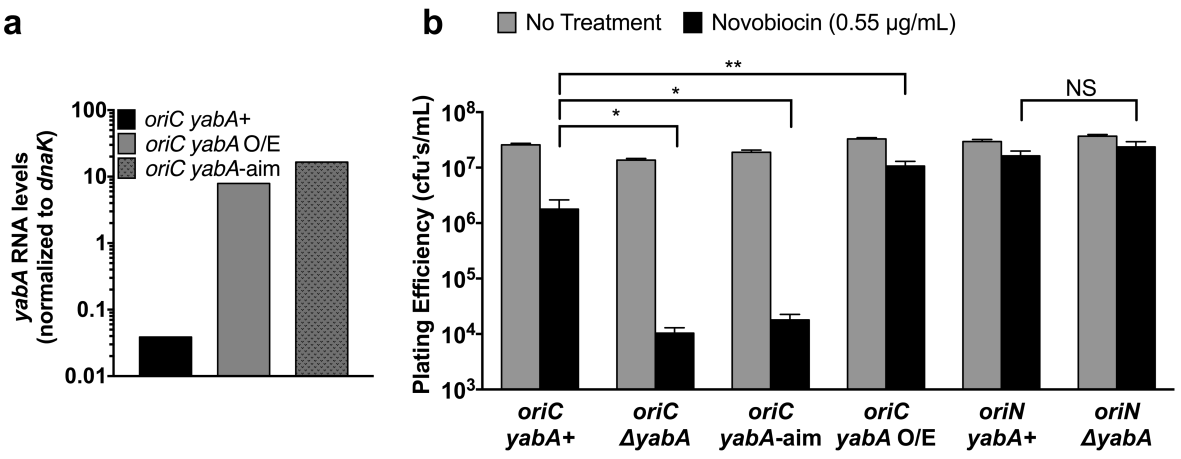

Figure 2.9. Regulation of initiation by YabA increases the ability of cells to survive DNA gyrase inhibition. A) RNA levels for *yabA* (normalized to *dnaK*) for wild-type cells, *yabA* over-expression ($P_{spank\ (hy)}$ - *yabA*) with inducer (1 mM IPTG), and $P_{spank\ (hy)}$ – *yabA-aim* with inducer (1 mM IPTG). Data shown are averages from 3 biological replicates. B) Colony forming units per mL of exponentially growing wild-type cells, Δ*yabA*, *yabA-aim* (YabA-DnaA interaction mutant), *yabA* over-expression mutant, *oriN* Δ*oriC-S*, and *oriN* Δ*oriC-S* Δ*yabA* (OD600 = 0.3) plated on LB and LB supplemented with 0.55 µg/mL novobiocin. Data shown are averages from at least 6 biological replicates. Statistical significance was calculated using *t*-test (* $p < 0.05$, ** $p < 0.01$).

We found that in the absence of YabA, cells are significantly more sensitive to novobiocin. Survival of *yabA* deletion mutants was 2–3 logs lower than wild-type (Fig. 2.9 B). Conversely, YabA over-expression increased survival efficiency on novobiocin by 1–2 logs (Fig. 2.9 B). These data are consistent with the findings presented above, and suggest that sensitivity to gyrase inhibition is strongly influenced by changes in regulation of DnaA association and activity at *oriC*.

We found that initiation mutants with deletions in *yabA* are highly sensitive to novobiocin (Fig. 2.9 B). To further confirm that this is due to the activity of these proteins at *oriC*, we constructed *yabA* deletions in the *oriN* background and quantified survival of these mutants on novobiocin. In contrast to cells initiating replication from *oriC*, we did not observe any increase in novobiocin sensitivity in *yabA* deletion mutants initiating replication from *oriN* (Fig. 2.9 B). The

plating efficiency for these mutants remained high, with no detectable decrease in survival, as is seen with cells that initiate replication from *oriN* (Fig. 2.9 B).

Experiments using the *yabA-aim* mutants, where YabA–DnaA interactions are disrupted, provided results consistent with the overall hypothesis we have developed based on the data presented above. We grew *yabA-aim* mutants on increasing concentrations of novobiocin with 1 mM IPTG (to induce expression of *yabA-aim*) and found that loss of YabA–DnaA interactions (*yabA-aim*) increases novobiocin sensitivity by up to 3 logs (Fig. 2.9 B). This suggests that it is specifically the interaction of YabA with DnaA that is important for modulation of novobiocin survival and not indirect effects found in strains lacking YabA.

Discussion

In vitro work has demonstrated the importance of gyrase and negative supercoiling for melting of the DUE (130, 177). Both our work and previous *in vitro* studies are in agreement that gyrase activity is important for replication initiation. However, our findings strongly suggest that gyrase is important for replication initiation at an earlier step than DUE melting *in vivo*. Our results point to a model where gyrase negatively regulates DnaA association with *oriC*, and decreases replication initiation frequency in *B. subtilis*.

A previous study reported that novobiocin treatment actually decreases initiation in *B. subtilis* (178). Ogasawara and colleagues reported that only a limited region near the origin of replication is replicated in the presence of novobiocin (178). This result is not surprising as replication and transcription can both be completely inhibited at high concentrations of novobiocin (162, 163). However, based on the marker frequency patterns presented, had Ogasawara *et al*. measured origin-to-terminus ratios, they would have likely seen an increase in initiation frequency similar to what we found. Nevertheless, at lower concentrations of novobiocin such as those used in our study, the impact of gyrase on initiation is clearly detectable.

There are various ways in which gyrase might regulate DnaA-dependent replication initiation. One possibility is that inhibition of gyrase indirectly affects DnaA binding to the origin through changes in DNA topology at the DnaA consensus binding sites, which are adjacent to the transcriptionally active *dnaA* gene. The origin of replication must be negatively supercoiled for initiation to proceed. However, given that gyrase introduces negative supercoils into DNA, our data suggest that negative supercoiling beyond what is necessary for DUE melting is actually inhibitory to DnaA association and/or function at *oriC*. Another possible model for how topology might impact initiation dynamics is through indirect effects of superhelical torsion on replication elongation, which could be communicated to the origin specifically through DnaA regulation. The Grossman group previously reported that in elongation-arrested *B. subtilis* cells, DnaA association at the origin of replication and copy number of origin-proximal genes increases (39). This is consistent with our findings using MMC. However, in the context of gyrase inhibition, we find that elongation block alone cannot explain the observed effects on DnaA and *oriC* firing. Cells initiating replication from *oriN* continue replication elongation unaltered upon gyrase inhibition. Furthermore, unlike with novobiocin inhibition of gyrase, the effects of blocking replication elongation through MMC is not specific to *oriC*. These results argue against the model that gyrase inhibition targets DnaA-dependent initiation through arrest of replication elongation.

Given the global role of gyrase on chromosome topology, we cannot rule out the possibility that supercoiling effects on DnaA are indirect. However, we did not detect changes in mRNA levels of several regulators of DnaA, including: YabA, SirA, Spo0A and DnaA upon gyrase inhibition. These results argue against an indirect effect, but do not rule it out. It is possible that the impact of gyrase inhibition on replication initiation is independent of both origin topology and DNA replication. For example, recent work by Magnan *et al*. showed that chromosome tethering at sites as far as 1 Megabase away from the origin of replication can alter global DNA topology and inhibit replication initiation (179). Furthermore, inhibition of gyrase may affect replication initiation indirectly. Further experimentation is required to dissect these models.

Interestingly, it appears that dis-regulation of replication initiation can be lethal for cells if the topological status of the chromosome is compromised. Our studies suggest that over-initiation becomes lethal if positive supercoiling is not resolved around the chromosome. In the case of other regulators such as YabA, over-initiation is not lethal, perhaps because gyrase is able to resolve topological problems that arise away from the origin, in front of converging replication forks.

We propose a model where the topological status of the origin is used as a regulatory mechanism for DnaA binding at an early step prior to the melting of the origin. This model can explain previous observations from studies in *E. coli*, where changes in DNA supercoiling or transcriptional activity at promoters near *oriC* were shown to impact replication initiation dynamics (158, 159, 180). Transcriptional activation of *gidA*, which is adjacent to *oriC* in *E. coli*, can alter topology at the origin by introducing negative supercoiling within the region (158, 159). Furthermore, decreased supercoiling was shown to lead to asynchronous replication initiation (181, 182). Additionally, initiation phenotypes observed in the temperature sensitive alleles of *dnaA* could be suppressed by mutations in *topA* (Topoisomerase I) (183). All of these observations point to a possible regulatory role for topology in DnaA binding and activity during replication initiation. However, to our knowledge, a role for gyrase in DnaA association and initiation from *oriC* has not been demonstrated *in vivo* prior to our study. This role may or may not be direct, and the mechanism of DnaA regulation by gyrase should be further investigated.

Additionally, this work establishes a role for topology in DnaA activity at the origin in *B. subtilis*. Since DnaA, gyrase and topological constraints are ubiquitously found across bacterial species, we anticipate that regulation of DnaA association or activity by gyrase at *oriC* is not specific to *B. subtilis*. Topology-mediated DnaA binding may, therefore, be one of the few common mechanisms that regulate replication initiation across both Gram-negative and Gram-positive organisms.

CHAPTER 3. Investigation of the error-prone polymerases acting at TC-NER sites

Introduction

Faithful replication of bacterial chromosomes is essential for life. There are many obstacles to DNA replication, including DNA lesions, which cells must resolve to survive and ensure transfer of genetic material to progeny cells. Bacteria have conserved, redundant mechanisms for repairing DNA damage. While the fidelity of DNA replication and repair is important for maintaining the integrity of essential processes, the ability of cells to adapt to changing conditions depends on controlled introduction of mutations. As such, cells have highly targeted and regulated mechanisms for introducing mutations during DNA replication. These include the selective use of error-prone translesion synthesis (TLS) polymerases, which facilitate replication past bulky lesions (184). While DNA repair pathways generally reduce genomic instability, recent work has highlighted the role of transcription-coupled nucleotide excision repair (TC-NER), the repair process which removes template strand lesions that block RNA polymerase (RNAP), in promoting mutagenesis (110–112).

Mutagenesis is essential to the survival and adaptation of bacterial populations to a variety of environmental conditions. Therefore, identifying the mechanisms by which bacteria acquire mutations is important. While there have been extensive studies investigating which proteins are involved in TC-NER and what their specific roles in this pathway are (185), we still do not understand how TC-NER is mutagenic and which polymerase(s) drive this mutagenesis. Previous studies from other groups have implicated Pol I, the DNA polymerase responsible for replacing RNA primers at Okazaki fragments, in prokaryotic nucleotide excision repair (116, 117). These studies were based on *in vitro* experiments measuring repair-synthesis and excision activity in the presence of different combinations of purified proteins and polymerases (116, 117). Other polymerases, like the main replicative polymerase DNA Pol III, were also tested and their involvement was ruled out. However, these studies were done prior to the discovery of TLS

polymerases. We have preliminary data indicating that the two TLS polymerases in *Bacillus subtilis*, YqjH and YqjW, may act in this repair pathway. Due to the predicted role of Pol I in TC-NER, the known interactions between Pol I and TLS polymerases, and the requirement of Pol I for TLS polymerase mediated mutagenesis (126), it is plausible that error-prone polymerases are recruited to TC-NER sites to fill in gaps through Pol I. Based on this, I hypothesized that TLS polymerases work together with DNA polymerase I to increase mutations at TC-NER sites through gap filling. To better understand which polymerases are introducing mutations at TC-NER sites – and whether specific polymerases are working together or independently of each other – I used a genetic approach, measuring mutation rates for TC-NER and polymerase mutants.

Results

TC-NER promotes mutagenesis in *B. subtilis*

Mechanisms by which bacteria evolve are required for survival and fitness in the face of changing environments. TC-NER is a highly conserved DNA repair pathway that contributes to bacterial evolution through increasing point mutations at transcribed genes (109). This can have implications for bacterial adaptation and antibiotic resistance development. Our lab has shown that TC-NER promotes antibiotic resistance development against multiple classes of antibiotics in *Bacillus subtilis*, *Salmonella enterica*, *Pseudomonas aeruginosa* and *Mycobacterium tuberculosis* (Ragheb et al., unpublished). Additionally, deletions in TC-NER genes reduce spontaneous mutagenesis, as measured by mutations in the highly transcribed gene *rpoB* that confer resistance to rifampicin. Deletion of nucleotide excision repair proteins that recognize and process DNA lesions – UvrA, UvrB, and UvrC – result in 2-3-fold lower mutation rates, as compared to WT cells (Fig. 3.1). To determine if UvrABC increase mutations through transcription-coupled repair, I tested mutation rates in *mfd* deletion mutants in combination with deletions of various *uvrABC* genes. Mutation rates for the double deletion mutants are epistatic

with the single *mfd* mutant (Fig. 3.1). This is consistent with previous reports that mutation frequency is lower in TC-NER mutants (109–112). All together, these findings led us to ask why this repair pathway is mutagenic.

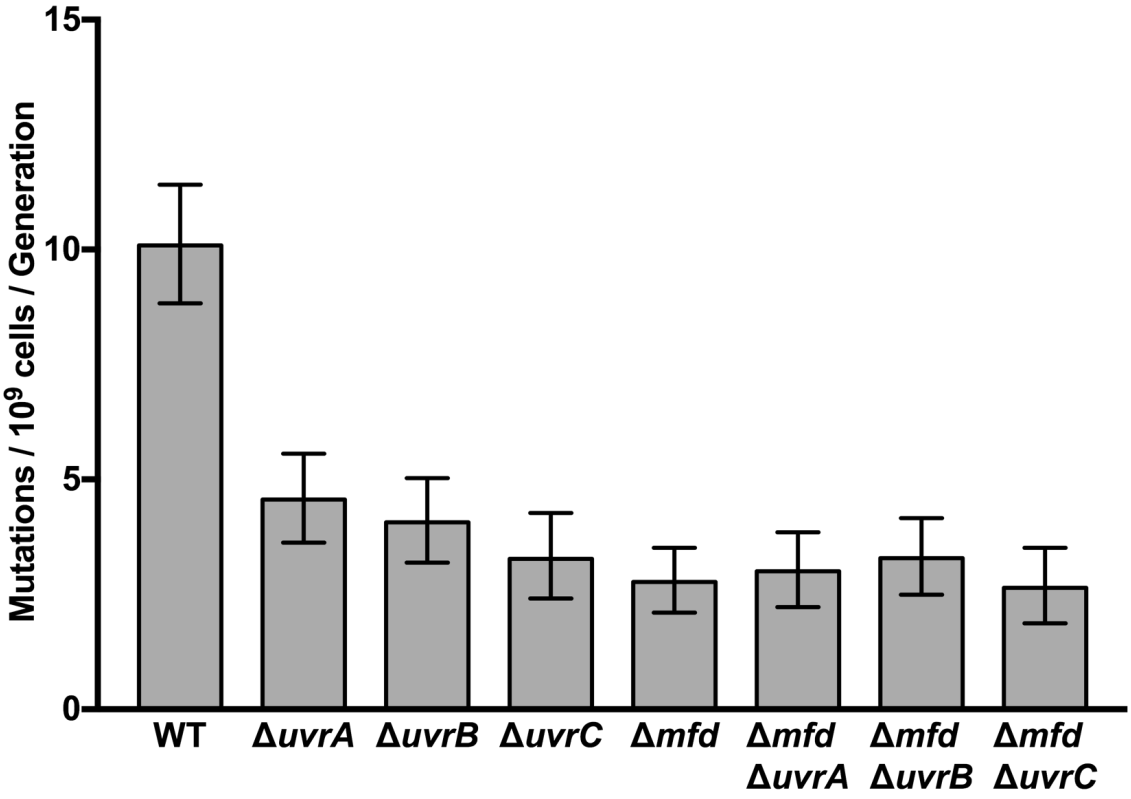

Figure 3.1. TC-NER promotes spontaneous mutagenesis in *Bacillus subtilis*. Mutation rates represent mutations that confer rifampicin resistance. N= 55-114 biological replicates. Error-bars represent 95% confidence intervals.

TLS polymerases may act in the same pathway as TC-NER to promote mutagenesis

Our lab has previously shown that TC-NER is required for transcription-dependent mutagenesis in *B. subtilis* (109). Through epistasis analysis, we found that the TLS-polymerase, YqjH, may act in this TC-NER pathway (109). The contribution of these factors to transcription-dependent mutagenesis was observed by measuring reversion rates in three reporter strains, each containing an inactive biosynthesis gene with a premature stop codon or missense codon (*hisC952*, *metB5*, and *leuC27*), under conditions where these genes are transcribed at low or high levels (109). To test if these mechanisms increase mutagenesis at highly transcribed, endogenous genes, and facilitate antibiotic resistance development, I measured the contribution of TC-NER and TLS polymerases to rifampicin resistance development. In support of our previous results, I found that mutations at the highly transcribed gene, *rpoB*, are TC-NER and TLS polymerase-dependent (Fig. 3.2).

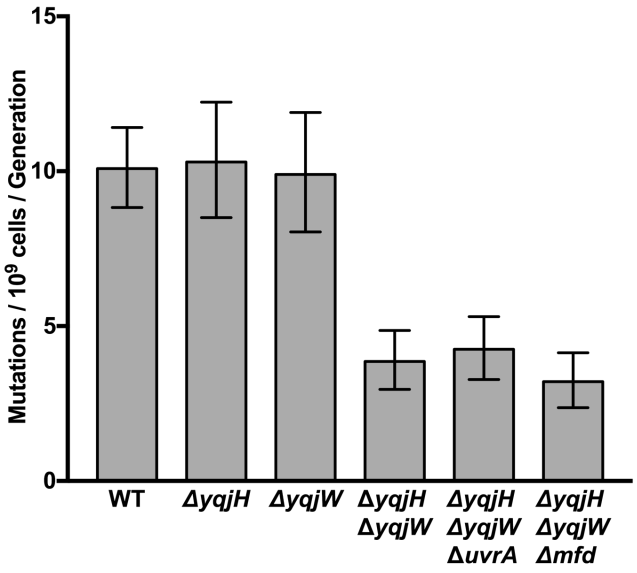

Figure 3.2. TLS polymerases increase spontaneous mutagenesis. Epistasis analysis indicates that TLS polymerases may act in the same pathway as TC-NER. Mutation rates represent mutations that confer rifampicin resistance. N= 55-114 biological replicates. Error-bars represent 95% confidence intervals.

In the established model of TC-NER, Pol I is involved in repair-synthesis (116, 117). However, due to the high fidelity of Pol I (186), this model may be incomplete. Specifically, it fails to address why we observe an increase in mutations associated with TC-NER. It is plausible that Pol I and TLS polymerases would act together, as Pol I physically interacts with TLS polymerases, and is required for TLS polymerase-mediated mutagenesis in *B. subtilis* (126).

There are several models that might explain why this repair pathway is mutagenic. 1) Pol I facilitates TLS polymerase-mediated gap filling at TC-NER sites. 2) Both Pol I and TLS polymerases perform gap filling at TC-NER sites. 3) Pol I and TLS polymerases perform repair synthesis independently of each other, with the activity of specific polymerases changing depending on protein levels, and variations in stoichiometry. These models are illustrated in **Figure 3.3**. While TC-NER has been well studied, it is still unclear why this pathway is error-prone.

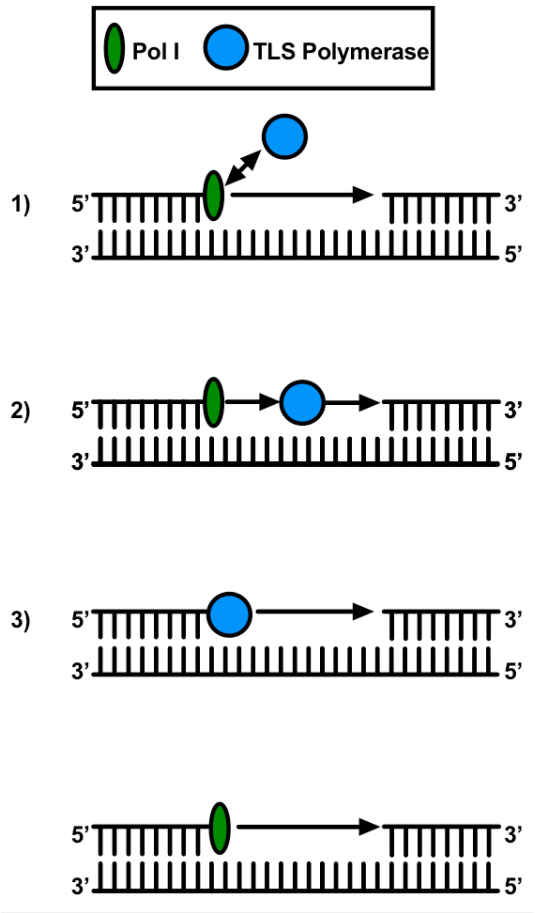

Figure 3.3. Models for TC-NER gap filling by Pol I and/or TLS polymerases. 1) Pol I recruits TLS polymerases to fill in gaps TC-NER sites. 2) Pol I and TLS polymerases work together to perform gap filling at TC-NER sites. 3) Pol I and TLS polymerases can each perform repair synthesis, and work independently of each other.

Pol I may act in the same pathway as TC-NER to promote mutagenesis

In *Bacillus subtilis*, DNA polymerase I acts in error-prone translesion synthesis mediated by Y-family polymerases (126). To investigate the role of Pol I in gap filling at TC-NER sites, I measured the contribution of Pol I to TC-NER mediated rifampicin resistance development. In agreement with previous *in vitro* work, I found that mutations at the highly transcribed gene, *rpoB*, are Pol I and TC-NER dependent (**Figure 3.4**). Additionally, as predicted, epistasis analysis indicates that Pol I may act in the TC-NER pathway.

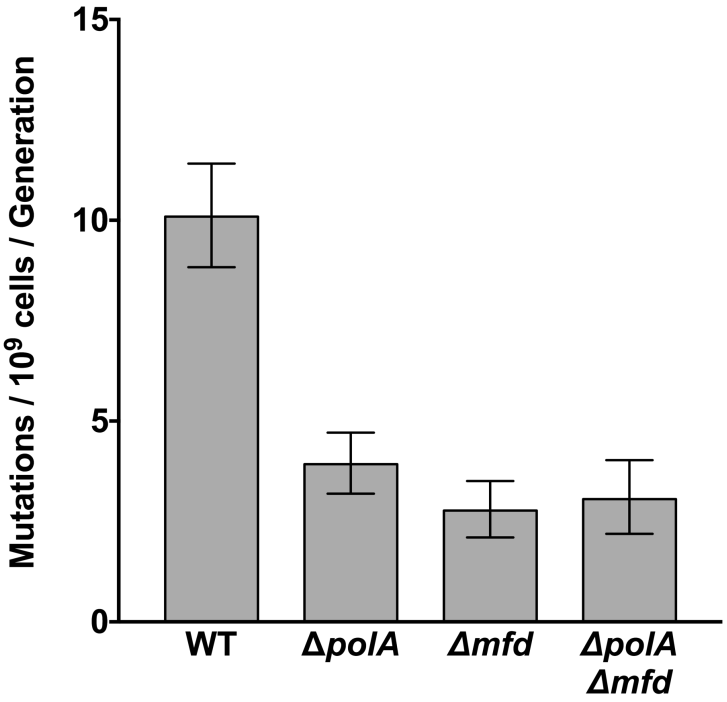

Figure 3.4. Pol I and Mfd are epistatic. Epistasis analysis indicates that Pol I may act in the same pathway as TC-NER. Mutation rates represent mutations that confer rifampicin resistance. N= 60-130 biological replicates. Error-bars represent 95% confidence intervals.

Pol I and TLS polymerases may act in together to promote mutagenesis through TC-NER

Whether Pol I and TLS polymerases act together or independently to fill in gaps at TC-NER sites is not clear. However, we know that *B. subtilis* Y-family polymerases YqjH and YqjW interact physically with Pol I (126), and that interactions between Pol I, YqjH and DnaN have also been observed by three-hybrid analysis (126). Interestingly, Pol I is required for YqjH-dependent spontaneous mutagenesis and for UV-induced YqjW-dependent mutagenesis (126). Given the role Pol I plays in Y-family polymerase-mediated mutagenesis, and the known protein-protein interactions, it is plausible that there may be a mechanism for polymerase switching at TC-NER sites.

Epistasis analysis was used to determine if Pol I and TLS polymerases are working together or separately to perform gap filling at TC-NER sites. I measured the contribution of Pol I to TC-NER mediated rifampicin resistance development. In agreement with previous *in vivo* work in *B. subtilis*, using epistasis analysis, I found that mutations at the highly transcribed gene, *rpoB*, are through Pol I and the TLS polymerases (YqjH and YqjW) working together (**Figure 3.5**).

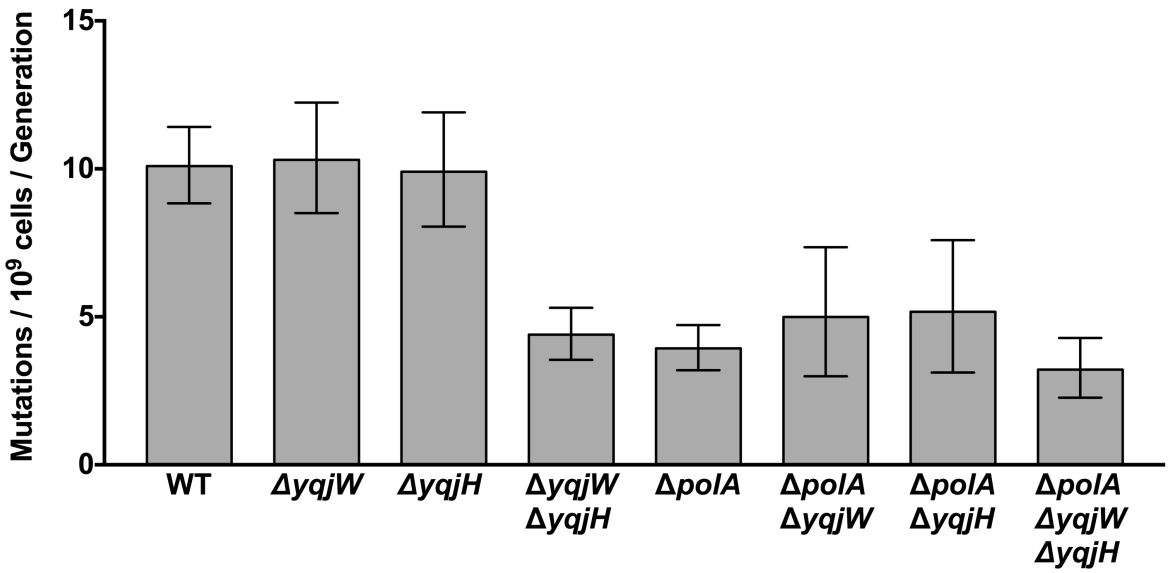

Figure 3.5. Pol I and TLS polymerases are epistatic. Epistasis analysis indicates that Pol I may act together with TLS polymerases, YqjH and YqjW. Mutation rates represent mutations that confer rifampicin resistance. N=20-130 biological replicates. Error-bars represent 95% confidence intervals.

Discussion

Together, my results indicate that Pol I may facilitate error-prone gap filling at TC-NER sites, and act in the same pathway as TLS polymerases. These results helped to narrow down the models we had for gap filling during TC-NER. Our current models for gap-filling are illustrated in **Figure 3.6**. We now have *in vivo* evidence suggesting that Pol I and TLS polymerases are working together in this mutagenic repair pathway. My *in vivo* work showing that Pol I is epistatic with TC-NER is in agreement with previous, *in vitro* studies (116, 117). Additionally, my results showing that these polymerases may be working together are consistent with previous findings in *B. subtilis* (126).

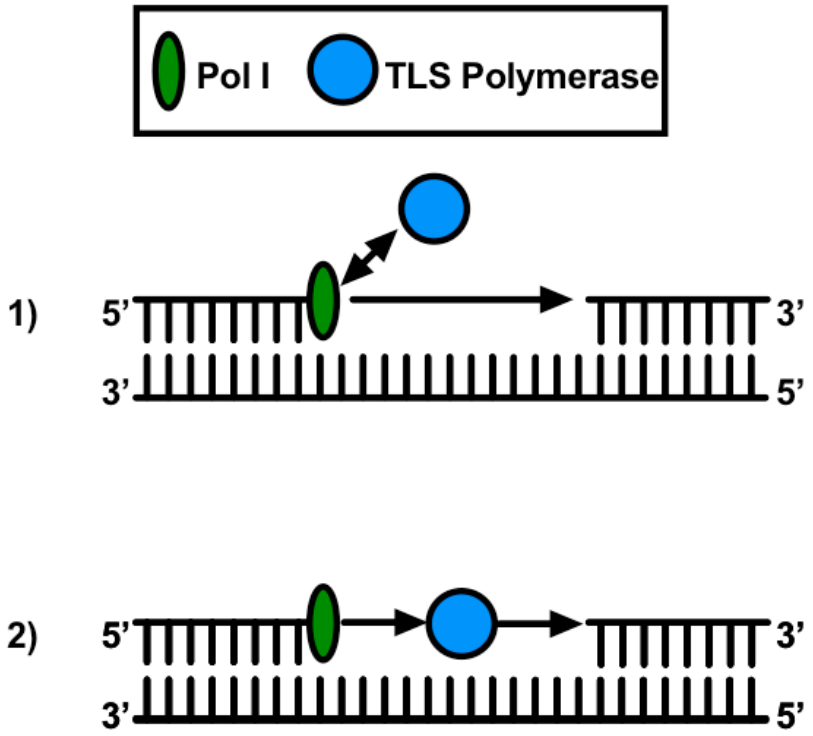

Figure 3.6. Models for cooperative TC-NER gap-filling by Pol I and TLS polymerases. 1) Pol I recruits TLS polymerases to fill in gaps TC-NER sites. 2) Pol I and TLS polymerases work together to perform gap filling at TC-NER sites.

Further *in vivo* and *in vitro* work must be done to determine if and how Pol I and TLS polymerases are acting to perform gap filling at TC-NER sites. These models and various approaches to testing them are outlined below in the "Future Directions" section.

CHAPTER 4. Future Directions

4.1 Role of DNA topology in regulating replication initiation

How is gyrase inhibiting DnaA binding to *oriC*?

Through my work, we have learned that gyrase activity inhibits DnaA binding to the origin of replication *in vivo* (187). However, how gyrase inhibits DnaA association at *oriC* is not yet understood. There are various models for how gyrase-mediated DnaA inhibition may work – several of these are discussed below.

1) *Gyrase introduces negative supercoiling at oriC*

It is possible that gyrase-dependent remodeling of *oriC* is required for proper DnaA oligomerization and replication initiation timing. However, testing for this variable in a controlled manner would be challenging. Creating an experimental condition where gyrase can only act at *oriC* and not genome-wide where it also acts does not seem possible with the tools we have now. Furthermore, this would likely lead to replication arrest which would further confuse our interpretation of the results. Instead, we can test if gyrase activity promotes negative supercoiling at the origin of replication *in vivo* by using conditions with and without novobiocin, isolating the *oriC* region, and determining its supercoiling status under the two conditions. A method for excising “chromatin circles” which include a region of interest (in our case *oriC*) from the chromosome and determining its supercoiling status has been described (188). If this model is correct, in the absence of novobiocin, when gyrase can act, we would expect to see more negative supercoiling at *oriC*. Additionally, with novobiocin treatment (when gyrase is inhibited), we would expect negative supercoiling to be reduced at this region. If gyrase is introducing negative supercoiling at this region *in vivo*, it would not prove that this change in supercoiling is necessarily important for regulation, however it would provide further support for a model in which gyrase activity regulates DnaA binding at *oriC* through modulating the topology of that region.

2) *Gyrase introduces negative supercoiling globally, along the chromosome.*

As described above, it is difficult to tease apart the roles of gyrase at a specific site versus genome-wide. And furthermore, showing causation is difficult. However, if through the above experiment it appears that gyrase is not important for maintaining the supercoiling status of *oriC*, its role in relaxing positive supercoiling and introducing negative supercoiling along the chromosome may be a more important factor for controlling initiation timing. As replication forks proceed, changes in DNA topology and topoisomerase activity along the chromosome may be important for communicating the status of replication progression to the origin of replication. Furthermore, gyrase activity genome-wide may regulate DnaA activity at *oriC*.

3) *Gyrase association with oriC prevents cooperative DnaA oligomerization.*

Another, not mutually exclusive, mechanism for gyrase-mediated inhibition of DnaA oligomerization could be through formation of a physical barrier. Gyrase association with DnaA-boxes and surrounding sites could prevent DnaA oligomerization at *oriC*. It is not clear whether gyrase binds to and modifies the topology of the origin of replication. However, based on its function in DNA remodeling in cells, and *in vivo* work showing a correlation between increased negative supercoiling and increased DNA gyrase binding near the origin in *E. coli* (189) it is not unlikely that gyrase would associate with this region. In order to test gyrase binding to *oriC*, Chromatin Immunoprecipitation (ChIP) experiments can be performed. It is possible that even if gyrase preferentially associates with this region, if this association is transient, the detection of gyrase at this region may be difficult. Averaging relative gyrase association with *oriC* from a population of cells that are each initiating replication at different times may weaken any potential signal for gyrase enrichment at *oriC*. As such, it would be useful to perform these experiments in synchronized cells, and to harvest cultures at multiple time points (including: prior to initiation

release, multiple time points following the initiation of replication, and at multiple other time points throughout the cell cycle).

4) *Gyrase interactions with DnaA prevent cooperative DnaA association at oriC.*

There are various DnaA regulators that control replication initiation in *B. subtilis* by interacting with and preventing DnaA from binding cooperatively to the origin of replication. Based on this, it is plausible that direct interactions between gyrase and DnaA could be inhibiting DnaA oligomerization at *oriC*. To our knowledge, such an interaction has not been described in the literature. Based on the well-studied role of gyrase in altering DNA topology, and the importance of DNA topology for DNA replication, it is more likely that changes in supercoiling are impacting DnaA association at *oriC*. However, further experiments would need to be performed to test this model. Co-immunoprecipitations and 2-hybrid analyses could be used to test for *in vivo* interactions between gyrase and DnaA.

When is gyrase inhibiting DnaA binding to *oriC*?

The experiments where I observed clear initiation phenotypes with gyrase inhibition were performed in asynchronous populations of cells. I measured averages for the origin-to-terminus ratios, DnaA ChIPs, and survival assays, where within a given culture every cell is initiating replication at a different time. Due to this, I was unable to determine if gyrase inhibition is important for initiation control during the entire cell cycle or at a specific time interval. An open question that stems from my thesis work is: at what step during initiation does gyrase control initiation?

There are several ways to address this question. A simple way to test the impact of gyrase activity on initiation control at different time points during DNA replication would be to perform the above experiments with and without novobiocin, but in synchronized cells, with DnaA temperature sensitive (Ts) mutants. Shifting between permissive and non-permissive temperatures allows for initiation of replication to be synchronized within a population of Ts mutants. Another exciting

approach would be to visualize and quantify DnaA binding to *oriC* in the presence and absence of novobiocin, and at different time points (prior to replication initiation, during replication initiation, replication elongation, and replication termination). The Graumann lab has developed a series of strains where both DnaA and the origin of replication are fluorescently labeled (190). The origin is marked through fluorescently labeled LacI proteins that bind to *lacO* arrays inserted near *oriC* (190). These markers would be useful in temperature-sensitive initiation mutants that can be synchronized. Using these strains, with and without novobiocin treatment (where gyrase is active or inactive), we can perform microscopy to better understand if gyrase activity controls DnaA binding at *oriC* throughout the entire replication cycle or whether it is at a specific time.

Does topoisomerase I activity regulate replication initiation?

Based on the involvement of gyrase in regulating DnaA activity at *oriC* (187) and the opposing activities of gyrase and topoisomerase I (142), it is plausible that topoisomerase I may also serve as a regulator of replication initiation. We still do not understand the mechanism of how gyrase activity could alter DnaA-dependent initiation. However, if it is through introducing negative supercoiling, it is plausible that opposing topoisomerase I activity (relaxing negative supercoiling) may also be important for controlling replication initiation frequency – and fine tuning the timing of this process.

There is *in vivo* work indicating that topoisomerase I may alter initiation of replication – however a thorough investigation of this has not yet been performed. Deletion of the gene encoding for topoisomerase I in *E. coli* increases negative supercoiling and suppresses the temperature sensitivity of *dnaA46* replication initiation mutants (183). It would be interesting to further test if topoisomerase I is important for initiation timing by comparing initiation phenotypes for wild-type and deletion mutants, with origin-to-terminus ratios and DnaA ChIPs at *oriC*. My

prediction is that if topoisomerase I is important for initiation control, due to its role in opposing DNA gyrase activity, it would act as a positive regulator of DnaA.

4.2 Mechanism of TC-NER mediated mutagenesis

Building on the work of a previous graduate student in our lab, Sam Million-Weaver, I continued to investigate the mechanism behind transcription and TC-NER mediated mutagenesis. My preliminary results rely heavily on genetic-based approaches and could be complemented well with more biochemical approaches. Therefore, there is much more work to be done to further test our models. In the sections below, I will go through the questions we are still trying to answer and various experiments that could help address them.

Which DNA polymerases can perform error-prone gap filling at TC-NER sites?

Previous, *in vitro* work was done with *E. coli* proteins to test the ability of various polymerases to perform TC-NER gap-filling (116, 117). From these studies, Pol I was shown to incorporate nucleotides on the TC-NER substrates and the other polymerases tested (DNA Polymerase III, T4 polymerase, and Klenow) were ruled out. In these experiments, however, TLS polymerases were not tested. Based on our preliminary mutation rate analyses showing that Pol I, TLS polymerases, and TC-NER are epistatic, it is worth further investigating TLS polymerase activity on TC-NER substrates.

To measure if TLS polymerases increase repair synthesis at TC-NER sites, gap-filling can be quantified using an established *in vitro* method (197). To do this, cell-free extract (CFE) can be isolated from: WT cells (positive control), Δ*uvrA* mutants (negative control, no TC-NER), as well as single, double, and triple polymerase mutants (Pol I, YqjH, YqjW). CFE from these strains can be incubated with UV-treated and undamaged plasmid (pDR3274), which contains a single highly expressed gene, *uvrC*, in the presence and absence of rifampicin (to turn transcription of

uvrC off and on, respectively). As an indication of gap filling, incorporation of radiolabeled nucleotides at *uvrC* can be measured using autoradiography. Based on previous studies, we expect that deletion of Pol I should reduce gap filling. I predict that deletion of both TLS polymerases will also decrease gap filling, and that deletion of Pol I in addition to TLS polymerases will result in the same decrease in repair synthesis. As a control, TC-NER mediated gap filling should be abolished in the presence of rifampicin.

Which DNA polymerases are enriched at TC-NER sites?

Using a genetic approach, we have supporting evidence for Pol I and TLS polymerases acting in the same pathway as TC-NER. In support of our work in *B. subtilis*, *in vitro* work in mammalian cells shows that the TLS polymerase, Pol Kappa, fills in gaps at NER sites (196). However, we still lack direct evidence that these polymerases act at the repair-synthesis step of bacterial TC-NER. To further investigate the role of Pol I and TLS polymerases in TC-NER mediated mutagenesis, it would be useful to test if these polymerases are enriched at TC-NER sites. If these polymerases are filling in gaps at TC-NER sites, we would expect to observe enrichment of these polymerases at TC-NER sites *in vivo*.

In vitro Chromatin Immunoprecipitation (ChIP) experiments can be used to measure enrichment of polymerases at a TC-NER site. To do this, *B. subtilis* cell free extract (CFE) must be isolated from strains with His-tagged YqjH, YqjW and Pol I in either the wild-type background or in strains lacking TC-NER (*mfd* deletion). CFE can then be incubated with an established transcription-repair substrate: UV-irradiated pDR3274, which contains a highly transcribed gene, *uvrC* (197). UV-treatment increases lesions that stall RNAP, increasing our ability to detect TC-NER polymerases at *uvrC*. Experiments should be performed with UV-treated and untreated (control) plasmid, in the presence and absence of rifampicin, which will inhibit transcription of *uvrC*. Polymerase association at *uvrC* (+/- transcription, +/- UV treatment) can be measured by ChIP-

sequencing. As a control, RNA polymerase (RNAP) enrichment at *uvrC* should be measured to confirm RNA polymerase stalling. I predict that both Pol I and TLS polymerases will be enriched at the *uvrC* gene, and that this will be both transcription and Mfd dependent. If enrichment of these polymerases is abolished in the absence of Mfd, this will more directly show that these polymerases are working downstream of transcription-coupled lesion recognition.

An alternative, *in vivo* approach can also be used to test for polymerase activity during TC-NER. This can be done by tagging the TLS polymerases with fluorescent proteins and using single cell microscopy to quantify foci formation (TLS polymerase association on the chromosomal DNA) in wild-type cells that have TC-NER (which have Mfd and stalled RNA polymerases) and in TC-NER mutants that do not have Mfd. In wild-type cells we predict to see TLS polymerase activity (i.e. foci), however in *mfd* deletion mutants, and *rpoB** mutants, where TC-NER cannot occur or is greatly reduced, we predict that TLS polymerase foci will be reduced. If there is a reduction in TLS polymerase activity (foci formation) under these conditions, this will provide further evidence to support our model that these TLS polymerases are acting through the TC-NER pathway.

How are polymerases recruited to TC-NER sites?

Lastly, an open question that we would like to address is how polymerases are recruited to TC-NER sites. Are polymerases able to directly associate with TC-NER intermediates? *In vitro*, we know that DNA polymerase I can fill the 12-13 nucleotide gaps. However, *in vivo*, there are many other factors to consider. For instance, there may be other proteins that are necessary for the efficient recruitment of polymerases to these sites. If so, this type of regulation could be through polymerase interactions with the β-clamp, single-stranded DNA binding proteins coating these exposed fragments to recruit polymerases. Or DNA polymerase I may directly bind these sites, and through its known interactions with TLS polymerases, recruit them for gap filling.

As described above, there are many possible models for how polymerase recruitment might occur *in vivo*. To test these, interaction mutants can be made and compared to wild-type and deletion strains to determine the impact of these interactions on: 1) the mutational signature of highly transcribed genes, 2) mutation rates of a highly transcribed genes, and 3) polymerase association at highly transcribed regions by *in vitro* and *in vivo* ChIPs.

What is the mutational footprint of TC-NER?

In order to supplement the genetic approach from my preliminary results, measuring mutation rates of TC-NER and polymerase mutants, it would be useful to know what kinds of mutations are introduced during TC-NER. By determining the mutational signature of highly transcribed (head-on and co-directional) genes, we can learn how transcription-dependent repair mechanisms are mutagenic. Furthermore, it can help us identify the polymerases responsible for transcription-dependent mutagenesis, which have well characterized mutational footprints. One way to test this using a non-biased, highly sensitive approach is to use maximum-depth sequencing (191). This error-corrected, high-throughput sequencing method is preferred over other sequencing techniques because of its ability to detect extremely rare mutations within a population, in the absence of selection.

By identifying mutations enriched in WT cells that are absent in TC-NER and polymerase mutant backgrounds we can infer the mutational footprint of TC-NER (i.e. the types of mutations caused by this repair pathway) and identify which polymerases might be filling in gaps at TC-NER sites. Do the types of mutations enriched at highly transcribed genes align with the mutational signature of a specific error-prone polymerase? Furthermore, maximum depth sequencing can be used to address the following questions: 1) What is the mutational footprint of TC-NER? 2) Is the mutational footprint of TC-NER dependent on Pol I and/or TLS polymerases?

The mutational footprint of TLS polymerases is well-characterized. We also know that TLS polymerase-dependent mutagenesis in *B. subtilis* is dependent on Pol I. Based on these, if the polymerases are working together at TC-NER sites, I would expect the mutational signature of TC-NER to match the mutational signature of the TLS polymerases. Based on work on TLS polymerases in *E. coli*, these mutations would likely include a high frequency of -1 frameshifts, T→G, T→A, and G→T transversions, and T→C and A→G transitions (192–195).

CHAPTER 5. Materials and Methods

Table 5.1 Strain List

Strain	Relevant Genotype	Reference
HM1 (JH642)	*trpC2*, *pheA1* (Wild Type)	Perego et al., 1988 (198)
HM 345	*trpC2, pheA1 yqjW::cat*	Million-Weaver et al., 2015
HM 391	*trpC2, pheA1 yqjH::cat*	Million-Weaver et al., 2015
HM2 (AIG109)	*trpC2*, *pheA1 yabA*::*cat*	Goranov et al., 2009 (199)
HM3 (AIG80)	*trpC2*, *pheA1*, *amyE*::[$P_{spank(hy)}$-*yabA spec*^{R}]	Goranov et al., 2009 (199)
HM77 (MMB170)	*trp*$^+$ *pheA1 122 spoIIIJ*::[*oriN repN kan*] *oriC-S*	Goranov et al., 2009 (199)
HM78 (AIG185)	*trp*$^+$ *pheA1 122 spoIIIJ*::[*oriN repN kan*] *oriC-S yabA*::*cat*	Goranov et al., 2009 (199)
HM89	*yabA*::*cat amyE*::[$P_{spank(hy)}$-*yabA*(N85D) *spec*^{R}]	Samadpour et al., 2018 (187)
HM313 (LAS40)	*recA-mgfp-mut2(A206K)-spec*	Simmons et al., 2007 (200)
HM 2632	*trpC2, pheA1 yqjW::cat yqjH::Er*	Unpublished
HM 2633	*trpC2, pheA1 uvrA::Er*	Unpublished
HM 2634	*trpC2, pheA1 uvrB::Er*	Unpublished
HM 2635	*trpC2, pheA1 uvrC::Er*	Unpublished
HM 2521	*trpC2, pheA1 mfd::Er*	Unpublished
HM 2472	*trpC2, pheA1 Δmfd uvrA::Er*	Unpublished
HM 2473	*trpC2, pheA1 Δmfd uvrB::Er*	Unpublished

HM 2474	*trpC2, pheA1 Δmfd uvrC::Er*	Unpublished
HM 2666	*trpC2, pheA1 yqjW::cat ΔyqjH uvrA::Er*	Unpublished
HM 2667	*trpC2, pheA1 yqjW::cat ΔyqjH uvrB::Er*	Unpublished
HM 2668	*trpC2, pheA1 yqjW::cat ΔyqjH uvrC::Er*	Unpublished
HM 2669	*trpC2, pheA1 yqjW::cat ΔyqjH mfd::Er*	Unpublished
HM3387	*trpC2*, *pheA1*, *gyrB*(R138L)	Samadpour et al., 2018 (187)
HM 3533	*trpC2, pheA1 polA::Er*	Unpublished
HM 3548	*trpC2, pheA1 yqjW::cat polA::Er*	Unpublished
HM 3549	*trpC2, pheA1 yqjH::cat polA::Er*	Unpublished
HM 3550	*trpC2, pheA1 Δmfd polA::Er*	Unpublished
HM 3567	*trpC2, pheA1 yqjW::cat ΔyqjH polA::Er*	Unpublished

Table 5.2 Primer List

Primer	Sequence
HM20	5` – CGAAAAGAGGATTGTCCTTTCTGTCTGTCATTC – 3`
HM21	5` –GAATGACAGACAGAAAGGACAATCCTCTTTTCG – 3`
HM192	5`- CCGTCTGACCCGATCTTTTA -3`
HM193	5`-GTCATGCTGAATGTCGTGCT -3`
HM457	5’ - ACCATTGCAAGCTCTCGTTT - 3’
HM458	5’- CCACACTTTGTGGATAAAGAGGA -3’
HM459	5’- GGGAAAGTGTGAATAACTTTTCG -3’
HM460	5’- GTAGGGCCTGTGGATTTGTG -3’
HM770	5` - TCTCCAGCTGTGATAAACGGTA – 3`
HM771	5` - AAAACGGCATTGATTTGTCA – 3`
HM1583	5` – GATCAATCGGGGAAAGTGTG – 3`
HM1584	5` – GTAGGGCCTGTGGATTTGTG – 3`
HM1585	5` – TCCATATCCTCGCTCCTACG – 3`
HM1586	5` – ATTCTGCTGATGTGCAATGG – 3`
HM2510	5` – GAATTCCTTCAGGCCATTGA – 3`
HM2511	5` – GATTTCTGGCGAATTGGAAG – 3`
HM2967	5`- GCAGCTGGGGGATTTGAAGC -3`
HM2968	5`- GTCCAGCCGTTTGCGCAAATG -3`

HM2995	5`- GCCAATCACTATTTCGGCCGGG -3`
HM2996	5`- GCTGCTTTTCAAGGCTTGTCC -3`
HM3011	5` – GTCGAGATGGTGGCGATCG – 3`
HM3012	5` –CGCGGCATGTCTCTGAGTAC – 3`
HM3015	5` – GATACGGCATTACAGCATGC – 3`
HM3016	5` – GCTTTTAATCAGAATGAGCTGTCC – 3`
HM3017	5` – GTGCTCACTGAAGACGATCTTCCC – 3`
HM3018	5` – CATCTTCTTGAAGGGTTCCGAC – 3`
HM3021	5` – CGTTTGTAAGAGGGGCGCACC – 3`
HM3022	5` –GGTGATTGCGTCATGATCCGTACC – 3`
HM4654	5`- CCTGTGGAACCAAGCCCTTGCTC -3`
HM4655	5`- GGCAAATTCATTGGGAGCCGTG -3`
HM4855	5` – GCTGTCAAGTGGACATGTC – 3`
HM4856	5` – GTATTCGCGGTGTGAAAACCTTG – 3`
HM4849	5`- TAACGGACAGGAATGCCTGT -3`
HM4850	5`ACGGCCTTTTTCGTGACATC -3`
HM4853	5` – CCTTATCGTTCGGTATCGTC – 3`
HM4854	5` – GCTTTGCAATGCGC TTG – 3`

Bacterial culture conditions. Cells were grown overnight at 378C on Luria–Bertani (LB) agar plates supplemented with 10 μg/ml chloramphenicol, 100 μg/ml spectinomycin, 5 μg/ml kanamycin or 500 μg/ml erythromycin and 12.5 μg/ml lincomycin, when appropriate. Cultures were started from single colonies and grown at 30°C or 37°C with aeration (260 rotations per minute), in LB broth, supplemented with 5 μg/ml chloramphenicol, 50 μg/ml spectinomycin, 2.5 μg/ml kanamycin or 250 ng/ml erythromycin and 6.25 μg/ml lincomycin, when appropriate. Sporulating cells were prepared by growing cells in 2 ml LB media at 37°C with aeration (260 rotations per minute). Mid-exponential phase cultures (OD 0.3–0.5) were pelleted, LB supernatant was removed, and cells were back diluted (to OD 0.05) into 10 ml of sporulation media, using a previously described recipe (201). Cells were grown for 18.5 hours, harvested in methanol (1:1 ratio), and pelleted for genomic DNA extraction.

Plating efficiencies. Cultures were started from single colonies and grown at 37°C with aeration (260 rotations per minute) in LB media. Cultures were grown to OD 0.3, and serial dilutions were plated on LB alone and LB supplemented with varying concentrations of novobiocin or MMC. Plates were incubated at 30°C. Total viable cells were quantified after 24–72 hours of incubation. Novobiocin concentrations used include: 0.45, 0.55, 0.65, 0.75 and 0.85 μg/ml. Mitomycin C concentrations used include: 20 and 30 ng/ml.

Origin-to-Terminus Ratios and Marker Frequency Analysis. Cultures were started from single colonies and grown at 37°C with aeration (260 rotations per minute) in LB media. Cultures were grown to exponential phase (optical density 0.3-0.5), set back to OD 0.05 in LB media and grown at 30°C. Cultures were grown to OD 0.2, divided into 5mL cultures with no treatment, 0.50 μg/mL novobiocin, 0.75 μg/mL novobiocin, and 1 μg/mL Mitomycin C. After 40 minutes of growth at 30°C, cells were harvested in methanol (1:1 ratio) and pelleted. Genomic DNA was isolated by phenol-

chloroform extractions. The copy number of the origin and terminus were quantified by quantitative PCR (qPCR). QPCR was done using SSoAdvanced SYBR Green master mix and CFX96 Touch Real-Time PCR system (Bio-Rad).

Primers used to amplify the origin and terminus were the same as previously described (202). Quantification of *oriC* was done using primers: HM1583 and HM1584. Quantification of the origin in strains that initiate replication at *oriN* was done using primers: HM2510 and HM2511. Quantification of the terminus region was done using primers: HM1585 and HM1586. Origin-to-terminus ratios were determined by dividing the number of sequence reads (as indicated by the Cq values measured through qPCRs) from the origin by the number of sequence reads quantified at the terminus. Ratios were normalized to the origin-to-terminus ratio of sporulating *B. subtilis* cells, which were quantified using primers HM1583 and HM1584.

For marker frequency analysis, quantification of DNA at six additional chromosomal positions was measured: 22.5°, 45°, 135°, 225°, 315°, 337.5°. Primers HM4853 and HM4854 amplify DNA at position 22.5°. HM3011 and HM3012 amplify DNA at position 45°. Primers HM3015 and HM3016 amplify DNA at position 135°. Primers HM3017 and HM3018 amplify DNA at position 225°. Primers HM3021 and HM3022 amplify DNA at position 315°. Primers HM4855 and HM4856 amplify DNA at position 337.5°. Marker frequency ratios were determined by dividing the number of sequence reads quantified at each site (as indicated by the Cq values measured through qPCRs) by the number of sequence reads quantified at the terminus (using primers HM1585 and HM1586). These values were normalized to ratios measured for sporulating *B. subtilis* cells.

Chromatin Immunoprecipitations. Cultures were started from single colonies and grown at 37°C with aeration (260 rotations per minute) in LB media. Cultures were grown to exponential phase (optical density 0.3-0.5), set back to OD 0.05 in 25 mL LB media and grown at 30°C. After

reaching OD 0.2, cultures were grown for 40 more minutes at 30°C with no treatment or 0.75 µg/mL novobiocin. Cultures were processed for ChIPs as described (108). ChIPs were performed using 2 µl anti-DnaA rabbit polyclonal antiserum (18). Quantitative PCR was done using SSoAdvanced SYBR green master mix and Bio-Rad CFX96 Touch Real-Time PCR system. DnaA association at the DNA unwinding element (DUE) was normalized to DnaA association at *yhaX*, a control locus that does not have increased DnaA association. Enrichment of the DUE was detected using primers HM459 and HM460. Enrichment upstream of *dnaA* (referred to in the text as P*dnaA*) was done using primers HM457 and HM458. Enrichment of *yhaX* was detected using primers HM192 and HM193.

DNA Sequencing. Cultures were prepared as described under the "origin-to-terminus ratios" section. Whole genomic DNA was sonicated using a Covaris ultrasonicator and sequenced on an Illumina Next-Seq yielding approximately 15 million reads. Reads were mapped to the *B. subtilis* strain JH642 (GenBank: CP007800.1) genome using Bowtie 2 (203). The resulting sam file was processed using SAMtools, view, and sort functions. PCR and optical duplicates were then removed using Picard (204). The resulting .sam file was processed by SAMtools mpileup functions to produce wiggle plots. To account for differences in read depth between samples, the signal at each base position was normalized to total signal for the genome. The resulting total-normalized wiggle files were then visualized in MochiView.

Quantification of RNA Levels. RNA levels were quantified by growing cultures from single colonies at 37°C with aeration (260 rotations per minute) in LB media. Cultures were grown to exponential phase (optical density 0.3-0.5), set back to OD 0.05 in LB media (with and without 1mM IPTG), and grown to OD=0.3. Cultures were mixed with ice-cold Methanol (1:1 ratio). Cells were pelleted and RNA was extracted using the Thermo Scientific GeneJET RNA Purification kit. DNase was added to 1µg RNA samples for 30 minutes at 37°C, and inactivated by adding 1µL

EDTA to the reaction and incubating at 65°C for 10 minutes. Reverse Transcriptase PCR was performed to make cDNA. Samples were diluted 1:5 and qPCR was performed using the housekeeping gene *dnaK* as a control locus. QPCR was done using SSoAdvanced SYBR Green master mix and CFX96 Touch Real-Time PCR system (Bio-Rad). Primers to amplify *dnaK* were HM770 and HM771. Primers to amplify *yabA* were HM2967 and HM2968. Primers to amplify *sirA* were HM2995 and HM2996. Primers to amplify *spo0A* were HM4849 and HM4850. Primers to amplify *dnaA* were HM4654 and HM4655.

Replica Plating. Wild-type exponential phase cells were plated on novobiocin. After 24-48 hours of incubation at 30°C, colony forming units were quantified. Using sterile velvet cloths, cells were transferred to LB plates and incubated overnight. The number and location of colonies was recorded and compared to what was observed on the antibiotic plates.

Microscopy. Cultures were started from single colonies and grown at 37°C with aeration (260 rotations per minute) in LB media. Cultures were grown to exponential phase (optical density 0.3-0.5), set back to OD 0.05 in LB media and grown at 30°C. Cultures were grown to OD 0.2, divided into 5 mL cultures with no treatment, 0.50 µg/mL novobiocin. Cells were then fixed with 4% formaldehyde (vol/vol), stained with DAPI (4-,6-diamidino-2-phenylindole), and transferred to 1% agarose pads for visualization by microscopy. Images were taken using a Leica inverted microscope with CCD camera fitted with a 60× oil objective. DAPI fluorescence was used to quantify total cells and GFP fluorescence was used to quantify total RecA-GFP foci. DAPI-stained nucleoids and RecA-GFP foci were counted using ImageJ. At least 2,000 cells from 3 biological replicates were counted per condition.

Strain Construction. *Bacillus subtilis* strains are isogenic with the strain JH642, and contain the *trpC2* and *pheA1*alleles, unless indicated otherwise. New strains were confirmed by PCR and

sequencing. HM89 was constructed using site-directed mutagenesis by a previously described method (205). Primers HM20 and HM21 were used to make the point mutation. This point mutation has been made and characterized by Noirot-Gros and colleagues (176). The gyrase mutant (HM3387) was isolated by plating a large saturated culture of wild type *B. subtilis* onto LB supplemented with 4 µg/mL novobiocin. The mutation in *gyrB*, R138L, was identified by amplification of *gyrB* by PCR, followed by sequencing. The *parE* gene was also amplified and sequenced. As expected, no mutations in this gene were found.

Mutation Rates. Cultures were grown from single colonies at 37°C with aeration (260 rotations per minute) in 18-mm culture tubes containing 2mL LB media. Exponential phase cultures (OD = 0.3) were diluted back to OD = 0.0005 into 10 parallel cultures containing 3mL LB broth, and plated following 4.5 hours of growth at 37°C with aeration (260 rotations per minute). 1.5 mL of each culture were plated on 50 µg/mL rifampicin to quantify the number of *rpoB* mutants that confer Rifampicin resistance and serially diluted and plated on LB to quantify total viable cells. Colonies were quantified after overnight incubation at 37°C (for rifampicin plates) and 30°C (for LB plates). Mutation rates were calculated using the Fluctuation Analysis Calculator (206), which utilizes the Ma-Sandri-Sarkar Maximum Likelihood method.

References

1. **Mangiameli SM**, **Veit BT**, **Merrikh H**, **Wiggins PA**. 2017. The Replisomes Remain Spatially Proximal throughout the Cell Cycle in Bacteria. PLoS Genet **13**.
2. **Kubitschek HE**, **Freedman ML**. 1968. Chromosome replication and the division cycle of Escherichia coli. J Mol Biol **31**:519–540.
3. **Ogawa T**, **Okazaki T**. 1980. Discontinuous DNA Replication. Annu Rev Biochem **49**:421–457.
4. **Wu CA**, **Zechner EL**, **Marians KJ**. 1992. Coordinated leading- and lagging-strand synthesis at the Escherichia coli DNA replication fork: I. Multiple effectors act to modulate Okazaki fragment size. J Biol Chem **267**:4030–4044.
5. **Beattie TR**, **Reyes-Lamothe R**. 2015. A replisome's journey through the bacterial chromosome. Front Microbiol.
6. **Sakamoto Y**, **Nakai S**, **Moriya S**, **Yoshikawa H**, **Ogasawara N**. 1995. The Bacillus subtilis dnaC gene encodes a protein homologous to the DnaB helicase of Escherichia coli. Microbiology **141**:641–644.
7. **Marceau AH**. 2012. Functions of single-strand DNA-binding proteins in DNA replication, recombination, and repair. Methods Mol Biol **922**:1–21.
8. **Fuller RS**, **Funnell BE**, **Kornberg A**. 1984. The dnaA protein complex with the E. coli chromosomal replication origin (oriC) and other DNA sites. Cell **38**:889–900.
9. **Rozgaja TA**, **Grimwade JE**, **Iqbal M**, **Czerwonka C**, **Vora M**, **Leonard AC**. 2011. Two oppositely oriented arrays of low-affinity recognition sites in oriC guide progressive binding of DnaA during Escherichiacoli pre-RC assembly. Mol Microbiol **82**:475–488.

10. **Kaur G**, **Vora MP**, **Czerwonka CA**, **Rozgaja TA**, **Grimwade JE**, **Leonard AC**. 2014. Building the bacterial orisome: High-affinity DnaA recognition plays a role in setting the conformation of oriC DNA. Mol Microbiol **91**:1148–1163.

11. **Krause M**, **Rückert B**, **Lurz R**, **Messer W**. 1997. Complexes at the replication origin of Bacillus subtilis with homologous and heterologous DnaA protein. J Mol Biol **274**:365–380.

12. **Smits WK**, **Goranov AI**, **Grossman AD**. 2010. Ordered association of helicase loader proteins with the Bacillus subtilis origin of replication in vivo. Mol Microbiol **75**:452–461.

13. **Bramhill D**, **Kornberg A**. 1988. Duplex opening by dnaA protein at novel sequences in initiation of replication at the origin of the E. coli chromosome. Cell **52**:743–755.

14. **Kowalski D**, **Eddy MJ**. 1989. The DNA unwinding element: a novel, cis-acting component that facilitates opening of the Escherichia coli replication origin. Embo J **8**:4335–4344.

15. **Moriya S**, **Atlung T**, **Hansen FG**, **Yoshikawa H**, **Ogasawara N**. 1992. Cloning of an autonomously replicating sequence (ars) from the Bacillus subtilis chromosome. Mol Microbiol **6**:309–315.

16. **Schaper S**, **Messer W**. 1995. Interaction of the initiator protein DnaA of Escherichia coli with its DNA target. J Biol Chem **270**:17622–17626.

17. **McGarry KC**, **Ryan VT**, **Grimwade JE**, **Leonard AC**. 2004. Two discriminatory binding sites in the Escherichia coli replication origin are required for DNA strand opening by initiator DnaA-ATP. Proc Natl Acad Sci **101**:2811–2816.

18. **Smith JL**, **Grossman AD**. 2015. In Vitro Whole Genome DNA Binding Analysis of the Bacterial Replication Initiator and Transcription Factor DnaA. PLoS Genet **11**:e1005258.

19. **Leonard AC**, **Grimwade JE**. 2011. Regulation of DnaA Assembly and Activity: Taking Directions from the Genome. Annu Rev Microbiol **65**:19–35.

20. **Miller DT**, **Grimwade JE**, **Betteridge T**, **Rozgaja T**, **Torgue JJ-C**, **Leonard AC**. 2009. Bacterial origin recognition complexes direct assembly of higher-order DnaA oligomeric structures. Proc Natl Acad Sci **106**:18479–18484.

21. **Jameson K**, **Wilkinson A**. 2017. Control of Initiation of DNA Replication in Bacillus subtilis and Escherichia coli. Genes (Basel) **8**:22.

22. **Kohiyama M**. 1968. DNA Synthesis in Temperature Sensitive Mutants of Escherichia coli. Cold Spring Harb Symp Quant Biol 317–324.

23. **Messer W**. 2002. The bacterial replication initiator DnaA. DnaA and oriC, the bacterial mode to initiate DNA replication. FEMS Microbiol Rev.

24. **Messer W**, **Blaesing F**, **Majka J**, **Nardmann J**, **Schaper S**, **Schmidt A**, **Seitz H**, **Speck C**, **Tüngler D**, **Wegrzyn G**, **Weigel C**, **Welzeck M**, **Zakrzewska-Czerwinska J**. 1999. Functional domains of DnaA proteins, p. 819–825. *In* Biochimie.

25. **Sutton MD**, **Kaguni JM**. 1997. The Escherichia coli dnaA gene: Four functional domains. J Mol Biol **274**:546–561.

26. **Rahn-Lee L**, **Merrikh H**, **Grossman AD**, **Losick R**. 2011. The sporulation protein SirA inhibits the binding of DnaA to the origin of replication by contacting a patch of clustered amino acids. J Bacteriol **193**:1302–1307.

27. **Jameson KH**, **Rostami N**, **Fogg MJ**, **Turkenburg JP**, **Grahl A**, **Murray H**, **Wilkinson AJ**. 2014. Structure and interactions of the Bacillus subtilis sporulation inhibitor of DNA replication, SirA, with domain I of DnaA. Mol Microbiol **93**:975–991.

28. **Nozaki S**, **Ogawa T**. 2008. Determination of the minimum domain II size of Escherichia coli DnaA protein essential for cell viability. Microbiology **154**:3379–84.

29. **Molt KL**, **Sutera VA**, **Moore KK**, **Lovett ST**. 2009. A role for nonessential domain II of initiator protein, DnaA, in replication control. Genetics **183**:39–49.

30. **Noirot-Gros MF**, **Velten M**, **Yoshimura M**, **McGovern S**, **Morimoto T**, **Ehrlich SD**, **Ogasawara N**, **Polard P**, **Noirot P**. 2006. Functional dissection of YabA, a negative regulator of DNA replication initiation in Bacillus subtilis. Proc Natl Acad Sci U S A **103**:2368–2373.

31. **Scholefield G**, **Murray H**. 2013. YabA and DnaD inhibit helix assembly of the DNA replication initiation protein DnaA. Mol Microbiol **90**:147–159.

32. **Cho E**, **Ogasawara N**, **Ishikawa S**. 2008. The functional analysis of YabA, which interacts with DnaA and regulates initiation of chromosome replication in Bacillus subtils. Genes Genet Syst **83**:111–125.

33. **Duan Y**, **Huey JD**, **Herman JK**. 2016. The DnaA inhibitor SirA acts in the same pathway as Soj (ParA) to facilitate oriC segregation during Bacillus subtilis sporulation. Mol Microbiol **102**:530–544.

34. **Roth a**, **Messer W**. 1995. The DNA binding domain of the initiator protein DnaA. EMBO J **14**:2106–2111.

35. **Fujikawa N**, **Kurumizaka H**, **Nureki O**, **Terada T**, **Shirouzu M**, **Katayama T**, **Yokoyama S**. 2003. Structural basis of replication origin recognition by the DnaA protein. Nucleic Acids Res **31**:2077–2086.

36. **Sekimizu K**, **Bramhill D**, **Kornberg A**. 1987. ATP activates dnaA protein in initiating replication of plasmids bearing the origin of the E. coli chromosome. Cell **50**:259–265.

37. **Washington TA**, **Smith JL**, **Grossman AD**. 2017. Genetic networks controlled by the bacterial replication initiator and transcription factor DnaA in Bacillus subtilis. Mol Microbiol **106**:109–128.

38. **Collier J**, **Murray SR**, **Shapiro L**. 2006. DnaA couples DNA replication and the expression of two cell cycle master regulators. EMBO J **25**:346–356.

39. **Goranov AI**, **Kuester-Schoeck E**, **Wang JD**, **Grossman AD**. 2006. Characterization of the global transcriptional responses to different types of DNA damage and disruption of replication in Bacillus subtilis. J Bacteriol **188**:5595–5605.

40. **Messer W**, **Weigel C**. 1997. DnaA initiator-also a transcription factor. Mol Microbiol **24**:1–6.

41. **Wang Q**, **Kaguni JM**. 1987. Transcriptional repression of the dnaA gene of Escherichia coli by dnaA protein. MGG Mol Gen Genet **209**:518–525.

42. **Ogura Y**, **Imai Y**, **Ogasawara N**, **Moriya S**. 2001. Autoregulation of the dnaA-dnaN operon and effects of DnaA protein levels on replication initiation in Bacillus subtilis. J Bacteriol **183**:3833–3841.

43. **Breier AM**, **Grossman AD**. 2009. Dynamic association of the replication initiator

and transcription factor DnaA with the bacillus subtilis chromosome during replication stress. J Bacteriol **191**:486–493.

44. **Katayama T**, **Ozaki S**, **Keyamura K**, **Fujimitsu K**. 2010. Regulation of the replication cycle: conserved and diverse regulatory systems for DnaA and oriC. Nat Rev Microbiol **8**:163–170.

45. **Okumura H**, **Yoshimura M**, **Ueki M**, **Oshima T**, **Ogasawara N**, **Ishikawa S**. 2012. Regulation of chromosomal replication initiation by oriC-proximal DnaA-box clusters in Bacillus subtilis. Nucleic Acids Res **40**:220–234.

46. **Nozaki S**, **Yamada Y**, **Ogawa T**. 2009. Initiator titration complex formed at datA with the aid of IHF regulates replication timing in Escherichia coli. Genes to Cells **14**:329–341.

47. **Braun RE**, **O'Day K**, **Wright A**. 1985. Autoregulation of the DNA replication gene dnaA in E. coli K-12. Cell **40**:159–169.

48. **Nishida S**, **Fujimitsu K**, **Sekimizu K**, **Ohmura T**, **Ueda T**, **Katayama T**. 2002. A nucleotide switch in the Escherichia coli DnaA protein initiates chromosomal replication. Evidence from a mutant DnaA protein defective in regulatory ATP hydrolysis in vitro and in vivo. J Biol Chem **277**:14986–14995.

49. **Donczew R**, **Mielke T**, **Jaworski P**, **Zakrzewska-Czerwińska J**, **Zawilak-Pawlik A**. 2014. Assembly of helicobacter pylori initiation complex is determined by sequence-specific and topology-sensitive DnaA-oric interactions. J Mol Biol **426**:2769–2782.

50. **Donczew R**, **Weigel C**, **Lurz R**, **Zakrzewska-Czerwińska J**, **Zawilak-Pawlik A**. 2012. Helicobacter pylori oriC-the first bipartite origin of chromosome replication

in Gram-negative bacteria. Nucleic Acids Res **40**:9647–9660.

51. **Bonilla CY**, **Grossman AD**. 2012. The primosomal protein DnaD inhibits cooperative DNA binding by the replication initiator DnaA in Bacillus subtilis. J Bacteriol **194**:5110–5117.

52. **Keyamura K**, **Katayama T**. 2011. DnaA protein DNA-binding domain binds to Hda protein to promote inter-AAA+ domain interaction involved in regulatory inactivation of DnaA. J Biol Chem **286**:29336–29346.

53. **Kasho K**, **Tanaka H**, **Sakai R**, **Katayama T**. 2017. Cooperative DnaA Binding to the Negatively Supercoiled datA Locus Stimulates DnaA-ATP Hydrolysis. J Biol Chem **292**:1251–1266.

54. **Fujimitsu K**, **Katayama T**. 2004. Reactivation of DnaA by DNA sequence-specific nucleotide exchange in vitro. Biochem Biophys Res Commun **322**:411–419.

55. **Boye E**, **Løbner-Olesen A**, **Skarstad K**. 2000. Limiting DNA replication to once and only once. EMBO Rep **1**:479–83.

56. **Leonard AC**, **Grimwade JE**. 2010. Initiation of DNA Replication. EcoSal Plus **4**.

57. **Rahn-Lee L**, **Gorbatyuk B**, **Skovgaard O**, **Losick R**. 2009. The conserved sporulation protein YneE inhibits DNA replication in Bacillus subtilis. J Bacteriol **191**:3736–3739.

58. **Wagner JK**, **Marquis KA**, **Rudner DZ**. 2009. SirA enforces diploidy by inhibiting the replication initiator DnaA during spore formation in Bacillus subtilis. Mol Microbiol **73**:963–974.

59. **Noirot-Gros M-F**, **Dervyn E**, **Wu LJ**, **Mervelet P**, **Errington J**, **Ehrlich SD**,

Noirot P. 2002. An expanded view of bacterial DNA replication. Proc Natl Acad Sci U S A **99**:8342–8347.

60. **Merrikh H**, **Grossman AD**. 2011. Control of the replication initiator DnaA by an anti-cooperativity factor. Mol Microbiol **82**:434–446.

61. **Soufo CD**, **Soufo HJD**, **Noirot-Gros MF**, **Steindorf A**, **Noirot P**, **Graumann PL**. 2008. Cell-Cycle-Dependent Spatial Sequestration of the DnaA Replication Initiator Protein in Bacillus subtilis. Dev Cell **15**:935–941.

62. **Ishigo-Oka D**, **Ogasawara N**, **Moriya S**. 2001. DnaD protein of Bacillus subtilis interacts with DnaA, the initiator protein of replication. J Bacteriol **183**:2148–2150.

63. **Smits WK**, **Merrikh H**, **Bonilla CY**, **Grossman AD**. 2011. Primosomal proteins DnaD and DnaB are recruited to chromosomal regions bound by DnaA in Bacillus subtilis. J Bacteriol **193**:640–648.

64. **Scholefield G**, **Whiting R**, **Errington J**, **Murray H**. 2011. Spo0J regulates the oligomeric state of Soj to trigger its switch from an activator to an inhibitor of DNA replication initiation. Mol Microbiol **79**:1089–1100.

65. **Scholefield G**, **Errington J**, **Murray H**. 2012. Soj/ParA stalls DNA replication by inhibiting helix formation of the initiator protein DnaA. EMBO J **31**:1542–55.

66. **Camara JE**, **Breier AM**, **Brendler T**, **Austin S**, **Cozzarelli NR**, **Crooke E**. 2005. Hda inactivation of DnaA is the predominant mechanism preventing hyperinitiation of Escherichia coli DNA replication. EMBO Rep **6**:736–741.

67. **Schaaper RM**. 1993. Base selection, proofreading, and mismatch repair during DNA replication in Escherichia coli. J Biol Chem **268**:23762–23765.

68. **Fijalkowska IJ**, **Schaaper RM**, **Jonczyk P**. 2012. DNA replication fidelity in

Escherichia coli: A multi-DNA polymerase affair. FEMS Microbiol Rev.

69. **Kunkel TA**. 2004. DNA Replication Fidelity. J Biol Chem.

70. **Lenhart JS**, **Pillon MC**, **Guarné A**, **Biteen JS**, **Simmons LA**. 2016. Mismatch repair in Gram-positive bacteria. Res Microbiol.

71. **Foster PL**. 2007. Stress-induced mutagenesis in bacteria. Crit Rev Biochem Mol Biol.

72. **Galhardo RS**, **Hastings PJ**, **Rosenberg SM**. 2007. Mutation as a stress response and the regulation of evolvability.Critical reviews in biochemistry and molecular biology.

73. **Fonville NC**, **Ward RM**, **Mittelman D**. 2012. Stress-induced modulators of repeat instability and genome evolution. J Mol Microbiol Biotechnol.

74. **Battesti A**, **Majdalani N**, **Gottesman S**. 2011. The RpoS-mediated general stress response in Escherichia coli. Annu Rev Microbiol **65**:189–213.

75. **Patten CL**, **Kirchhof MG**, **Schertzberg MR**, **Morton RA**, **Schellhorn HE**. 2004. Microarray analysis of RpoS-mediated gene expression in Escherichia coli K-12. Mol Genet Genomics **272**:580–591.

76. **Layton JC**, **Foster PL**. 2003. Error-prone DNA polymerase IV is controlled by the stress-response sigma factor, RpoS, in Escherichia coli. Mol Microbiol **50**:549–561.

77. **Radman M**. 1975. SOS repair hypothesis: phenomenology of an inducible DNA repair which is accompanied by mutagenesis. Basic Life Sci 355–67.

78. **Schlacher K**, **Goodman MF**. 2007. Lessons from 50 years of SOS DNA-damage-induced mutagenesis. Nat Rev Mol Cell Biol.

79. **Gudas LJ**, **Pardee a B**. 1975. Model for regulation of Escherichia coli DNA repair functions. Proc Natl Acad Sci U S A **72**:2330–2334.

80. **Gudas LJ**, **Pardee AB**. 1976. DNA synthesis inhibition and the induction of protein X in Escherichia coli. J Mol Biol **101**:459–477.

81. **Brent R**, **Ptashne M**. 1981. Mechanism of action of the lexA gene product. Proc Natl Acad Sci U S A **78**:4204–8.

82. **Courcelle J**, **Khodursky A**, **Peter B**, **Brown PO**, **Hanawalt PC**. 2001. Comparative Gene Expression Profiles Following UV Exposure in Wild-Type and SOS-Deficient Escherichia coli Genetics **158**:41 LP-64.

83. **Hauryliuk V**, **Atkinson GC**, **Murakami KS**, **Tenson T**, **Gerdes K**. 2015. Recent functional insights into the role of (p)ppGpp in bacterial physiology. Nat Rev Microbiol.

84. **Atkinson GC**, **Tenson T**, **Hauryliuk V**. 2011. The RelA/SpoT Homolog (RSH) superfamily: Distribution and functional evolution of ppgpp synthetases and hydrolases across the tree of life. PLoS One **6**.

85. **Wendrich TM**, **Blaha G**, **Wilson DN**, **Marahiel MA**, **Nierhaus KH**. 2002. Dissection of the mechanism for the stringent factor RelA. Mol Cell **10**:779–788.

86. **Gallant J**, **Palmer L**, **Pao CC**. 1977. Anomalous synthesis of ppGpp in growing cells. Cell **11**:181–185.

87. **Kanjee U**, **Ogata K**, **Houry WA**. 2012. Direct binding targets of the stringent response alarmone (p)ppGpp. Mol Microbiol **85**:1029–1043.

88. **Merrikh H**. 2017. Spatial and Temporal Control of Evolution through Replication–Transcription Conflicts. Trends Microbiol.

89. **Paul S**, **Million-Weaver S**, **Chattopadhyay S**, **Sokurenko E**, **Merrikh H**. 2013. Accelerated gene evolution through replication-transcription conflicts. Nature **495**:512–5.

90. **Rocha EPC**, **Danchin A**. 2003. Gene essentiality determines chromosome organisation in bacteria. Nucleic Acids Res **31**:6570–6577.

91. **Rocha EPC**. 2004. The replication-related organization of bacterial genomes. Microbiology.

92. **Jaskunas SR**, **Nomura M**. 1977. Organization of ribosomal protein genes of Escherichia coli as analyzed by polar insertion mutations. J Biol Chem **252**:7337–7343.

93. **Brewer BJ**. 1988. When polymerases collide: Replication and the transcriptional organization of the E. coli chromosome. Cell.

94. **Guy L**, **Roten CAH**. 2004. Genometric analyses of the organization of circular chromosomes: A universal pressure determines the direction of ribosomal RNA genes transcription relative to chromosome replication. Gene **340**:45–52.

95. **Merrikh H**, **Zhang Y**, **Grossman AD**, **Wang JD**. 2012. Replication-transcription conflicts in bacteria. Nat Rev Microbiol.

96. **Merrikh H**, **Machón C**, **Grainger WH**, **Grossman AD**, **Soultanas P**. 2011. Co-directional replication-transcription conflicts lead to replication restart. Nature **470**:554–7.

97. **Million-Weaver S**, **Samadpour AN**, **Merrikh H**. 2015. Replication restart after replication-transcription conflicts requires RecA in Bacillus subtilis. J Bacteriol **197**:2374–2382.

98. **French S**. 1992. Consequences of replication fork movement through transcription units in vivo. Science **258**:1362–1365.

99. **Mangiameli SM**, **Merrikh CN**, **Wiggins PA**, **Merrikh H**. 2017. Transcription leads to pervasive replisome instability in bacteria. Elife **6**.

100. **Sankar TS**, **Wastuwidyaningtyas BD**, **Dong Y**, **Lewis SA**, **Wang JD**. 2016. The nature of mutations induced by replication-transcription collisions. Nature **535**:178–181.

101. **Lang KS**, **Hall AN**, **Merrikh CN**, **Ragheb M**, **Tabakh H**, **Pollock AJ**, **Woodward JJ**, **Dreifus JE**, **Merrikh H**. 2017. Replication-Transcription Conflicts Generate R-Loops that Orchestrate Bacterial Stress Survival and Pathogenesis. Cell **170**:787–799.e18.

102. **Srivatsan A**, **Tehranchi A**, **MacAlpine DM**, **Wang JD**. 2010. Co-orientation of replication and transcription preserves genome integrity. PLoS Genet **6**.

103. **Hamperl S**, **Cimprich KA**. 2016. Conflict Resolution in the Genome: How Transcription and Replication Make It Work. Cell.

104. **Trautinger BW**, **Jaktaji RP**, **Rusakova E**, **Lloyd RG**. 2005. RNA polymerase modulators and DNA repair activities resolve conflicts between DNA replication and transcription. Mol Cell **19**:247–258.

105. **Tehranchi AK**, **Blankschien MD**, **Zhang Y**, **Halliday JA**, **Srivatsan A**, **Peng J**, **Herman C**, **Wang JD**. 2010. The Transcription Factor DksA Prevents Conflicts between DNA Replication and Transcription Machinery. Cell **141**:595–605.

106. **Voloshin ON**, **Camerini-Otero RD**. 2007. The DinG protein from Escherichia coli is a structure-specific helicase. J Biol Chem **282**:18437–18447.

107. **Washburn RS**, **Gottesman ME**. 2011. Transcription termination maintains chromosome integrity. Proc Natl Acad Sci **108**:792–797.

108. **Merrikh CN**, **Brewer BJ**, **Merrikh H**. 2015. The B. subtilis Accessory Helicase PcrA Facilitates DNA Replication through Transcription Units. PLoS Genet **11**.

109. **Million-Weaver S**, **Samadpour AN**, **Moreno-Habel DA**, **Nugent P**, **Brittnacher MJ**, **Weiss E**, **Hayden HS**, **Miller SI**, **Liachko I**, **Merrikh H**. 2015. An underlying mechanism for the increased mutagenesis of lagging-strand genes in Bacillus subtilis. Proc Natl Acad Sci U S A **112**:E1096-105.

110. **Hasegawa K**, **Yoshiyama K**, **Maki H**. 2008. Spontaneous mutagenesis associated with nucleotide excision repair in Escherichia coli. Genes to Cells **13**:459–469.

111. **Ross C**, **Pybus C**, **Pedraza-Reyes M**, **Sung HM**, **Yasbin RE**, **Robleto E**. 2006. Novel role of mfd: Effects on stationary-phase mutagenesis in Bacillus subtilis. J Bacteriol **188**:7512–7520.

112. **Gómez-Marroquín M**, **Martin HA**, **Pepper A**, **Girard ME**, **Kidman AA**, **Vallin C**, **Yasbin RE**, **Pedraza-Reyes M**, **Robleto EA**. 2016. Stationary-Phase Mutagenesis in Stressed Bacillus subtilis Cells Operates by Mfd-Dependent Mutagenic Pathways. Genes (Basel) **7**.

113. **Selby CP**, **Sancar a**. 1993. Molecular mechanism of transcription-repair coupling. Science **260**:53–58.

114. **WITKIN EM**. 1956. Time, temperature, and protein synthesis: a study of ultraviolet-induced mutation in bacteria. Cold Spring Harb Symp Quant Biol **21**:123–140.

115. **Mellon I**, **Hanawalt PC**. 1989. Induction of the *Escherichia coli* lactose operon selectively increases repair of its transcribed DNA strand. Nature **342**:95–98.

116. **Husain I**, **Van Houten B**, **Thomas DC**, **Abdel-Monem M**, **Sancar A**. 1985. Effect of DNA polymerase I and DNA helicase II on the turnover rate of UvrABC excision nuclease. Proc Natl Acad Sci U S A **82**:6774–8.

117. **Caron PR**, **Kushner SR**, **Grossman L**. 1985. Involvement of helicase II (uvrD gene product) and DNA polymerase I in excision mediated by the uvrABC protein complex. Proc Natl Acad Sci U S A **82**:4925–4929.

118. **Goodman MF**, **Woodgate R**. 2013. Translesion DNA polymerases. Cold Spring Harb Perspect Biol **5**.

119. **Boudsocq F**, **Kokoska RJ**, **Plosky BB**, **Vaisman A**, **Ling H**, **Kunkel TA**, **Yang W**, **Woodgate R**. 2004. Investigating the role of the little finger domain of Y-family DNA polymerases in low fidelity synthesis and translesion replication. J Biol Chem **279**:32932–32940.

120. **Ohmori H**, **Friedberg EC**, **Fuchs RPP**, **Goodman MF**, **Hanaoka F**, **Hinkle D**, **Kunkel TA**, **Lawrence CW**, **Livneh Z**, **Nohmi T**, **Prakash L**, **Prakash S**, **Todo T**, **Walker GC**, **Wang Z**, **Woodgate R**. 2001. The Y-family of DNA Polymerases. Mol Cell.

121. **Sale JE**, **Lehmann AR**, **Woodgate R**. 2012. Y-family DNA polymerases and their role in tolerance of cellular DNA damage. Nat Rev Mol Cell Biol **13**:141–52.

122. **Goodman MF**, **Tippin B**. 2000. The expanding polymerase universe. Nat Rev Mol Cell Biol **1**:101–9.

123. **Tang M**, **Pham P**, **Shen X**, **Taylor J-S**, **O'Donnell ME**, **Woodgate R**, **Goodman**

MF. 2000. Roles of E. coli DNA polymerases IV and V in lesion-targeted and untargeted SOS mutagenesis. Nature **404**:1014–1018.

124. **Ling H**, **Boudsocq F**, **Woodgate R**, **Yang W**. 2001. Crystal structure of a Y-family DNA polymerase in action: A mechanism for error-prone and lesion-bypass replication. Cell **107**:91–102.

125. **Sung HM**, **Yeamans G**, **Ross CA**, **Yasbin RE**. 2003. Roles of YqjH and YqjW, homologs of the Escherichia coli UmuC/DinB or Y superfamily of DNA polymerases, in stationary-phase mutagenesis and UV-induced mutagenesis of Bacillus subtilis. J Bacteriol **185**:2153–2160.

126. **Duigou S**, **Ehrlich SD**, **Noirot P**, **Noirot-Gros MF**. 2005. DNA polymerase I acts in translesion synthesis mediated by the Y-polymerases in Bacillus subtilis. Mol Microbiol **57**:678–690.

127. **Kaguni JM**, **Bertsch LL**, **Bramhill D**, **Flynn JE**, **Fuller RS**, **Funnell B**, **Maki S**, **Ogawa T**, **Ogawa K**, **van der Ende A**, **et al.** 1985. Initiation of replication of the Escherichia coli chromosomal origin reconstituted with purified enzymes. Basic Life Sci **30**:141–150.

128. **Funnell BE**, **Baker TA**, **Kornberg A**. 1986. Complete enzymatic replication of plasmids containing the origin of the Escherichia coli chromosome. J Biol Chem **261**:5616–5624.

129. **Funnell BE**, **Baker TA**, **Kornberg A**. 1987. In vitro assembly of a prepriming complex at the origin of the Escherichia coli chromosome. J Biol Chem **262**:10327–10334.

130. **Kornberg A**. 1987. Enzyme systems initiating replication at the origin of the

Escherichia coli chromosome. J Cell Sci Suppl **7**:1–13.

131. **Smelkova N**, **Marians KJ**. 2001. Timely Release of Both Replication Forks from oriC Requires Modulation of Origin Topology. J Biol Chem **276**:39186–39191.
132. **Vos SM**, **Tretter EM**, **Schmidt BH**, **Berger JM**. 2011. All tangled up: How cells direct, manage and exploit topoisomerase function. Nat Rev Mol Cell Biol.
133. **Wang JC**. 1998. Moving one DNA double helix through another by a type II DNA topoisomerase: The story of a simple molecular machine. Q Rev Biophys.
134. **Zechiedrich EL**, **Cozzarelli NR**. 1995. Roles of topoisomerase IV and DNA gyrase in DNA unlinking during replication in Escherichia coli. Genes Dev **9**:2859–2869.
135. **Hardy CD**, **Crisona NJ**, **Stone MD**, **Cozzarelli NR**. 2004. Disentangling DNA during replication: a tale of two strands. Philos Trans R Soc Lond B Biol Sci **359**:39–47.
136. **Champoux JJ**. 2001. DNA topoisomerases: structure, function, and mechanism. Annu Rev Biochem **70**:369–413.
137. **Wang JC**. 1971. Interaction between DNA and an Escherichia coli protein omega. J Mol Biol **55**:523–533.
138. **Cheng B**, **Zhu C-X**, **Ji C**, **Ahumada A**, **Tse-Dinh Y-C**. 2003. Direct interaction between Escherichia coli RNA polymerase and the zinc ribbon domains of DNA topoisomerase I. J Biol Chem **278**:30705–30710.
139. **Liu LF**, **Wang JC**. 1987. Supercoiling of the DNA template during transcription. Proc Natl Acad Sci **84**:7024–7027.
140. **Massé E**, **Drolet M**. 1999. Escherichia coli DNA topoisomerase I inhibits R-loop

formation by relaxing transcription-induced negative supercoiling. J Biol Chem **274**:16659–16664.

141. **Gellert M**, **Mizuuchi K**, **O'Dea MH**, **Nash HA**. 1976. DNA gyrase: an enzyme that introduces superhelical turns into DNA. Proc Natl Acad Sci **73**:3872–3876.

142. **DiNardo S**, **Voelkel K a**, **Sternglanz R**, **Reynolds a E**, **Wright a**. 1982. Escherichia coli DNA topoisomerase I mutants have compensatory mutations in DNA gyrase genes. Cell **31**:43–51.

143. **Pruss GJ**, **Manes SH**, **Drlica K**. 1982. Escherichia coli DNA topoisomerase I mutants: Increased supercoiling is corrected by mutations near gyrase genes. Cell **31**:35–42.

144. **Levine C**, **Hiasa H**, **Marians KJ**. 1998. DNA gyrase and topoisomerase IV: Biochemical activities, physiological roles during chromosome replication, and drug sensitivities. Biochim Biophys Acta - Gene Struct Expr.

145. **Hiasa H**, **Shea ME**. 2000. DNA gyrase-mediated wrapping of the DNA strand is required for the replication fork arrest by the DNA gyrase-quinolone-DNA ternary complex. J Biol Chem **275**:34780–34786.

146. **Ullsperger C**, **Cozzarelli NR**. 1996. Contrasting enzymatic activities of topoisomerase IV and DNA gyrase from Escherichia coli. J Biol Chem **271**:31549–31555.

147. **Gellert M**, **Mizuuchi K**, **O'Dea MH**, **Nash HA**. 1976. DNA gyrase: an enzyme that introduces superhelical turns into DNA. Proc Natl Acad Sci USA **73**:3872–6.

148. **Hiasa H**, **Marians KJ**. 1994. Topoisomerase IV can support oriC DNA replication in vitro. J Biol Chem **269**:16371–16375.

149. **Cozzarelli NR**. 1980. DNA gyrase and the supercoiling of DNA. Science **207**:953–960.

150. **Peter BJ**, **Ullsperger C**, **Hiasa H**, **Marians KJ**, **Cozzarelli NR**. 1998. The structure of supercoiled intermediates in DNA replication. Cell **94**:819–827.

151. **Peng H**, **Marians KJ**. 1993. Escherichia coli topoisomerase IV: Purification, characterization, subunit structure, and subunit interactions. J Biol Chem **268**:24481–24490.

152. **Crisona NJ**, **Strick TR**, **Bensimon D**, **Croquette V**, **Cozzarelli NR**. 2000. Preferential relaxation of positively supercoiled DNA by E. coli topoisomerase IV in single-molecule and ensemble measurements. Genes Dev **14**:2881–2892.

153. **Kato J ichi**, **Nishimura Y**, **Imamura R**, **Niki H**, **Hiraga S**, **Suzuki H**. 1990. New topoisomerase essential for chromosome segregation in E. coli. Cell **63**:393–404.

154. **Prescott DM**, **Kuempel PL**. 1972. Bidirectional replication of the chromosome in Escherichia coli. Proc Natl Acad Sci U S A **69**:2842–5.

155. **Magnan D**, **Bates D**. 2015. Regulation of DNA Replication Initiation by Chromosome Structure. J Bacteriol **197**:3370–7.

156. **Fuller RS**, **Kornberg A**. 1983. Purified dnaA protein in initiation of replication at the Escherichia coli chromosomal origin of replication. Proc Natl Acad Sci U S A **80**:5817–5821.

157. **Erzberger JP**, **Mott ML**, **Berger JM**. 2006. Structural basis for ATP-dependent DnaA assembly and replication-origin remodeling. Nat Struct Mol Biol **13**:676–683.

158. **Asai T**, **Takanami M**, **Imai M**. 1990. The AT richness and gid transcription

determine the left border of the replication origin of the E. coli chromosome. EMBO J **9**:4065–4072.

159. **Bogan J a**, **Helmstetter CE**. 1997. DNA sequestration and transcription in the oriC region of Escherichia coli. Mol Microbiol **26**:889–896.

160. **Wang JC**. 1991. DNA topoisomerases: Why so many? J Biol Chem **266**:6659–6662.

161. **Khodursky a B**, **Peter BJ**, **Schmid MB**, **DeRisi J**, **Botstein D**, **Brown PO**, **Cozzarelli NR**. 2000. Analysis of topoisomerase function in bacterial replication fork movement: use of DNA microarrays. Proc Natl Acad Sci U S A **97**:9419–9424.

162. **Smith DH**, **Davis BD**. 1967. Mode of action of novobiocin in Escherichia coli. J Bacteriol **93**:71–79.

163. **WL. S**. 1975. Novobiocin-a specific inhibitor of semiconservative DNA replication in permeabilized Escherichia coli cells. J Mol Biol **1**:201–5.

164. **Cozzarelli NR**. 1977. The mechanism of action of inhibitors of DNA synthesis. Annu Rev Biochem **46**:641–668.

165. **Sugino A**, **Higgins NP**, **Brown PO**, **Peebles CL**, **Cozzarelli NR**. 1978. Energy coupling in DNA gyrase and the mechanism of action of novobiocin. Proc Natl Acad Sci U S A **75**:4838–42.

166. **Sugino a**, **Peebles CL**, **Kreuzer KN**, **Cozzarelli NR**. 1977. Mechanism of action of nalidixic acid: purification of Escherichia coli nalA gene product and its relationship to DNA gyrase and a novel nicking-closing enzyme. Proc Natl Acad Sci U S A **74**:4767–71.

167. **Lewis RJ**, **Singh OM**, **Smith C V**, **Skarzynski T**, **Maxwell A**, **Wonacott AJ**, **Wigley DB**. 1996. The nature of inhibition of DNA gyrase by the coumarins and the cyclothialidines revealed by X-ray crystallography. EMBO J **15**:1412–20.

168. **Fujimoto-Nakamura M**, **Ito H**, **Oyamada Y**, **Nishino T**, **Yamagishi JI**. 2005. Accumulation of mutations in both gyrB and parE genes is associated with high-level resistance to novobiocin in Staphylococcus aureus. Antimicrob Agents Chemother **49**:3810–3815.

169. **Orr E**, **Staudenbauer WL**. 1982. Bacillus subtilis DNA gyrase: Purification of subunits and reconstitution of supercoiling activity. J Bacteriol **151**:524–527.

170. **Berkmen MB**, **Grossman AD**. 2007. Subcellular positioning of the origin region of the Bacillus subtilis chromosome is independent of sequences within oriC, the site of replication initiation, and the replication initiator DnaA. Mol Microbiol **63**:150–165.

171. **Hassan AKM**, **Moriya S**, **Ogura M**, **Tanaka T**, **Kawamura F**, **Ogasawara N**. 1997. Suppression of initiation defects of chromosome replication in Bacillus subtilis dnaA and oriC-deleted mutants by integration of a plasmid replicon into the chromosomes. J Bacteriol **179**:2494–2502.

172. **Tanaka T**, **Ogura M**. 1998. A novel Bacillus natto plasmid pLS32 capable of replication in Bacillus subtilis. FEBS Lett **422**:243–246.

173. **Moriya S**, **Hassan a K**, **Kadoya R**, **Ogasawara N**. 1997. Mechanism of anucleate cell production in the oriC-deleted mutants of Bacillus subtilis. DNA Res **4**:115–126.

174. **Munoz R**, **Bustamante M**, **De la Campa AG**. 1995. Ser-127-to-leu substitution in

the DNA gyrase B subunit of Streptococcus pneumoniae is implicated in novobiocin resistance. J Bacteriol.

175. **Hayashi M**, **Ogura Y**, **Harry EJ**, **Ogasawara N**, **Moriya S**. 2005. Bacillus subtilis YabA is involved in determining the timing and synchrony of replication initiation. FEMS Microbiol Lett **247**:73–79.

176. **Noirot-Gros M-F**, **Velten M**, **Yoshimura M**, **McGovern S**, **Morimoto T**, **Ehrlich SD**, **Ogasawara N**, **Polard P**, **Noirot P**. 2006. Functional dissection of YabA, a negative regulator of DNA replication initiation in Bacillus subtilis. Proc Natl Acad Sci U S A **103**:2368–73.

177. **Baker TA**, **Sekimizu K**, **Funnell BE**, **Kornberg A**. 1986. Extensive unwinding of the plasmid template during staged enzymatic initiation of DNA replication from the origin of the Escherichia coli chromosome. Cell **45**:53–64.

178. **Ogasawara N**, **Seiki M**, **Yoshikawa H**. 1979. Effect of novobiocin on initiation of DNA replication in Bacillus subtilis. Nature **281**:702–704.

179. **Magnan D**, **Joshi MC**, **Barker AK**, **Visser BJ**, **Bates D**. 2015. DNA replication initiation is blocked by a distant chromosome-membrane attachment. Curr Biol **25**:2143–2149.

180. **Baker TA**, **Kornberg A**. 1988. Transcriptional activation of initiation of replication from the E. coli chromosomal origin: An RNA-DNA hybrid near oriC. Cell **55**:113–123.

181. **von Freiesleben U**, **Rasmussen K V.** 1991. DNA replication in Escherichia coli gyrB(Ts) mutants analysed by flow cytometry. Res Microbiol **142**:223–227.

182. **Freiesleben U Von**, **Rasmussen K V**. 1992. The level of supercoiling affects the

regulation of DNA replication in Escherichia coli. Res Microbiol **143**:655–663.

183. **Louarn J**, **Bouché JP**, **Patte J**, **Louarn JM**. 1984. Genetic inactivation of topoisomerase I suppresses a defect in initiation of chromosome replication in Escherichia coli. MGG Mol Gen Genet **195**:170–174.

184. **Fuchs RP**, **Fujii S**. 2013. Translesion DNA synthesis and mutagenesis in prokaryotes. Cold Spring Harb Perspect Biol **5**.

185. **Hanawalt PC**, **Spivak G**. 2008. Transcription-coupled DNA repair: two decades of progress and surprises. Nat Rev Mol Cell Biol **9**:958–70.

186. **Patel PH**, **Suzuki M**, **Adman E**, **Shinkai A**, **Loeb LA**. 2001. Prokaryotic DNA polymerase I: evolution, structure, and ``base flipping" mechanism for nucleotide selection. J Mol Biol **308**:823–37.

187. **Samadpour AN**, **Merrikh H**. 2018. DNA gyrase activity regulates DnaA-dependent replication initiation in *Bacillus subtilis*. Mol Microbiol.

188. **Kouzine F**, **Sanford S**, **Elisha-Feil Z**, **Levens D**. 2008. The functional response of upstream DNA to dynamic supercoiling in vivo. Nat Struct Mol Biol **15**:146–154.

189. **Lal A**, **Dhar A**, **Trostel A**, **Kouzine F**, **Seshasayee AS**, **Adhya S**. 2016. Genome scale patterns of supercoiling in a bacterial chromosome. Nat Commun **7**:11055.

190. **Schenk K**, **Hervás AB**, **Rösch TC**, **Eisemann M**, **Schmitt BA**, **Dahlke S**, **Kleine-Borgmann L**, **Murray SM**, **Graumann PL**. 2017. Rapid turnover of DnaA at replication origin regions contributes to initiation control of DNA replication. PLoS Genet **13**.

191. **Jee J**, **Rasouly A**, **Shamovsky I**, **Akivis Y**, **Steinman SR**, **Mishra B**, **Nudler E**. 2016. Rates and mechanisms of bacterial mutagenesis from maximum-depth

sequencing. Nature **534**:693–696.

192. **Kobayashi S**, **Valentine MR**, **Pham P**, **O'Donnell M**, **Goodman MF**. 2002. Fidelity of Escherichia coli DNA polymerase IV. Preferential generation of small deletion mutations by dNTP-stabilized misalignment. J Biol Chem **277**:34198–34207.

193. **Neeley WL**, **Delaney S**, **Alekseyev YO**, **Jarosz DF**, **Delaney JC**, **Walker GC**, **Essigmann JM**. 2007. DNA polymerase V allows bypass of toxic guanine oxidation products in vivo. J Biol Chem **282**:12741–12748.

194. **Kokoska RJ**, **Bebenek K**, **Boudsocq F**, **Woodgate R**, **Kunkel TA**. 2002. Low fidelity DNA synthesis by a Y family DNA polymerase due to misalignment in the active site. J Biol Chem **277**:19633–19638.

195. **Wagner J**, **Nohmi T**. 2000. Escherichia coli DNA polymerase IV mutator activity: Genetic requirements and mutational specificity. J Bacteriol **182**:4587–4595.

196. **Ogi T**, **Lehmann AR**. 2006. The Y-family DNA polymerase kappa (pol kappa) functions in mammalian nucleotide-excision repair. Nat Cell Biol **8**:640–642.

197. **Selby CP**, **Sancar A**. 1991. Gene- and strand-specific repair in vitro: partial purification of a transcription-repair coupling factor. Proc Natl Acad Sci U S A **88**:8232–6.

198. **Perego M**, **Spiegelman GB**, **Hoch JA**. 1988. Structure of the gene for the transition state regulator, abrB: regulator synthesis is controlled by the spo0A sporulation gene in Bacillus subtilis. Mol Microbiol **2**:689–699.

199. **Goranov AI**, **Breier AM**, **Merrikh H**, **Grossman AD**. 2009. Yaba of bacillus subtilis controls DnaA-mediated replication initiation but not the transcriptional

response to replication stress. Mol Microbiol **74**:454–466.

200. **Simmons LA**, **Grossman AD**, **Walker GC**. 2007. Replication is required for the RecA localization response to DNA damage in *Bacillus subtilis*. Proc Natl Acad Sci U S A **104**:1360–1365.

201. **Sterlini JM**, **Mandelstam J**. 1969. Commitment to sporulation in *Bacillus subtilis* and its relationship to development of actinomycin resistance. Biochem J **113**:29–37.

202. **Murray H**, **Errington J**. 2008. Dynamic Control of the DNA Replication Initiation Protein DnaA by Soj/ParA. Cell **135**:74–84.

203. **Li H**, **Handsaker B**, **Wysoker A**, **Fennell T**, **Ruan J**, **Homer N**, **Marth G**, **Abecasis G**, **Durbin R**. 2009. The Sequence Alignment/Map format and SAMtools. Bioinformatics **25**:2078–2079.

204. **Langmead B**, **Salzberg SL**. 2012. Fast gapped-read alignment with Bowtie 2. Nat Methods **9**:357–359.

205. **Fabret C**, **Ehrlich SD**, **Noirot P**. 2002. A new mutation delivery system for genome-scale approaches in Bacillus subtilis. Mol Microbiol **46**:25–36.

206. **Hall BM**, **Ma C-X**, **Liang P**, **Singh KK**. 2009. Fluctuation analysis CalculatOR: a web tool for the determination of mutation rate using Luria-Delbruck fluctuation analysis. Bioinformatics **25**:1564–5.